DISRUPTION OF NOREPINEPHRINE RELEASE AND CLEARANCE MECHANISMS IN SYMPATHETIC NERVES ASSOCIATED WITH MESENTERIC ARTERIES BUT NOT VEINS IN SALT-SENSITIVE HYPERTENSION

By

Hua Dong

A DISSERTATION

Submitted to
Michigan State University
In partial fulfillment of the requirements
For the degree of

DOCTOR OF PHILOSOPHY

Chemistry

2009

ABSTRACT

DISRUPTION OF NOREPINEPHRINE RELEASE AND CLEARANCE MECHANISMS IN SYMPATHETIC NERVES ASSOCIATED WITH MESENTERIC ARTERIES BUT NOT VEINS IN SALT-SENSITIVE HYPERTENSION

By

Hua Dong

Norepinephrine (NE) is a vasoconstrictor neurotransmitter released from sympathetic nerves that innervate the smooth muscle cells in arteries and veins. Once released, NE diffuse across the junctional cleft, bind briefly to receptor to elicit smooth muscle contraction. The sympathetic nerves system regulates blood pressure and its function is altered in animal models and human essential hypertension. The altered function is associated with altered NE release. However, little is known about the characteristics of local NE release from periarterial and perivenous sympathetic nerves in normal and hypertensive animals. I seek a better understanding of the functional differences between sympathetic neurotransmission in mesenteric arteries (MA) and veins (MV), and how this process is altered in hypertension. Deoxycorticosterone-acetate (DOCA) salt rats were used as a model of salt-sensitive hypertension. Continuous amperometry with a microelectrode measures the local concentration of endogenous NE at the surface of a blood vessel as an oxidation current. Since NE release is a multi-step process, one way the mechanisms can be probed is

by studying the temperature dependence of neurotransmitter release and clearance.

The results of this dissertation study revealed important findings regarding adrenergic neurotransmission in MA and MV from normotensive and DOCA-salt hypertensive rats. 1) NE release and clearance from rat periarterial and perivenous sympathetic nerves are regulated differently. This difference is based largely on the function of prejunctional α_2 adrenergic receptors (α_2ARs), NE transporter (NET), calcium channels, but may also include different distribution of vesicles that contain NE. NE release and clearance is regulated by α_2ARs and NET in MA but not in MV. 2) Adrenergic neurotransmission to MA is impaired in DOCA-salt hypertension. The increased NE overflows and temperature sensitivity in DOCA-salt MA is at least partially due to the impaired function of α_2AR and NET. These changes are not due to the alterations in calcium handling in the nerve terminal. 3) Oxidative stress alters sympathetic neurotransmission in DOCA-salt hypertensive rats by impairing pertussis toxin-sensitive G proteins which couple to α_2AR at the nerve terminal. Chronic antioxidant treatment lowers blood pressure and restores sympathetic nerve function at the neuroeffector junction in DOCA-salt hypertensive rats.

Together, these results reveal the different supply of sympathetic nerves to MA and MV may contribute to their different hemodynamic functions. Furthermore, they reveal the importance of sympathetic nerve endings as a therapeutic target and support a new mechanism for the beneficial effect of antioxidant treatment in salt-sensitive hypertension.

ACKNOWLEDGEMENTS

The research work conducted in this thesis was completed with the guidance, support, and encouragement of many people.

First and foremost, I would like to thank my advisor, Dr. Greg M. Swain, and my co-advisor Dr. James Galligan, for their continued support and guidance throughout the course of my research. They offered valuable insight and direction in guiding my research work. Under their excellent guidance, I learned how to conduct research in the academic area. I appreciate all that they have done for me during my PhD study.

I am indebted to the members of my committee, Dr. Gary Blanchard and Dr. Gregory Fink, for their valuable suggestions, comments, and the time they shared with me. In addition, I would like to thank my previous group members, Dr. Jinwoo Park and Dr. Shihua Wang for their friendship and academic support on my research.

My gratitude also goes to members of Dr. Swain's lab: Dr. Hong Zhao, Dr. Liang Guo, Dr. Doo Young Kim, Vernon Matthew Swope, Ayten Ay, Matthew Fhaner, David Woodbury, Chen Qiu, Xingyi Yang, and Kelly Hutchins, for their help and suggestions during my PhD study. I would also like to express my deep appreciation to colleagues and friends from Dr. Galligan's Lab: Dr. Hui Xu, Dr. Xiaochun Bian, Hui Wang, Emmy Sangsiri, Vinoo Naidoo, and Dima Decker, for their inspiring ideas and assistance. I was fortunate to have worked with these talented researchers and students.

Last but not the least, I owe my family much gratitude. I would like to thank my parents, sister and husband for their unwavering encouragement, understanding, and endless love along this journey. They were always there whenever I needed them and their constant support was my strong crutch for the completion of my PhD study.

TABLE OF CONTENTS

LIST OF TABLES

LIST OF FIGURES

CHAPTER 1

GENERAL INTRODUCTION

1.1 Hypertension

Hypertension is defined as a sustained systolic blood pressure greater than 140 mmHg, and/or diastolic blood pressure over 90 mmHg [American Heart Association]. Known as the "silent killer," hypertension often produces few obvious symptoms. However, uncontrolled high blood pressure can damage the heart, eyes, kidneys, blood vessels, and the brain and can lead to congestive heart failure, heart attack, kidney failure, or stroke. Hypertension occurs more commonly among people over 35 and it is particularly prevalent in African Americans, obese people, heavy drinkers and women who take birth control pills. Every year, approximately 7.1 million deaths worldwide occur as a result of hypertension related illness [1]. The goal of hypertension treatment is to lower blood pressure and to protect the brain, heart, kidneys and other organs from damage. Although the treatment rate is 75% or higher, less than 50% of hypertensive patients achieve control of blood pressure to goal levels [2].

There are two types of hypertension, essential (primary) and secondary hypertension. About 90 to 95% of the hypertension is essential hypertension, which arises from unknown causes. Secondary hypertension accounts for 5 to 10% of all hypertension cases and high blood pressure in these patients is a result of other diseases, such as kidney disease or hormone secreting tumors. Although the evidence shows that some forms of essential hypertension involve primarily the sympathetic nervous system, mechanisms leading to increased

sympathetic nerve activity are poorly understood [3]. Therefore, it is important to study hypertension and its connection to increased sympathetic nerve activity. My research was designed to further understand the causes of hypertension which may help develop improved treatments for this disease.

1.2 Blood pressure regulation

The mean arterial blood pressure (MAP) is the product of cardiac output (CO) and total peripheral resistance (TPR). CO is the volume of blood being pumped by the left ventricle of the heart per minute. CO is the product of heart rate and stroke volume. TPR is the sum of the resistance to blood flow through all peripheral blood vessels. TPR is determined largely by the diameter of small arteries and arterioles. Humoral factors, the central and the peripheral nervous systems, and kidney function are important factors regulating blood pressure. Acute changes in blood pressure are regulated by the baroreflex arc, which also contributes to the long-term blood pressure regulation [4]. Baroreflexes and central signals from higher brain centers dominate the moment-to-moment control of blood pressure through the sympathetic and parasympathetic nervous system (SNS and PNS), are part of the autonomic nervous system [5]. The SNS influences the distribution of blood throughout the body by constricting and dilating the blood vessels. SNS activation can increase TPR and CO to increase blood pressure. Effects of sympathetic activation on the kidney and the rennin-angiotensin system can also influence the blood pressure regulation [6]. The PNS can slow the heart and decrease blood pressure by activation of vagal

nerves. Other factors, such as the endothelin system, vascular function, and circulating epinephrine all contribute to the blood pressure regulation.

1.3 Sympathetic nervous system and hypertension

1.3.1 Sympathetic nervous system (SNS)

The nervous system plays an essential role in short and long term blood pressure regulation [7] and SNS innervating the splanchnic circulation are particularly important [8]. SNS is the part of the autonomic nervous system. It, in general, inhibits or opposes the physiological effects of the parasympathetic nervous system, as in tending to reduce digestive secretions, speeding up the heart, and contracting blood vessels [9]. The cell bodies of the preganglionic sympathetic neurons are located in the intermediolateral gray matter of the spinal cord, between levels T1 and L3 (see Figure. 1.1). After convergence and divergence, most of the axons from these preganglionic neurons synapse with postganglionic sympathetic neurons located within ganglia of the paravertebral sympathetic chain, as well as within prevertebral ganglia. The synapse in the sympathetic ganglion uses acetylcholine (ACh) as a neurotransmitter. ACh binds with nicotinic receptors on the post synaptic neurons in sympathetic ganglia. The synapse of the post-ganglionic neuron with the target organ uses norepinephrine (NE), adenosine 5'-triphosphate (ATP) as neurotransmitters and neuropeptide Y (NPY) as a neuromodulator [10]. Over the past several years, beta-nicotinamide adenine dinucleotide (beta-NAD) was also found to be a neurotransmitter released from the SNS [11]. The SNS is the primary short term regulator of blood

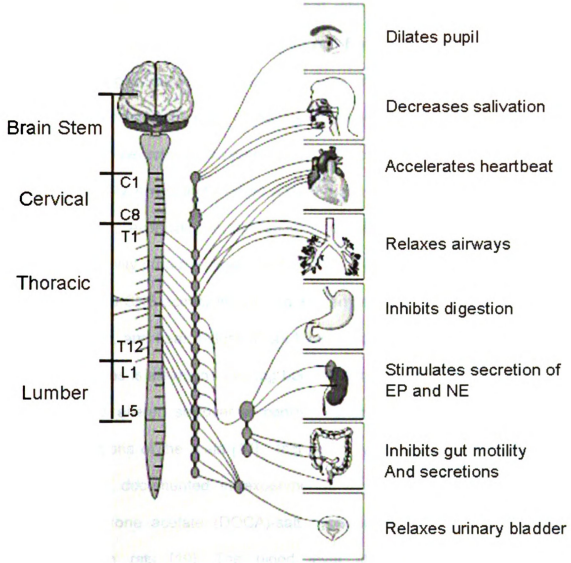

Figure 1.1 Sympathetic divisions of the autonomic nervous system

[http://www.goodpsych.com/storage/Sympathetic_Nervous_System_L.jp]

pressure regulation and plays an important role in long term blood pressure regulations. Sympathetic nerves originating from the celiac and superior mesenteric ganglia supply arteries and veins in the splanchnic circulation. Sympathetic nerves travel along blood vessels near the adventitial medial border where they form neuromuscular junctions with vascular smooth muscle cells [12-14]. Quantitatively, sympathetic nerve activity is the most critical factor controlling venoconstriction, especially in the splanchnic circulation [15, 16]. Increased sympathetic activity produces vasoconstriction.

Enhanced SNS activity is involved in many cardiovascular diseases, such as hypertension, and heart failure. Work by Esler demonstrated that NE release from renal nerves is elevated in young borderline hypertensive patients and that they also have altered spillover of central monoamine neurotransmitters from subcortical regions of the brain [17]. Increased sympathetic neurotransmission has also been documented in experimental hypertension models, such as deoxycorticosterone acetate (DOCA)-salt hypertension [18] and spontaneous hypertension in rats [19]. The blood level of the principal sympathetic neurotransmitters, NE, is elevated in these models to suggest increased neurotransmitter release from sympathetic nerves. Increased NE release in hypertension indicates that alteration may take place at the sympathetic nerve endings.

1.3.2 Neurotransmitters

NE. Among the neurotransmitters that are released by SNS, NE is the principle

neurotransmitter intimately regulate cardiovascular functions. And it is believed that the NE: ATP ratio in a sympathetic vesicle may be as high as 50:1 [20, 21]. NE is a catecholamine that is secreted by the adrenal medulla and sympathetic nerve endings to cause vasoconstriction, increase heart rate, blood pressure, and the sugar level of the blood [9]. NE performs its action mainly by act on adrenergic receptors on target cells. For example, NE bind with α_1 adrenergic receptor (α_1AR) post junctionally resulting in constriction of the smooth muscle cell. Many substances modulate NE release, some inhibiting it and some stimulating it, for instance, NE can bind to presynaptic α_2 receptors for the inhibition for its release by negative feedback mechanisms [21]. Details for the regulation of NE release and clearance will be introduced in section 1.4 (Prejunctional regulation of sympathetic neurotransmission). Numerous studies have indicated that there is increased NE release from perivascular sympathetic nerves and increased vasoconstriction in animal models of hypertension, particularly salt sensitive hypertension which is associated with hyperactivity of the sympathetic nervous system [22, 23].

ATP as a sympathetic neurotransmitter in the vasculature. ATP is a multifunctional nucleotide, and plays an important role in cell biology as an intracellular energy source [24]. In 1972, ATP was proposed as a neurotransmitter in non-adrenergic, non-cholinergic nerves in the gut and bladder [25]. It is an important signaling molecule in both the central and peripheral nervous system. Activity-dependent release of ATP from synapses, axons and

glia activates P2 (including P2X and P2Y family) purinergic membrane receptors that modulate intracellular calcium and cyclic AMP [26]. The P2X *ionotropic* receptor subgroup comprises seven members ($P2X_1$–$P2X_7$) which are ligand-gated Ca^{2+}-permeable ion channels that open when bound to an extracellular purine nucleotide [27]. The P2Y ($P2Y_1$–$P2Y_{15}$) receptors are G protein-coupled receptors and modulate mainly intracellular calcium and cyclic AMP levels. The level of ATP at nerve endings are primarily regulated by mitochondrial oxidative phosphorylation which generates ATP from ADP [28]. Upon nerve stimulation, ATP is released and then quickly degraded by ectonucleotidasesto to ADP and finally to adenosine [29, 30]. Adenosine can activate the A1 receptor on the nerve terminal to regulate neurotransmitter release via negative feedback.

For arteries, ATP (adenosine 5′ triphosphate) and NE are co-transmitters released by sympathetic nerves [31-33]. ATP is the dominant neurotransmitter in small mesenteric arteries in normotensive rats; however, in arteries from DOCA-salt hypertensive rats, NE is the major sympathetic neurotransmitter. As for the vein, NE is the neurotransmitter mediating neurogenic contractions of mesenteric veins from both sham and DOCA-salt rats [34]. This profile differs somewhat in guinea pig mesenteric arteries and veins where purinergic neurotransmission is more prominent in veins [31]. NE activates postjunctional α adrenergic receptors (αARs) in both arteries and veins [35]. However, there are differences in receptors that react to the nerve-released NE exist between arteries and veins. P2X receptors also play an important role besides αARs in regulating the arterial tone, while only αARs regulate venous tone [36].

Neuropeptide Y (NPY) is released by perivascular sympathetic nerves.. NPY is a 36-amino-acid peptide neurotransmitter in the central and peripheral nervous systems [37]. NPY is co-localized with NE in sympathetic nerves supplying the cardiovascular system and known to be of importance for the maintenance of blood pressure. It is released during high frequency sympathetic nerve stimulation and has a direct vasoconstrictor action, varying in intensity depending on the vascular bed examined [38]. The receptor protein that NPY operates on is a G-protein coupled receptor. Five subtypes of NPY receptor have been cloned and classified as Y1, Y2, Y3, Y4, Y5, and y6 based on their molecular and pharmacological profile [39]. Among them, Y1 and Y2 receptors are involved in peripheral effects. NPY increases the constriction induced by NE and ATP via the Y1 receptor post-junctionally [40] and inhibits NE release through Y2 receptor pre-junctionally [41]. NPY levels are increased in human diseases associated with sympathetic activation. For example, in human hypertension, venoarterial plasma NPY level is elevated [38]. NPY content is increased in nerves of the cerebral and mesenteric vasculature in spontaneously hypertensive rats [42]. Also, there are increased plasma NPY levels in DOCA-salt hypertension [43].

Beta-nicotinamide adenine dinucleotide (beta-NAD) as a sympathetic neurotransmitter. Beta-NAD is a coenzyme found in all living cells. Until recently, it was found to be a neurotransmitter released from sympathetic nerves in blood vessels and urinary bladder with NE, ATP, and NPY upon nerve stimulation [44]. Beta-NAD is released via a botulinum neurotoxin A-mediated

mechanism but not evoked either by the overflow of other neurotransmitters, e.g. NE, or the neuropeptides, e.g., substance P, in canine mesenteric artery [11] . The release of beta-NAD is sensitive to the voltage dependent calcium channel and depends on synaptosomal-associated protein of 25 kDa (SNAP-25) mediated exocytosis at a low level of nerve activation. It has found to work as an inhibitory neurotransmitter that contributes to enteric inhibitory regulation of visceral smooth muscles [45]. Since beta-NAD was just discovered to be a member of neurotransmitter family in the past several years, no work showing its function related with disease status, e.g. hypertension, has been altered.

1.4 Prejunctional regulation of sympathetic neurotransmission

Epinephrine is released from the adrenal medulla into the blood as a hormone, while NE is the primary neurotransmitter for postganglionic sympathetic adrenergic nerves where it is released from noradrenergic neurons. It performs its action by being released into the synaptic cleft, where it acts on adrenergic receptors, followed by the signal termination, either by degradation of norepinephrine, or by re-uptake. Figure 1.2 shows a diagram of NE synthesis, release and clearance.

1.4.1 NE synthesis

NE is synthesized from tyrosine as a precursor, and packed in to synaptic vesicles. As shown in Figure 1.2 and 1.3, first, the amino acid tyrosine (Tyr) is transported into the sympathetic nerve axon. Tyr is converted to

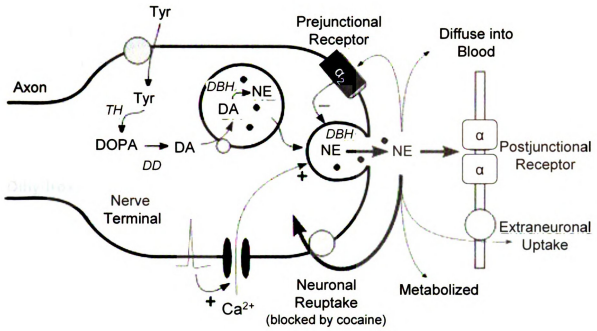

Tyr = tyrosine; TH = tyrosine hydroxylase; DD = DOPA decarboxylase;
DA = dopamine; DBH = dopamine β-hydroxylase; NE = norepinephrine

Figure 1.2 Diagram of NE synthesis, release and clearance

[www.cvpharmacology.com/norepinephrine.htm]

dihydroxyphenylalanine (DOPA) by tyrosine hydroxylase and this is the rate limiting step for NE synthesis. DOPA is then converted to dopamine (DA) by DOPA decarboxylase. Dopamine is transported into vesicles and then converted to NE by dopamine β-hydroxylase (DBH). NE can be further converted by phenylethanolamine-N-methyltransferase to epinephrine (EP), which is released into the blood from the adrenal glands and carried throughout the body [46].

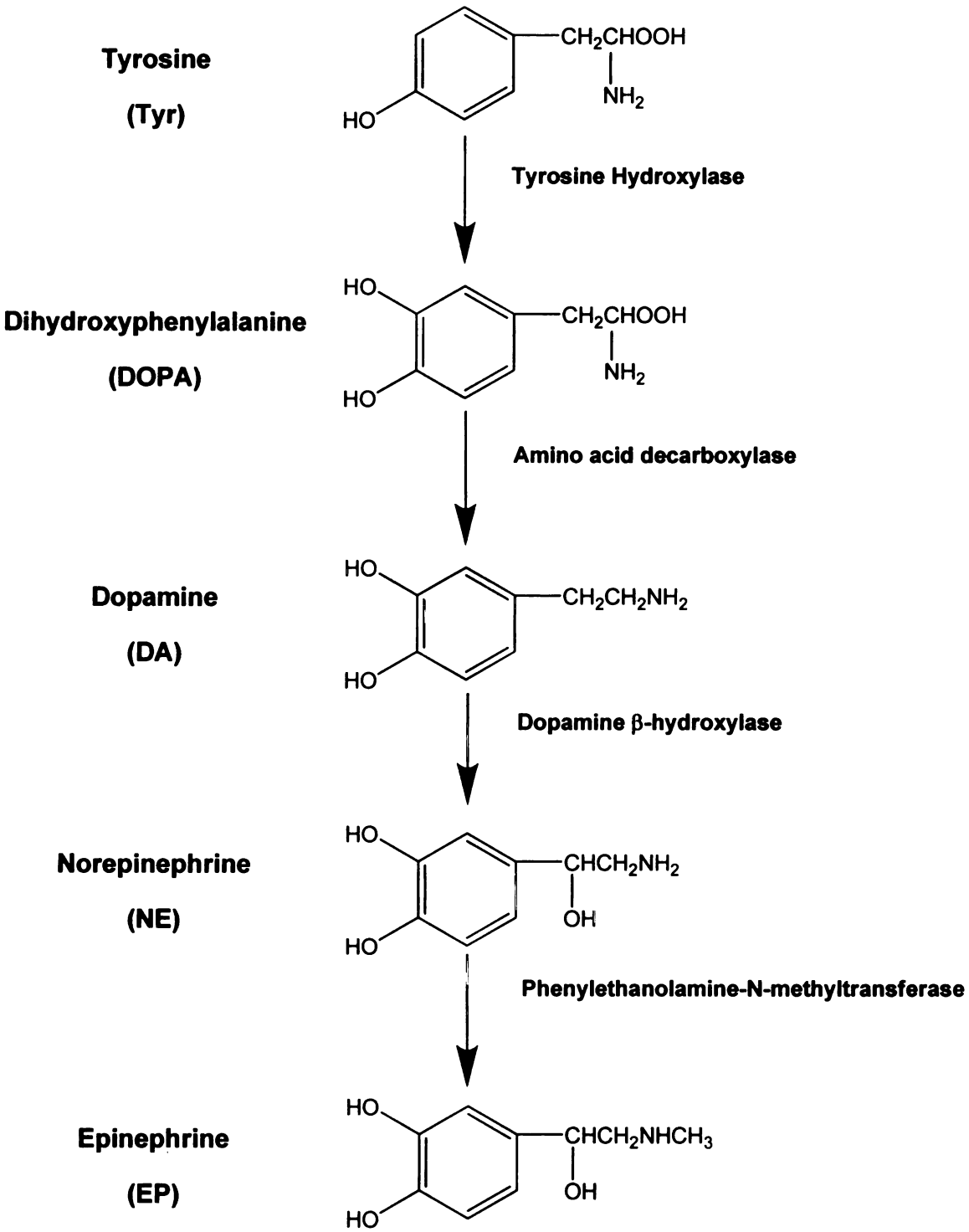

Figure 1.3 Steps for NE synthesis

1.4.2 NE release

After NE is synthesized inside the nerve axon, it is stored in vesicles and then released by the nerve when an action potential travels down the nerve. An action potential traveling down the axon depolarizes the membrane and causes Ca^{2+} influx to the nerve endings. The increased intracellular calcium causes the NE vesicles to migrate to the axonal membrane and fuse with the membrane. NE is then released through exocytosis along with other secondary neurotransmitters, such as ATP, into the junctional cleft. NE then binds with post-junctional adrenergic receptors to induce the smooth muscle cells (SMCs) constriction [47]. The store of NE in sympathetic nerve terminals is heterogeneous, with both large (~100 nm diameter) and small (~50 nm diameter) vesicles. It is believed that both vesicle populations participate in the release of NE [48]. There are several main factors that regulate NE release including the calcium channels, presynaptic α_2-adrenergic receptors and adenosine A1 receptors.

Ca^{2+} channels. There are two types of Ca^{2+} channels, voltage-dependent calcium channel (VDCC) and ligand-gated Ca^{2+} channels [49]. VDCCs are localized in the active zone and serve as one of the important mechanisms for Ca^{2+} influx into the cells, enabling the regulation of intracellular concentration of free Ca^{2+} [50]. Neurotransmission from central and peripheral nerves depends on the influx of Ca^{2+} through VDCCs [51]. Around 50-100 μM of internal calcium concentration is required for the synaptic vesicles to fuse with the plasma membrane [52]. Vesicle fusion requires binding of Ca^{2+} with two proteins in the

vesicle membrane, synaptobrevin/VAMP and synaptotagmin, and two proteins in the synaptic membrane: soluble NSF attathed protein SNAP-25 and syntaxin (which is closely associated with the VDCC) [53, 54]. There are several types of VDCCs, including L-, N-, P/Q , R, and T types [55]. Among them, N- and P/Q type VDCCs play a more prominent role in neurotransmitter release.

In a sympathetic nerve varicosity, more than 98% of the small synaptic vesicles are not releasable because they are tethered by synapsins to actin filaments. To become releasable, a synaptic vesicle has to be mobilized from this reserve pool, docking near a VDCC at the active zone, underwent activation and then triggered by Ca^{2+} for the exocytosis. All steps are Ca^{2+} independent [56, 57]. There is possibility that the transmitter release depends on two different nerve terminal action potential-initiated Ca^{2+} signals: one extremely fast, local, triggering signal, and the other slow, diffuse, regulatory signal. Near Ca^{2+} channels at the active zones are opened by the nerve terminal action potential which leads to the transient rise of Ca^{2+} concentration >>100 μM. Ca^{2+} binds to low affinity receptors and then trigger exocytosis. After Ca^{2+} channels have closed diffusion, it leads to a rise in global Ca^{2+} and Ca^{2+} binds to high affinity receptors and increases the availability of releasable vesicles at active zones [53]. Changes in the distribution of VDCCs may contribute to the altered synaptic transmission in hypertension, however, few work has been done for that [58].

α_2-adrenergic receptor (α_2-AR). Some of the NE released from the nerve terminal binds to prejunctional α_2ARs. α_2ARs are autoreceptors that couple to $G_{i/o}$

proteins and they play an important role in regulating NE release through pertussis toxin sensitive negative feedback mechanisms [59, 60]. After activation by NE, α_2ARs decrease adenylate cyclase activity and cyclic adenosine 3",-5' monophosphate (cAMP) production, inhibit N- and P/Q-type Ca^{2+} channel function, and activate pre-synaptic K^+ channels to inhibit NE release [61]. There are 3 subtypes of α_2-ARs: α_{2A}, α_{2B}, and α_{2C}. Studies in mice revealed that both the α_{2A} and α_{2C} subtypes were required for normal presynaptic control of transmitter release from sympathetic nerves in the heart and from central noradrenergic neurons. The α_{2A} subtype inhibits transmitter release at high stimulation frequencies, whereas the α_{2C} subtype modulates neurotransmission at lower levels of nerve activity [62]. Some studies have shown that ATP release is also regulated by α_2AR in arteries and veins, however, this prejunctional regulation of ATP are less marked than NE [21, 32, 63].

Previous work has demonstrated that the release of NE from sympathetic nerves supplying MA is tightly regulated by presynaptic α_2ARs through negative feedback [35, 60]. Importantly, impaired presynaptic α_2AR function is associated with hypertension in animals [7, 23, 59, 64] and humans [65, 66]. However, it is controversial whether or not the function of α_2AR is impaired in DOCA-salt rats. Both impaired [23, 59] and unaltered [67] α_2AR autoreceptors in the isolated MA have been reported.

Adenosine A1 receptors. The adenosine A1 receptor is a member of the adenosine receptor group of $G_{i/o}$ protein coupled receptors with adenosine as the

endogenous ligand [68]. The presynaptic adenosine A1 receptor is an important autoreceptor that regulates ATP release [69, 70]. After released from the nerve terminal, a large portion of ATP is enzymatically degraded rapidly to ADP, AMP, and adenosine as the final product, which activates the presynaptic A1 receptors [60]. The A1 receptor is a $G_{i/o}$ protein-coupled receptor and inhibits neurotransmitter release by reducing Ca^{2+} influx to the nerve terminal [70]. Similar as presynaptic α_2AR, adenosine A1 receptor inhibit NE release by decreasing adenylate cyclase activity and cAMP concentration, activating presynaptic K^+ channels and inhibiting N- and P/Q-type Ca^{2+} channels [71].

The function of prejunctional adenosine A1 receptors in hypertension remains controversial. In a hypertension model in which rats are treated chronically with the A1 receptor antagonist 1,3-dipropyl-8-sulphophenylxanthine (DPSX), adenosine plays a regulatory role by inhibiting NE release and maintaining blood pressure via an action at prejunctional A_1 autoreceptors [72]. However, in the SHR (spontaneously hypertensive rat), the enhanced noradrenergic neurotransmission is not due to defective modulation of neurotransmission by adenosine [73]. The effects of adenosine on noradrenergic neurotransmission in DOCA-salt hypertensive rat have not been studied.

1.4.3 NE metabolism and clearance

The actions of NE are carried out via the binding to adrenergic receptors. In the mesenteric arteries and veins, NE acts primarily via α_1 adrenergic receptor (α_1AR) to cause blood vessel constriction by triggering the specific second

massager pathways. The binding of NE to receptor depends on the concentration of NE in the vicinity of the receptor. When the nerve stops releasing NE, the concentration of NE in the junction decreases and NE will leave the receptor. There are several mechanisms for NE to get cleared from the junction: 1) most of the NE (around 90%) is transported back to the presynaptic junction by the NE transporter (NET) for repackaging into the synaptic vesicles, 2) some of the NE diffuses into capillaries and is carried out of the tissue by the circulation, 3) some of the NE is metabolized by catechol-O-methytransferase (COMT) and monoamine oxidase (MAO) with vanillylmandelic acid (VMA) as the final product of these pathways (as shown in Fig. 1.4), 4) a small portion of NE (around 5%) is taken up by an extraneuronal uptake system and metabolized [74].

NET is a monoamine transporter that transports NE from the synapse back to its vesicles for storage until later use [75]. It is consisted by 617 amino acids and has 12 transmembrane domains. NET function is regulated by several neurotransmitters, peptides, psychostimulant drugs, ionic environment, nucleotides and various pathological conditions [76]. It can be blocked by cocaine and therefore cocaine increases junctional NE concentrations by blocking its reuptake and subsequent metabolism. The function of NET in hypertension is not clear yet. Reduced reuptake has been observed to explain the elevated NE in DOCA-salt hypertension and human essential hypertension [77, 78]. However, unaltered neuronal reuptake of NE in DOCA-salt hypertensive rats [79, 80] and enhanced NE neuronal uptake in chronic hypertension model and spontaneously hypertensive rats arteries [81, 82] have also been reported.

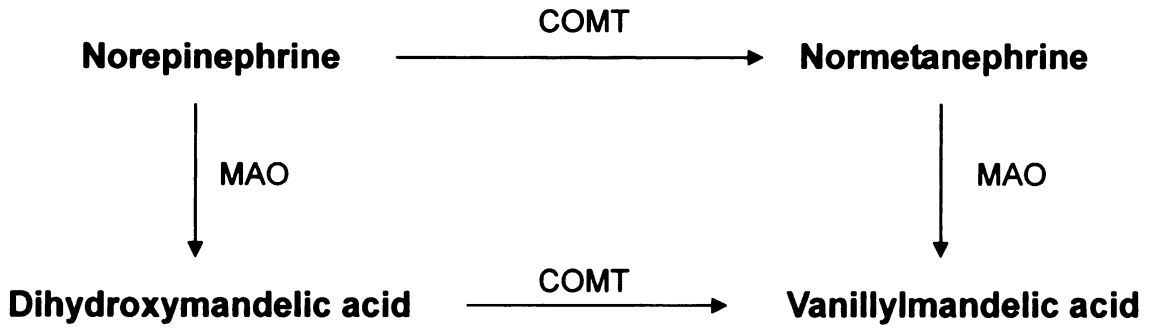

Figure 1.4 Metabolism of NE after release

1.5 Differential sympathetic innervations of mesenteric arteries *vs.* veins

The splanchnic region consists of liver, spleen, pancreas, small and large intestines. The splanchnic vascular bed holds around 33% of the total blood volume [83]. It is richly innervated by sympathetic nerves. Therefore, sympathetic control over the splanchnic vasculature may play an essential role in blood pressure regulation. Mesenteric arteries and veins are considered very important blood vessels in studies for the role of sympathetic nervous system in hypertension.

1.5.1 Artery and vein structure

Arteries are blood vessels that carry oxygenated blood away from the

heart. As shown in Figure 1.5, an artery has three layers: an outer adventitital layer, a muscular middle, and an inner layer of endothelial cells. The muscle in the middle is elastic and strong and the inner layer is very smooth. According to the size and function, arteries are divided into several types, the aorta, arteries, arterioles and capillaries. The arteries deliver the oxygen-rich blood to the capillaries where the exchange of oxygen and carbon dioxide occurs. The capillaries then deliver the carbon dioxide and waste-rich blood to the veins for transport back to the lungs and heart. Small arteries and arterioles are the main resistance blood vessels involved in blood pressure regulation. These small arteries are highly innervated by sympathetic nerves and respond to changes in nerve activity by constriction or dilation. Arteries are resistance vessels and their diameter changes lead to changes in total peripheral resistance and therefore, blood pressure.

Veins are blood vessels that carry blood toward the heart. As shown in Figure 1.5, a vein has a bigger lumen, and a thinner and less elastic smooth muscle layer compared to the artery. According to their size and function, there are several types of veins: superficial veins, deep veins, pulmonary veins, systemic veins, and venules. Veins are referred to as capacitance vessels and they contain 70% of the blood volume and 75% of which is in small veins and venules [84]. Constrictions mediated by sympathetic nervous system of veins can redistribute some of the stored blood from peripheral veins to the heart and then into the arterial circulation and therefore lead to the cardiac output increase [85].

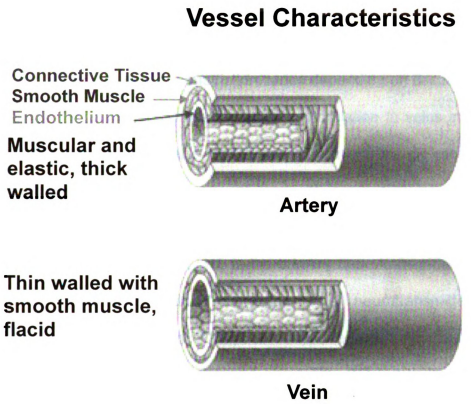

Figure 1.5 The structure of artery and vein

[http://www.colorado.edu/intphys/Class/IPHY3430-200/013bloodpressure.htm]

1.5.2 Sympathetic innervation of arteries and veins

Sympathetic nerves are the most important regulator of vasoconstriction, especially in the splanchnic circulation. Sympathetic nerve stimulation can reduce intestinal blood volume by up to 60% [86]. The sympathetic nerves projecting to the splanchnic bed originate from prevertebral and paravertebral ganglia. The sympathetic neurons innervating arteries and veins are differentially

located in the ganglia and they show different physiological properties [87, 88]. Veins are more sensitive to the nerve stimulation and vasoconstrictors in both physiological [89] and pathological conditions [34]. The relative contribution of ATP and NE to neurogenic constriction varies depending on tissue type, age and disease state of animal. Sympathetic nerve stimulation to veins induces a slow contraction, primarily mediated by NE acting at α_1 adrenergic receptors in rats. On the other hand, in small arteries from rat, nerve stimulation evokes short latency, fast contraction mediated mainly by ATP acting at P2X receptors [90] . While in guinea pig and dog, NE is the primary neurotransmitter in mesenteric arteries [47] and NE and ATP are the major neurotransmitters supplying mesenteric veins [31]. In DOCA-salt hypertension, NE is the primary neurotransmitter in both arteries and veins [34, 91], while in SHR model of essential hypertension, the sympathetic tone to veins is elevated [92]. This evidence supports the idea that there are fundamental differences in the sympathetic neural control of arteries and veins.

1.5.3 Venous function in hypertension.

Arteries have been studied extensively due to their important role in the blood pressure regulation. The role of veins in the development of hypertension could also important. Small veins and venules in the splanchinic region store the great majority of blood in the circulation and exhibit high active venoconstriction. Sympathetic venoconstrictor activity is the most important determinant of venomotor tone in splanchnic veins and the entire circulation [93]. The increase

of sympathetic nervous system activity could reduce vascular capacitance, which can cause venous return to transiently exceed cardiac output, thereby increasing central compartment blood volume and affects arterial blood pressure. Increased vascular resistance and reduced venous capacitance in the splanchnic circulation is found in established human and animal hypertension [94, 95]. The decreased venous capacitance in hypertension may be due to increased sympathetically mediated venoconstriction [96, 97]. This may be due to increased sympathetic activity [98], increased efficiency of neurotransmission [96] or both. It is possible that decreased venous capacitance, particularly in the splanchnic circulation, precedes and contributes to human [99] and experimental hypertension development [96].

1.6 Oxidative stress and hypertension

Oxidative stress results from an imbalance in the pro-oxidant-antioxidant equilibrium in favor of the prooxidants, which can lead to potential oxidative damage [100]. A number of diseases are associated with oxidative stress, such as atherosclerosis, Parkinson's disease, heart failure, and Alzheimer's disease. Reactive oxygen species (ROS) are ions or small molecules that include oxygen ions, free radicals, and peroxides. The major ROS resulting from oxidative stress are superoxide anion ($\cdot O_2^-$), hydrogen peroxide (H_2O_2), hydroxyl radical ($OH\cdot$) and peroxynitrite ($ONOO\cdot$). As shown in Figure 6, there are several pathways for endogenous oxidant and antioxidant. $\cdot O_2^-$ production is mediated by several enzymes, such as nicotinamide adenine dinucleotide phosphate (NADPH)

oxidase and xanthine oxidase [101]. $\cdot O_2^-$ is very reactive and can be converted to H_2O_2 either spontaneously or via superoxide dismutase (SOD). H_2O_2 is then converted to H_2O by and O_2 by catalase or to $OH\cdot$ by the further oxidation by transition metals: Fe and Cu [102].

Under physiological conditions, ROS are produced in a controlled manner at low concentration and act as signaling molecules regulating the growth and function of vascular smooth muscle cells [103]. Under pathological conditions, increased ROS production leads to endothelial dysfunction, increased contractility, and elevated sympathetic nervous system activity that all contribute to vascular damage in cardiovascular diseases [104, 105]. Compelling evidence supports the idea that an enhanced production of ROS and a decrease in the antioxidant reserve in plasma and tissue contributes to hypertension in DOCA-salt rats, the SHR [106], Dahl salt-sensitive rats [107], and angiotensin II hypertension in rats [108]. ROS are also elevated in patients with salt-sensitive hypertension and renovascular hypertension [109]. ROS play an important role in the development of hypertension, which is largely due to $\cdot O_2^-$ excess and decreased NO bioavailability in the vasculature and kidneys, and the ROS mediated cardiovascular remodeling.

A major source of $\cdot O_2^-$ is NADPH oxidase. $\cdot O_2^-$ and NADPH oxidase activity are elevated in the aorta of DOCA-salt rats, and in the aorta and cultured vascular smooth muscle cell of SHRs [106]. In addition to the increased level of NADPH oxidase, SOD activity was reduced in DOCA-salt rats which also leads to increased levels of $\cdot O_2^-$ [106]. Inhibition of ROS generation with the NADPH

oxidase inhibitor, apocynin, and radical scavenging with antioxidants or SOD mimetics decrease blood pressure and prevent development of hypertension in most hypertension models [110-112]. For example, the SOD mimetic, tempol (4-hydroxy-2,2,6,6-tetramethylpiperidinyloxy), lowers renal sympathetic nerve activity, heart rate, and mean arterial blood pressue in DOCA-salt hypertensive rats [113]. However, there is debate about whether or not tempol functions through a NO dependent manner to inhibit NE release from sympathetic nerves [105, 114]. There have been no studies focused on antioxidant treatment and NE release from the sympathetic nerve endings in DOCA-salt hypertensive rats.

There are also other mechanisms through which ROS can be produced as described earlier. These mechanisms contribute to the development of hypertension, as well. ROS have been shown to function mainly through oxidative modification of proteins, especially $G_{i/o}$ proteins, and activation of transcription factors that maintain vascular function and structure [115, 116]. ROS can be measured by the lucigenin assay [117], dihydroethidium staining [118], and cyanide-resistant oxygen consumption [119], *etc.* The role of ROS under pathological conditions can also be accessed pharmacologically using acute and chronic antioxidant treatments, such as apocynin, tempol and N-acetyl-cysteine [120].

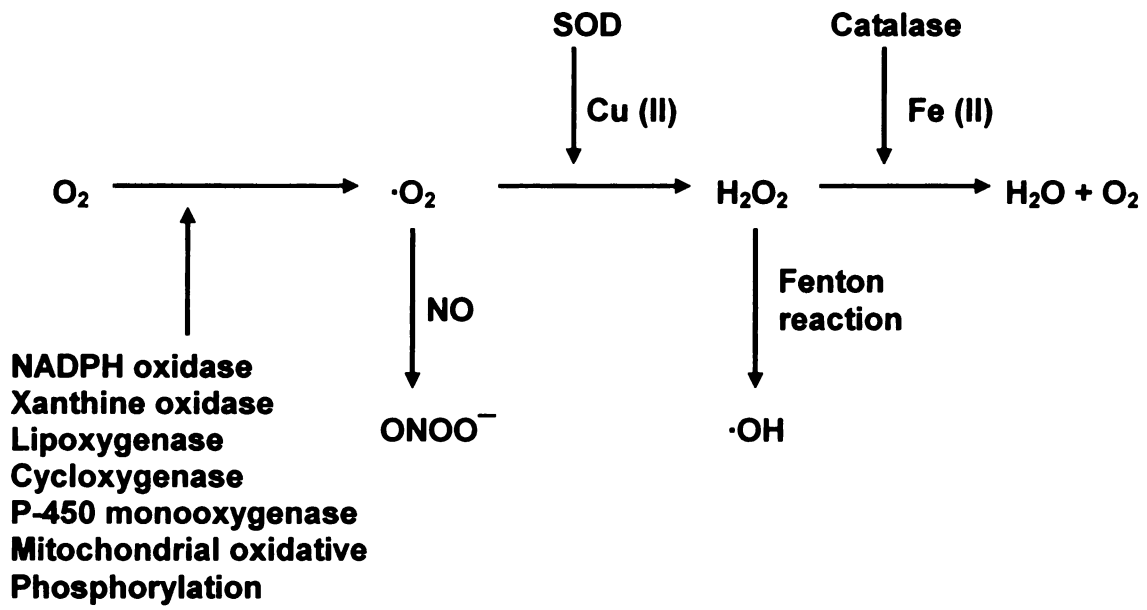

Figure 1.6 Endogenous oxidant and antioxidant pathways

1.7 The DOCA-salt hypertension animal model

There are several hypertensive animal models of primary and secondary hypertension. Rats are by far the most popular species in hypertension research, including SHR, Dahl-salt sensitive, Deoxycorticosterone (DOCA) -salt, two-kidney one-clip, and transgenic TGR (mRen2) 27 hypertensive models [121]. SHR is the most often used rat model, although it reflects only a rare subtype of human hypertension, such as, primary hypertension that is inherited in a Mendelian fashion.

The DOCA-salt hypertensive model is used to investigate the aspects of salt-sensitive human hypertension. Deoxycorticosterone is a steroid hormone that has mineralocorticoid activity and acts as a precursor to aldosterone. The administration of DOCA, in combination with a high salt diet and unilateral

nephrectomy induces a low rennin form of hypertension [122]. Specifically, administration of the mineralocorticoid affects Na^+/H^+ exchange and increases the rate of Na^+ reabsorption by kidney. High Na^+ increases water retention and leads to increased blood volume and blood pressure. The DOCA-salt hypertensive model is the only model in which rennin-angiotensin inhibition does not decrease blood pressure, nor end-organ function. Studies have shown that the periventricular areas of the hypothalamus in brain and the central sympathetic and baroreceptor systems are crucial for the development of hypertension in DOCA–salt ased sympathetic activity, elevated plasma NE content, altered neural angiotensin II function, and altered baroreflex responses have been found in DOCA-salt hypertension [77, 79, 123].

1.8 Approaches to measure NE release

NE overflow in the blood supply of tissues is an measure of sympathetic nerve activity in both physiological and pathological conditions. The release of NE has been widely studied in the heart, kidney and mesentery. There are several widely used methods to detect NE from these tissues, including mechanical bioassay, HPLC overflow technique and amperometry.

1.8.1 Mechanical bioassay

The pharmacologically isolated noradrenergic component of nerve stimulation induced smooth muscle contraction is often used to assess the release of NE. Specifically, the tissue can be stimulated either by nerve

stimulation or drugs to release NE. NE binds with postjunctional adrenergic receptors to induce contraction. Contraction amplitude is related to the amount of NE released from sympathetic nerve fibers. However, this technique can not exclude the contribution of other neurotransmitters, such as ATP, to the smooth muscle contraction. Furthermore, the measured contraction, which is a function of NE concentration at the receptors, is often poorly correlated with the per pulse release of NE and it is insensitive to subthreshold and saturating concentrations of released NE. The resolution of this method is poor and can not measure NE release from individual sites [124].

1.8.2 HPLC overflow technique

The nerve stimulation induced overflow of endogenous NE sampled either by collecting the perfusate or microdialysis can be detected by HPLC coupled with various detectors, such as electrochemistry, fluorescence, UV-Vis, *etc.* This technique is widely used to detect overflow of NE and ATP and their metabolites [125, 126]. However, this technique measures NE released offset by clearance. It reveals the average release of NE from multiple release sites at the nerve ending, but not release from individual sites, thus it provides little information about real time local release of NE from sympathetic nerves. The temporal resolution is poor and the kinetics of NE release can not be reflected.

1.8.3 Amperometry

Focal amperometric recording developed for dopamine measurement in

the brain has been successfully applied to NE release in mesenteric artery and rat tail artery [127, 128]. The nerve stimulation induced NE oxidation current can be recorded either by differential pulse amperometry or continuous amperometry. After release, the juncitonal concentration of NE decreases with time due to reuptake by the NET, extracellular metabolism and diffusion away. The diffusional fraction is what is detected electrochemically. Therefore, the oxidation current amplitude is proportional to the NE concentration in the vicinity of the releasing sites. It is by far the best technique to study nerve- released NE. Although this technique also measures NE released minus clearance and the metabolites of NE, its high sensitivity allows measurement of NE in real time and determine the time course of local release and clearance mechanisms. Details will be described later.

1.9 Electrochemical detection of NE *in vitro* using microelectrodes

Pioneered by Gonon and coworkers in 1984, electrochemical method with a microelectrode was applied to detect dopamine released in the brain [129]. Since then, this technique has been widely used to study neurotransmitter release kinetics *in vitro* and *in vivo* [127, 130-134]. Neurotransmitter can be detected by continuous amperometry, differential pulse amperometry and fast scan cyclic voltammetry. At a potential of 1V, NE can be detected by electrochemical method, as co-transmitters ATP and NPY are non-electroactive. NE can be detected as an oxidation current based on the following 2 electron / 2

proton redox reaction:

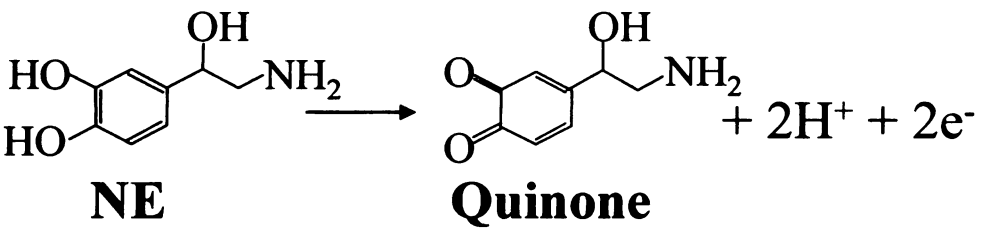

Figure 1.7 NE redox reaction

In continuous amperometric detection, the potential of the working electrode is adjusted to a value on the plateau of the voltammetirc curve (mass transfer-limited region). The current that flows between the recording and counter electrodes is measured and its amplitude is related to the diffusive overflow of NE from multiple neuroeffector junctions in the vicinity of the recording electrode. Since the potential is held at a certain value, the background current is low and therefore, the excellent temporal resolution and high sensitivity provided by amperometry allows measurement in real time to be made. This technique has been successfully applied to the measurement of neurotransmitter from tissues and single cells, such as adrenal chromaffin cells [131, 135]. The limit of detection of this technique can be as low as attomole and zeptomole for the neurotransmitter measurement from single synaptic vesicle [136].

In differential pulse amperometry, a fixed potential is held at the working electrode for most of the time, except for voltage pulses which are applied at regular intervals. The current flow is monitored prior to, and during the pulse. The current flow measured immediately prior to the pulse is subtracted from the current measured during the pulse. The advantage of this technique is it can

remove "baseline drift". [137, 138].

In fast scan cyclic voltammetry, a gradually increasing or decreasing potential is applied at the working electrode with a high scan rate (> 100 V/s). When the maximum or minimum desired potential is reached, the direction of the sweep is reversed. The current flow is measured during increases and decreases in electrode potential. The occurrence of a signal peak at a particular potential gives an indication of the type of substance present. At a high scan rate, a relatively large background current is seen and smaller faradaic current can only be detected by background subtraction. This technique has been applied to measurements of dopamine, NE, serotonin, and ascorbic acid especially in the central nervous system [134]. The advantage of this technique is that different compounds can be distinguished by the position of the peak in the voltammogram.

Most of the work to date using these methods with microelectrodes has focused on neurotransmitter release and clearance in the central nervous and peripheral nervous systems. There are several types of microelectrode, including spherical shape, disk shape, cylindrical shape, and band shape of microelectrode. Among them, disk and cylindrical shape of microelectrodes are the most widely used types in the *in vitro* and *in vivo* neurotransmitter detection. All types of microelectrode have a small tip dimension (less than 30 μm diameter) to allow measurement within a limited space, such as a single cell. Its small size provides a spatial resolution of 10-100 μm. The background current of microelectrode is much lower compared to the normal size microelectrode which

can enhance the signal to noise ratio (S/N) and thus the sensitivity of the detection. However, due to their small size, the faradaic current is also small and therefore, the requirement for instruments with low noise is higher. Since electrode capacitance is proportional to the area, the low capacitance of microelectrode allows the applied potential to be changed rapidly and this is extremely useful in the fast scan cyclic voltammetry. An important property of the microelectrode is that its diffusion layer is larger than its size, so that the current detected is under the steady state region, which is beneficial to the sensitivity of the detection.

1.10 Diamond and carbon fiber microelectrodes

A variety of materials can be used to fabricate microelectrodes. Nobel metal electrodes (eg., platinum electrode) have been used; however, they are not stable in biological environment [138]. Carbon fiber is the material that is often employed. Carbon fiber is a material consisting of extremely thin fibers about 0.005–0.010 mm in diameter and composed mostly of carbon atoms. The atomic structure of carbon fiber is similar to that of graphite, consisting of sheets of carbon atoms arranged in a regular hexagonal pattern, however, carbon fiber may be turbostratic or graphitic, or have a hybrid structure with both graphitic and turbostratic parts present. Carbon fibers derived from Polyacrylonitrile (PAN) are turbostratic, whereas carbon fibers derived from mesophase pitch are graphitic after heat treatment [139].

As shown in Figure 1.8, this kind of electrode material possesses a sp^2-

bonded carbon microstructure with an oxygenated surface, such as, carboxyl and hydroxyl functional groups [140]. Carbon fibers are resistance to drift when exposed to biological tissue and are attractive for *in vivo* measurement due to their small size and good conductivity. However, it is easy to get biomolecule adsorption due to the presence of the π electron system and carbon-oxygen functional groups. It is the oxidation/reduction reaction of the oxygenated functional groups that give rise to the background faradaic features in the voltammetry. The shifting of voltammetric background features of carbon fiber microelectrode with variation in pH leads to changes in background-subtracted voltammetric responses [141]. For *in vivo* experiments, the electrode's response to the hydronium ion is a particular concern because its voltammetric response occurs over a broad range of potentials that overlap those of the catecholamines. Simultaneous changes of the catecholamine concentration and pH occur in biological tissue as a result of coupling respiration and energy production to pH [142].

To remove surface oxide effects, a variety of surface pretreatments, such as chemical derivation, heat treatment and washes by organic solution have been developed. However, these pretreatments for carbon fiber are accompanied by a loss in signal amplitude for some electroactive neurotransmitters such as dopamine and NE [143]. Moreover, such surfaces absorb oxygen again over time and the pH dependence eventually returns and incorporates oxygen with time. Coating the carbon fiber with a ion-selective polymer, nafion, minimizes the fouling effect but results in decreased sensitivity and response time of the

electrode [144].

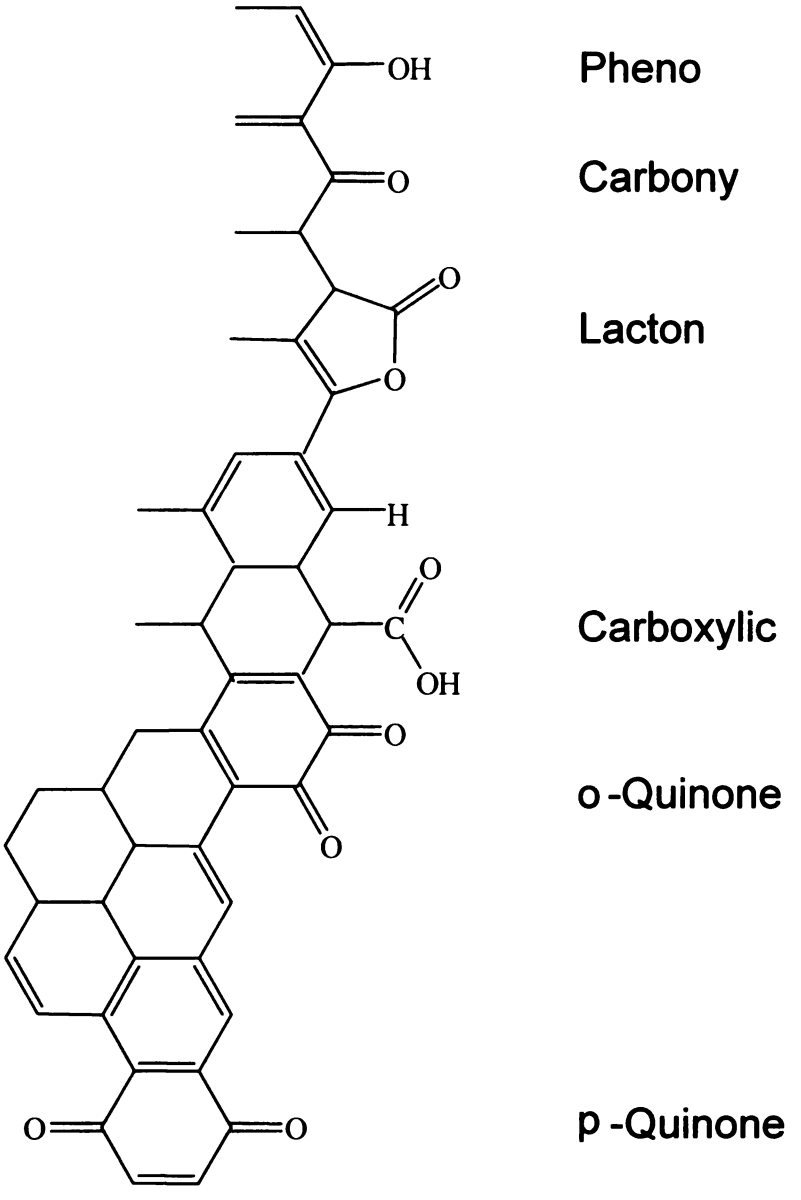

Figure 1.8. Representative functional groups that exist on oxidized sp^2 carbon surfaces

Given the above described issues with sp^2 carbon materials, it would be good to have an electrode that has no hassle with the pretreatment to remove the surface carbon-oxygen functional groups but is still responsive to the

analytes of interest. An oxygen-free boron-doped diamond electrode has the potential to be very useful for the *in vitro* and *in vivo* measurement of neurotransmitters. As shown in Figure 1.9, this kind of material consists of sp^3-bonded carbon atoms in a tetrahedral arrangement with hydrogen terminated surface. Its surface is hydrophobic, non-polar and chemically stable, low in surface oxygen (< 0.02 atomic %) and reacts slowly with the environment (O_2 /H_2O). Diamond has important properties like extreme hardness, high thermal conductivity, high chemical inertness, corrosion resistance and low compressibility. Diamond can be applied in several areas, such as electronics, thermal management, and optics [145]. Another very important application is for electrochemistry.

The first diamond electrode was developed in the mid 1980s [146]. Diamond naturally is a very good electrical insulator, however, it can be converted to possess semimetal electronic properties by controlled doping with impurities, such as boron. Boron is by far the widely used dopant since it has small covalent radius, which lead to easy incorporated into substitutional sites within the diamond without causing lattice distortion. Boron atom can substitute the carbon atom during the thin-film diamond growth [147]. It serves as an electron acceptor and promotes p-type semiconductivity with acceptor activation energy of 0.37 eV above the valence band. Valence band electrons are promoted to the boron acceptors thermally, and therefore leave free electrons in the dopant band and holes in the valence band to support current flow. Electrical conductivity of the electrode depends on the boron doping level, the grain

boundaries at the surface and the sp^2 carbon impurity [148].

Comparing with oxygen-containing sp^2 carbon electrodes, the hydrogen-terminated boron doped diamond electrode exhibits weak adsorption by polar molecules presumably because of the relative absence of polar carbon-oxygen functional groups which promote strong dipole-dipole and ion-dipole interactions with the adsorbate [148]. Therefore, diamond electrodes exhibit low background current without the redox-active surface carbon oxygen functional groups and this leads to improved signal to noise ratio (S/N). Boron doped diamond electrode also possess other outstanding properties, such as, a wide working potential window, pH independent background response, low limit of detection and improved response precision and stability [149]. These properties make boron doped diamond electrode a good choice when making measurements with complex samples. It has been demonstrated that diamond microelectrode is more stable when exposed to tissue for longer duration and the response attenuation is much smaller. Thus, boron doped diamond electrodes have a very wide application in the biological electrochemical study [150, 151].

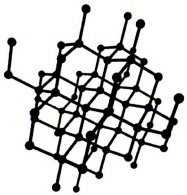

Figure 1.9 Structure for diamond sp^3 carbon

1.11 Temperature as a tool to probe the SNS differences in arteries and veins

Temperature variation has been used to probe molecular mechanisms controlling transmitter release and clearance in the central and peripheral nervous systems. In their classic studies, Katz and Miledi used data from temperature-dependence studies to propose that calcium entry during the falling phase of an action potential in the motor nerve terminal initiated a multi-step process that culminated in acetylcholine release at the neuromuscular junction [152]. Temperature has large effects on enzyme kinetics, plasma membrane state and synaptic transmission. As neurotransmitter release is a multi-step process, it is not surprising that synaptic transmission would be markedly altered by even small temperature changes. For example, small changes in temperature can alter synaptic vesicle movements and can change the dynamics of vesicle release responsible for synaptic plasticity in the central nervous system [153-155]. These studies showed treatments that increase synaptic efficacy reduce the temperature sensitivity of synaptic transmission. Increased synaptic efficacy is associated with an increased vesicle number and/or an increase in the content of synaptic vesicles that are replenished after release or an increase in the probability of release of the content of individual synaptic vesicles. It has been shown that re-uptake of NE is reduced by moderate cooling in rat mesenteric arteries [156].

There are also some studies focused on the effect of temperature on the smooth muscle response to exogenous and endogenous NE [22-28]. For

example, the effect of decreasing temperature on vascular smooth muscle responses to adrenergic agonists and neural activation has been shown. In 1968, Webb-Peploe and Shepherd [126, 157] reported that the vasoconstrictor response to local cooling in dog cutaneous veins was dependent on an intact sympathetic nervous system and was potentiated by a change in vascular responsiveness to incoming neural impulses. With regard to the deep vessels, it has been reported that cooling depressed the vasoconstrictor responses to exogenous NE in the canine femoral veins, while it increased the responses to electrical stimulation in canine mesenteric veins [158]. However, as for arteries, it is reported that, there is an increase in potency of NE at lower temperature from rabbit mesenteric artery [159] and decrease of NE from rat mesenteric artery [156]. For both of them there is no change in efficacy as measured by the maximum smooth muscle contractile response during cooling. Thus, temperature sensitivity would be a useful tool to probe physiological differences in either the mechanisms controlling release and clearance of NE from periarterial and perivenous nerves, or for the mechanisms regulating smooth muscle contraction.

However, almost no studies have been done related to temperature effects in DOCA-salt hypertensive rats. As discussed before, we can hypothesize that there are differences of NE release and blood vessel contractility between normotensive and hypertensive rats, and also between artery and vein. And temperature can be used as a tool to study these differences.

1.12 Research objective and specific aims

The sympathetic nervous system (SNS) plays an essential role in blood pressure regulation and its activity is increased in hypertension. As circulating levels of NE are related to SNS activity, studying the mechanisms of NE release from sympathetic nerves can improve our understanding of the causes of hypertension. Despite the prevailing focus on arteries, the role played by systemic veins in the development of certain types of hypertension is also important. The proposed study will focus on the DOCA-salt model of hypertension in rats. DOCA-salt hypertension is also associated with increased oxidative stress in the mesenteric vascular bed and this may contribute to alterations in sympathetic nervous system function in hypertension. At the vascular neuroeffector junction, prejunctional autoreceptor and NE transporter regulate NE overflow. Alterations in the function of proteins which regulate neurotransmitter release, such as the α_2AR, would impair the negative feedback pathway which controls NE release.

My research objective herein for this comprehensive study includes characterizing changes in the adrenergic component of NE neurotransmission at the neuroeffctor junction of mesenteric arteries and veins in DOCA-salt hypertension using chronoamperometry with microelectrodes. **I hypothesize that there are artery-vein differences in NE release and clearance mechanisms and these mechanisms are altered in DOCA-salt hypertensive rats associated with increased reactive oxygen species.** Since NE release is a multi-step process, one way to test the hypothesis is to study the release and

clearance temperature-dependent difference. The proposed work will address the hypothesis in the context of three specific aims:

Specific Aim 1: Study the differences of NE release and clearance mechanisms between normotensive mesenteric arteries and veins.

1a. The NE current released from mesenteric arteries and veins will be measured as a function of temperature. **1b.** The function of prejuntional autoreceptor α_2AR will be tested to verify if this accounts for the artery-vein differences in temperature sensitivity of NE transmission. **1c.** NE transporter function will be tested for the temperature dependent artery-vein NE transmission differences.

Specific Aim 2: Study how the mechanisms that regulate NE release and clearance have been altered in DOCA-salt hypertensive rats.

2a. Test the hypothesis that α_2 AR function is impaired in DOCA-salt rats and the impaired α_2AR function is related with the NE temperature dependent release and clearance differences between normotensive and hypertensive arteries and veins. **2b.** Test the hypothesis that NET function is impaired in arteries and veins of DOCA-salt rats and that NET activity contributes to artery-vein differences in temperature sensitivity of NE signaling in tissues from sham and DOCA-salt rats.

Specific Aim 3: Test the hypothesis that the impaired function of adrenergic neurotransmission is related with the increased oxidative stress in DOCA-salt hypertensive rats.

3a. Effects of chronic antioxidant treatments (apocynin and tempol) on NE release will be assessed by NE oxidation current measurement. **3b.** Effects of chronic antioxidant treatments on α_2AR function will be accessed. **3c.** The function of G protein which couples to α_2AR will be tested in normotensive and DOCA-salt hypertensive rats.

CHAPTER 2

EXPERIMENTAL SECTION

2.1 Boron doped diamond film growth

Boron-doped diamond films were grown on sharpened Pt wires (99.99%, Aldrich Chemical, 76 μm diam) by microwave-assisted chemical vapor deposition (CVD) [160-162]. Before growth, the etched wires were ultrasonically cleaned (5–10 min) in acetone and ultrasonically seeded (30 min) in a diamond powder suspension (5 nm particles, *ca.* 20 mg in 100 mL of ethanol, Tomei Diamond Co., Tokyo, Japan). The pretreated Pt wires were mounted horizontally on the top of a quartz plate (10×10×1 mm) in the center of the reactor. Boron-doped diamond films were deposited from a 0.5% CH_4/H_2 (v/v) source gas mixture with 4 ppm of diborane (0.1% B_2H_6 diluted in H_2) added. All source gases were ultrahigh purity grade (99.999%). During film growth, the system pressure was 45 Torr, the substrate temperature was approximately 750 °C (estimated by an optical pyrometer), the microwave power was 400 W, and the total gas flow was 200 standard cubic centimeters per minute (sccm). The deposition period was 10 h. Under the above conditions, the nominal growth rate was estimated to be on the order of 0.3 μm/h as the final film thickness was 3–5 μm. After the deposition, the diameter of the cylindrical portion of the exposed electrode was *ca.* 80 μm [151].

2.2 Diamond film characterization

The boron-doped diamond electrode surface microstructure and morphology were characterized by scanning electron microscopy (SEM) and Raman spectroscopy.

2.2.1 SEM

SEM was used to check the surface morphology and the dimensions of the electrode. It was performed with a JEOL 6400V electron microscope equipped with LaB6 emitter (Tokyo, Japan). The electrodes were attached to a specimen stub by using silver conductive epoxy. As shown in Figure 2.1 (left), a Pt wire was completely coated with a layer of polycrystalline boron-doped diamond without noticable cracks or exposure of Pt. A higher magnification image shown in Figure 2.1(right) demonstrates that the polycrystalline diamond consists of well faceted crystallites with a diameter from 0.5 to 3 μm.

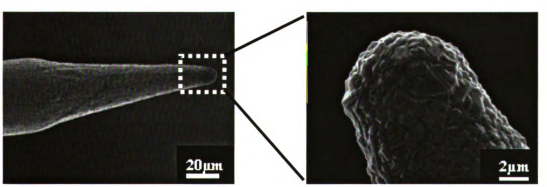

Figure 2.1 SEM image of a Pt wire coated with a polycrystalline boron-doped diamond film (left) and an expanded view of the microelectrode tip (right)

2.2.2 Raman spectroscopy

Raman spectroscopy was used to probe the film microstructure. Raman spectra were obtained using Raman 2000 instrument (Chromex, Albuquerque, NM), equipped with a 50-mW Nd:YAG laser (532 nm line). The laser beam was focused to a spot size of approximately 25 μm resulting in an estimated power density of *ca.* 150 kW/cm^2. Spectra were collected using a 10-s integration time. The spectrometer was calibrated using a single crystal diamond standard (100 orientation, Harris Diamond). Figure 2.2 shows a Raman spectrum for diamond thin film deposited on a Pt wire. An intense one-phonon diamond line is seen at 1332 cm^{-1} originating from the sp^3-bonded carbon structure [163-165]. There is minimal scattering intensity observed between 1500 and 1600 cm^{-1}, which arises from amorphous nondiamond carbon (i.e., sp^2 bonded carbon) impurity [151, 164, 166].

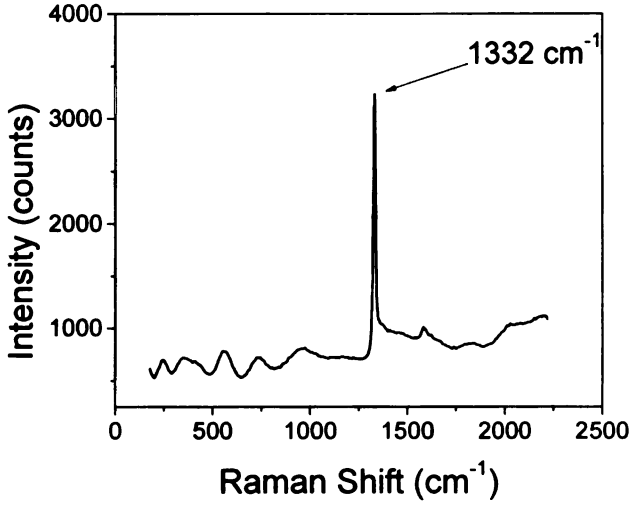

Figure 2.2 Raman spectrum for a diamond thin film deposited on a Pt wire. λ_{ex} = 532 nm. Laser power = 30 mW. Integration time = 10 s.

2.3 Microelectrode preparation

2.3.1. Preparation of the boron doped diamond microelectrode

The diamond-coated wire was attached to a copper wire with conductive silver epoxy. As shown in Figure 2.3, electrodes were then insulated with polypropylene [127]. Polypropylene is non-toxic to tissue and chemically resistant to the isopropyl alcohol (IPA) used to clean the microelectrodes before use. The resulting microelectrode was conically-shaped with an exposed length of *ca.* 500 μm and a tip diameter of *ca.* 10 μm [151]. The microelectrode diameter and length were be determined from SEM images. These dimensions were used to calculate the electrode area. The geometric area of the conically-shaped boron-doped diamond microelectrode was calculated using the following equation:

$$A = A_{cone} + A_{cylinder} = \pi r^2(H^2 + L)^{1/2} + 2\pi rh$$

where A is the electrode area (cm^2), r is the cone base radius (cm), L is the electrode length (cm), H is the ratio of the height of the cone and the radius of the cone base.

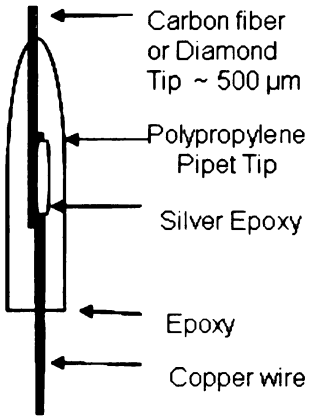

Figure 2.3 Diagram of the diamond and carbon fiber microelectrodes.

2.3.1. Preparation of carbon fiber microelectrode

A heat-treated (3000°C) pitch-base type (Textron Speciality) carbon fiber with a diameter of *ca.* 35 μm was inserted into a pipet tip and the tapered end was heated using the coil of the micropipette puller (Model P-30, Sutter Instrument, Novato, CA, USA). This softened the polypropylene and made a conformal layer around the carbon fiber. The portion of the carbon fiber in contact with the copper wire, and silver conductive epoxy CW2400 (Chemtronics, Kennesaw, GA), was insulated with the polypropylene. The carbon fiber tip was cut to a *ca.* 500 μm length with a scalpel under a microscope. The resulting cylindrical microelectrode was disk-shaped [166]. The microelectrode diameter and length were determined from scanning electron microscopy (SEM) images. These dimensions were used to calculate the electrode's area. The geometric area of the cylinder carbon fiber microelectrode was calculated by

$$A = A_{cylinder} + A_{disk} = 2\pi rL + \pi r^2$$

where A is the electrode area (cm^2), r is the electrode radius (cm) and L is the electrode length (cm).

2.4 Electrochemical measurement

Cyclic voltammetry was used to determine the exposed area of the electrode, to check the cracks and defects in the diamond layer, and to provide information on the kinetics of heterogeneous electron-transfer reactions. The physical, chemical and electronic properties of an electrode all influence the electrode reaction kinetics and mechanisms for the redox system. All voltammograms were

obtained using a CHI 650 potentiostat (CHI system, Inc.). A three electrodes system consisting of diamond or carbon fiber as a working electrode, carbon rod as a counter electrode and a home-made Ag/AgCl was used as a reference electrode. Solutions were deoxygenated with nitrogen for 15 min before a measurement.

Potassium ferrocyanide, $K_4Fe(CN)_6$ is a good redox system to check the electrode's response because the apparent heterogeneous electron transfer rate constant depends on surface cleanness, response sensitivity and stability due to it's inner-sphere redox mechanism [165]. Figure 2.4 shows the cyclic voltammetric i-E curves of a diamond (left) and carbon fiber (right) microelectrode in 1mM $K_4Fe(CN)_6$ in 1M KCl solution. Scan rate is 50 mV/s. In cyclic voltammetry, mass transport of the redox active molecule generally occurs solely by diffusion. Steady state current are observed in the i-E curves for both diamond and carbon fiber microelectrode. The $E_{1/2}$ value for diamond is about 292 mV *vs.* Ag/AgCl, which is 20 mV more positive than that for carbon fiber microelectrode. This reflects the slow electron transfer kinetics for diamond electrode [167]. These voltammograms indicate that the electrodes surfaces are clean, no blemish or crack and the response of diamond toward $K_4Fe(CN)_6$ redox system is similar to that for carbon fiber.

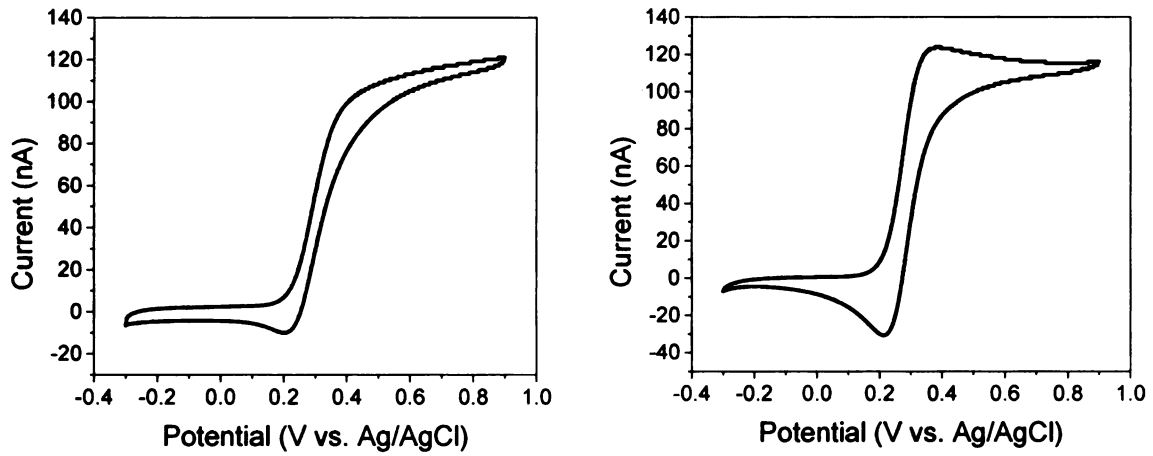

Figure 2.4 Cyclic voltammetric i-E curves for a diamond (left) and carbon fiber (right) microelectrode in 1.0 mM $K_4Fe(CN)_6$ in 1 M KCl. Scan rate is 50 mV/s.

Exposed electrode area can also be determined from the measured mass transport-limiting current. For the quasi-steady-state current, it holds that for the carbon fiber microelectrode, the limiting current is given by

$$i_{qss}^{cylinder} = \frac{2nFADC}{r \ln \tau}$$

Where $$\tau = \frac{4Dt}{r^2}$$

For diamond electrode, it has a mixed cylinder and cone geometry. Thus the limiting current for diamond electrode is given by

$$i_{\lim} = i_{qss}^{cylinder} + i_{ss}^{cone}$$

And the conical term is given by

$$i_{ss}^{cone} = 4nFDCr(1 + qH^p)$$

In the above equations, n is the number of electrons transferred per equivalent, F is the Faraday constant, which is 96485 C/mol, A is the electrode area (cm^2), D is the diffusion coefficient of the analyte (cm^2/s), C is the bulk concentration of the analyte (mol/cm^3), r is the cylinder or cone radius (cm), q = 0.30661, p =1.14466, and H is the aspect ratio h/r where h is height of the cone (cm). The measurement period, t (s), is the time of the forward voltammetric scan. The surface area of a cone is related to its aspect ratio according to the equation $A= \pi r^2(H + 1)^{1/2}$ [151] .

2.5 Drug effects on NE detection

For the drug effect studies with diamond and carbon fiber microelectrode work described in Chapter 3, the following experimental protocol was followed.

Cyclic voltammetric measurements were made using P-55 (r = 10 μm) and T-650 (r = 8 μm) carbon fiber (Amoco, Greenville, SC), and boron-doped diamond microelectrodes (r ≈ 40 μm). All measurements were made in a conventional, single-compartment glass cell using solutions purged for 10 min with N_2. A computer-controlled potentiostat (CHI-650, CH Instruments, Inc., Austin, TX) was used in a three-electrode configuration to control the working electrode potential and to measure the current flow through the cell. A home-made Ag/AgCl electrode (saturated KCl) was used as the reference and a large area carbon rod served as the auxiliary electrode. The potential of the reference was routinely checked against a standard SCE reference electrode in saturated KCl ($E_{Ag/AgCl}$ = -45 mV vs. SCE). A potential scan rate of 0.1 V/s was used in all

the measurements and the potential range scanned was from -0.5 to 1.2 V.

For each new microelectrode, a cyclic voltammetric *i-E* in a Krebs' buffer solution (pH 7.4) was first recorded followed by measurements in a Krebs' buffer solution containing NE (0.020 mM). Following these control measurements, the electrochemical response for the drug (0.10 mM) in Krebs' buffer was investigated. Finally, after drug wash out with the buffer, cyclic voltammetric *i-E* curves in Krebs' buffer and cyclic voltammetric *i-E* curves for NE were re-recorded. At least three measurements were made for each drug using a new microelectrode for each.

2.6 Normotensive and DOCA-salt hypertensive rats

All animal experiments were performed in accordance with the "Guide for the Care and Usage of Laboratory Animals" (National Research Council). All animal procedures were approved by the Institutional Animal Care and Use Committee at Michigan State University. Adult male Sprague Dawley rats (250-300g; Charles River Laboratories, Inc., Portage, MI) were uninephrectomized and subcutaneous implanted of DOCA (200 mg kg^{-1}) pellet under isoflurane anesthesia. Post-operatively, the rats were given drinking water containing 1% NaCl and 0.2% KCl. Normotensive controls (sham) to the hypertensive rats were uninephrectomized but no DOCA pellet was implanted and these rats were maintained on normal drinking water. Animals were housed two per cage with access to food and water while being kept on a 12:12 h light-dark cycle in a room with regulated temperature (22-24°C). Blood pressure was monitored by tail cuff

plethesmography and rats with systolic blood pressure ≥150 mmHg were considered hypertensive [8].

2.7 Chronic antioxidant treatment of DOCA-salt hypertensive rats

For the chronic antioxidant treatment work for DOCA-salt hypertension described in Chapter 6, adult male Sprague Dawley rats (250-300g) were uninephrectomized and implanted with radiotelemetry transmitters in their femoral arteries as previous described [168]. An opening was cut in left thigh area. A pocket was made by separating the skin and muscle in the abdomen region. The radiotelemetry transmitter's body was placed subcutaneously in the abdomen area. The tubing of the transmitter was pulled to the left thigh and the tip of the tubing was inserted into the abdominal artery through left femoral artery. Every animal was placed in an individual cage above a heating pad for recovery then was transferred to the telemetry animal room.

Rats were fed with either NaCl (control) alone or NaCl with either 2mM apocynin (apocynin group) or 1mM tempol (tempol group). After a 5 days recovery, transmitters were turned on for recording. The signals from transmitters were monitored by radiotelemetry receivers (RPC-1, Data Sciences International) which were connected to a data exchange matrix. Systolic blood pressure, diastolic blood pressue, and mean arterial pressure were recorded every 10 minutes for two control days. Animals were then implanted with a DOCA-salt pellet, and recordings were continued for the next 24 days. Data acquisition and

analysis were performed by custom software Dataquest ART 4.0 (Data Sciences International).

2.8 *In vitro* electrochemical measurement

For the work described in Chapters 4 to 6, continuous amperometry with diamond or carbon fiber microelectrodes combined with drug treatments of tissues in vitro were used for the measurement of nerve stimulation induced endogenous NE release from sympathetic nerve endings at mesenteric arteries and veins from normotensive and DOCA-salt hypertensive rats. The whole setup of the experiment is demonstrated in Figure 2.5.

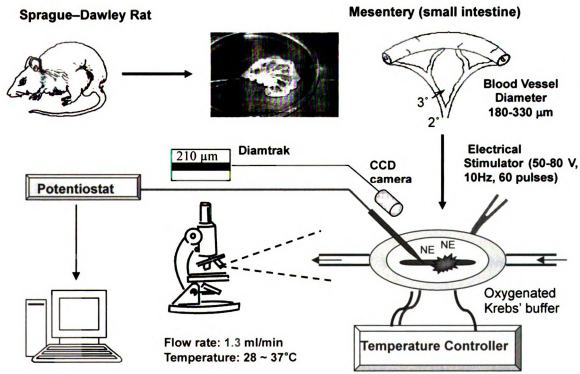

Figure 2.5 Diagram of the experimental set up for *in vitro* NE release from sympathetic nerve endings

2.8.1 Preparation of mesenteric arteries and veins

The sham and DOCA-salt rats were anesthetized with a lethal pentobarbital injection (i.p., 50 mg). The entire mesenteric arcade was removed from the rat and placed in an oxygenated (95% O_2, 5% CO_2) Krebs' buffer solution of the following composition (millimolar): 117 NaCl; 4.7 KCl; 2.5 $CaCl_2$; 1.2 $MgCl_2$; 25 $NaHCO_3$; 1.2 NaH_2PO_4, and 11 glucose. Secondary or tertiary MA and MV (150-320 μm) were separated from the surrounding connective tissue, isolated from the intestine, stretched gently and pinned to the bottom of a small silicone elastomer-lined chamber. The chamber was part of a single channel temperature-controller system (Biosciences Tools, CA, USA), which regulated the perfusate temperature. The chamber was mounted on the stage of an inverted microscope (Olympus CK 2, USA) and superfused with Krebs' solution (37 °C) at a flow rate of 1.5 ml/min. The flow rate was controlled by a peristaltic pump (Masterflex, Cole Parmer, USA). Tissues were perfused with Krebs' buffer at 37 °C for 30 minutes before use.

2.8.2 Focal stimulation of perivascular nerves

Electrical stimulation of perivascular sympathetic nerves was accomplished using a focal stimulating electrode composed of two parallel silver chloride-coated wires, shielded with a glass capillary. The wires were connected to a Grass Instruments stimulator (S88 Quincy, MA, USA). The stimulating electrode was positioned on the blood vessel using a micromanipulator. Nerves were stimulated using 60 stimuli at 10 Hz (stimulus duration, 0.5 ms; voltage, 50-80V).

2.8.3 Measurements of NE oxidation currents

The diamond or carbon fiber microelectrodes were immersed in distilled isopropyl alcohol (IPA) prior to use for at least 15 min in order to clean the electrode surface [169]. The microelectrode was affixed to a micromanipulator (MP-1, Narishige Instruments, Japan) for reproducible positioning along the blood vessel surface. As shown in Figure 2.6, the exposed microelectrode was positioned against the side of a MA or MV so that the NE flux from nearby neuroeffector junctions reached the entire surface. Such positioning also allowed the microelectrode to move in concert with the blood vessel when it contracted and relaxed, so as to maintain a constant electrode-vessel distance. The microelectrode and the tissue were placed in the center of the chamber. A platinum wire served as the counter electrode and a commercial 'no leak' Ag/AgCl electrode (3 M KCl, Cypress Systems Inc, USA) was used as the reference. Electrochemical measurement of NE was made using an Omni 90 analog potentiostat (Cypress Systems Inc., USA). Continuous amperometric i-t curves were recorded at a detection potential of 700 mV. At this potential, NE is oxidized at a mass-transfer limited rate. An analog-to-digital converter (MiniDigi, Axon Instruments, USA) and Axoscope software were used to collect the NE signal from the analog potentiostat. The analog voltage output from the potentiostat was low pass filtered at the time constant of 200 ms (5 Hz) before being digitized using and A/D converter at a sampling rate of 500 Hz. The data were then stored on the computer hard drive for subsequent analysis.

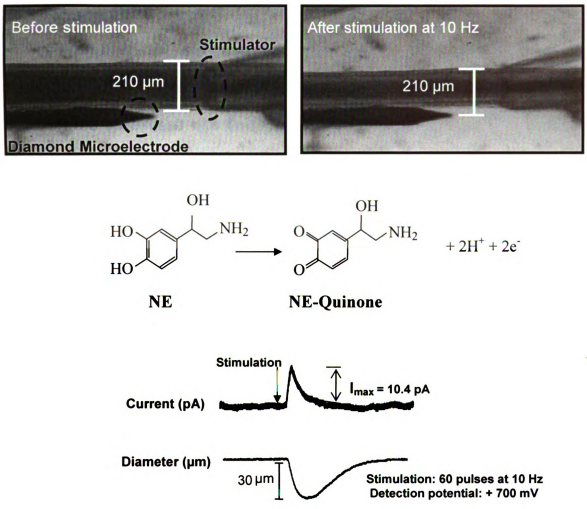

Figure 2.6 Video images of a mesenteric artery showing positions of the diamond microelectrode, the stimulator (top left) and the change in artery diameter in response to stimulation (top right). Temporal responses of the NE overflow oxidation current (bottom red trace) and vessel diameter (bottom blue trace) elicited by electrical stimulation.

2.8.4 Temperature Control

A TC-1 temperature controller (Biosciences Tools, CA, USA) was used to regulate the perfusate temperature in the chamber with a precision of 0.2 °C. Tissues were superfused with Krebs' solution and equilibrated for 20 minutes at 37 °C. Then nerves were stimulated to evoke NE release at 37 °C. The temperature was then progressively decreased from 37 to 28 °C (3 °C decrements). At each temperature, NE oxidation currents were measured in the absence and presence of drugs. Tissues were allowed to equilibrate at each temperature for 10 min before making an electrochemical measurement.

2.9 Chemical and drug application

The Opti-MEM I Reduced Serum Medium was obtained from Invitrogen company (California, USA). All other chemicals and drugs were obtained from Sigma-Aldrich Chemical company (St Louis, MO, USA). They were at least reagent grade quality and used without additional purification. Ultrapure water (distilled, deionized, and filtered over activated carbon, 17-18 MΩ, Barnstead E-Pure System) was used for solution preparation and cleaning. Agonists and antagonists were added to the superfusing Krebs' buffer for at least 20 minutes before making an electrochemical measurement.

2.10 Data analysis

Analysis of NE i-t curves was performed using Clampfit 9.0, which is a part of the pCLAMP 9.0 software package (Molecular Devices). Data are reported as mean ± S.E.M. with n values referring to the number of rats used for each study.

For comparisons of the NE peak current, 10-90% NE current rise slope, rise time, and decay slope between MA and MV or between sham and DOCA-salt, statistical significance were assessed by the Student's t-test. While the values were compared using student paired t-test for the comparison before and after drug treatment for the same type of tissue. The parameters of NE current obtained at different frequencies were analyzed using a one-way ANOVA with Newman-Keuls post hoc test or Student t-test for paired or unpaired data, as appropriate. Blood pressure was analyzed with a two-way ANOVA and followed by Newman-Keuls post hoc test at certain days. $P < 0.05$ was considered as statistically significant.

CHAPTER 3

Drug Effects on the Electrochemical Detection of NE with Carbon Fiber and Diamond Microelectrodes

3.1 Introduction

Electroanalytical methods with carbon fiber microelectrodes have been utilized for several decades now to measure electroactive neurotransmitters *in vitro* and *in vivo*; molecules such as dopamine (DA), norepinephrine (NE) and serotonin (5-HT) [134, 141, 170-173]. Two methods are routinely employed: continuous amperometry (CA) and fast-scan cyclic voltammetry (FSCV). In both methods, the electroactive neurotransmitter is measured as an oxidation or reduction current with a magnitude that is proportional to the time-dependent flux to the electrode. The flux depends on the balance between the rate of release and the rate of any clearance mechanisms (*e.g.*, reuptake) that might be operative. CA provides excellent sensitivity and temporal resolution but lacks qualitative information about the analyte being detected. In other words, at the constant detection potential employed, all electroactive species present at the electrode surface contribute to the current. In addition to good sensitivity and temporal resolution, FSCV also provides qualitative information about the analyte being detected based on differences in the oxidation or reduction potentials [141].

In recent years, these methods have been utilized to monitor neurotransmitters in the peripheral nervous system, specifically, NE released from sympathetic nerves innervating rat tail and mesenteric arteries [127, 128,

137, 174]. Sympathetic nerves project to the smooth muscle cells those makeup blood vessels. Neuroeffector junctions are formed where these nerve endings connect with the muscle cells and communication across these junctions is accomplished by three neurotransmitters: adenosine 5'-triphosphate (ATP), NE and neuropeptide Y (NPY). These neurotransmitters are stored in and released from sympathetic nerves via Ca^{+2}-dependent exocytosis. Our group has been using *in vitro* CA with a diamond microelectrode to study sympathetic neural control mechanisms of arteries and veins [127, 166]. When using electrochemical methods to investigate neurotransmission, drugs are often employed to probe mechanisms of release and clearance, post-junctional responses, and to confirm that the current measured is associated with a particular signaling molecule. For example, in studies of sympathetic neuroeffector transmission, yohimbine is often used. This drug is an α_2 adrenergic autoreceptor antagonist. α_2 autoreceptors are present at sympathetic nerve endings and function to mediate neurotransmitter release via negative feedback [23]. In CA measurements, NE oxidation currents will increase when this functional autoreceptor is blocked [91, 127, 131, 150, 166, 175].

When using drugs, it is necessary to verify that (i) the agent is not electrochemically active in the potential region where the neurotransmitter is detected and (ii) the drug does not attenuate the electrode response for the neurotransmitter by rapid molecular adsorption and electrode fouling. It has been reported in studies of dopaminergic neurotransmission that some drugs can decrease the carbon fiber sensitivity for dopamine (DA) *in vitro* [176, 177].

Although few in number, previous studies have described the influence of some drugs on the carbon fiber microelectrode response [133, 171].

We report herein on an investigation of the electroactivity of several commonly used sympathetic neuroeffector agonists and antagonists at carbon fiber and diamond microelectrodes. We also report how drug exposure affects the electrode sensitivity for NE oxidation. The microelectrode response was assessed using slow scan cyclic voltammetry and seven drugs were studied (Table 3.1): prazosin, an α_1 adrenergic receptor antagonist; yohimbine, an α_2 adrenergic receptor antagonist ; idazoxan, an α_2 adrenergic receptor antagonist; UK 14,304, an α_2 adrenergic agonist; cocaine, a norepinephrine transporter blocker; PPADS, a P_2X-purinoceptor antagonist; and capsaicin, a TRPV-1 receptor agonist [34, 91, 127, 178]. Along with the diamond microelectrodes, two types of carbon fiber were investigated: a more microstructurally-ordered pitch-base fiber (Thornel P-55) and a more microstructurally-disordered PAN-based fiber (Thornel T-650). Slow-scan rather than fast-scan cyclic voltammetry was used in these studies because the time scale of the measurements more closely mimics those for CA, and the technique readily provides information about half-wave potentials and oxidation currents.

Table 3.1. Drug Molecular Structure and Function

Redox System	Function	Structure
NE	Neurotransmitter in sympathetic nervous system	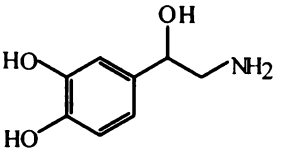
Capsaicin	Agonist for TRPV 1 channel	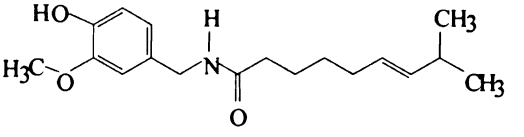
Cocaine	Antagonist for NE transporter	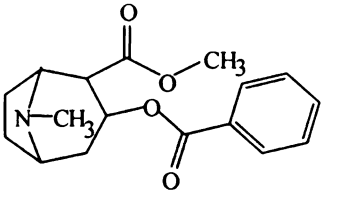
Idazoxan	Antagonist for alpha-2 autoreceptor	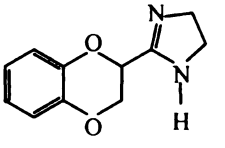
PPADS	Antagonist for P2X purinergic receptor	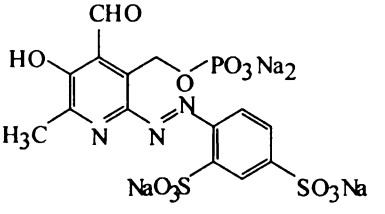
Prazosin	Antagonist for alpha-1 receptor	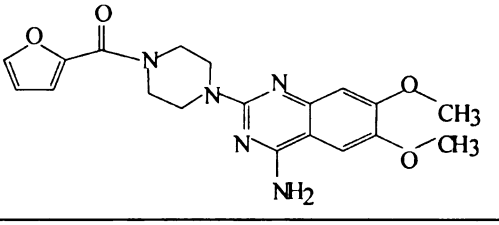

Table 3.1. Drug Molecular Structure and Function (continued)

UK 14,304	Agonist for alpha-2 autoreceptor	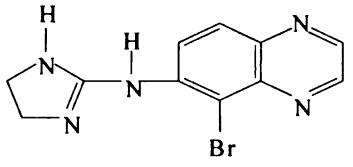
Yohimbine	Antagonist for alpha-2 autoreceptor	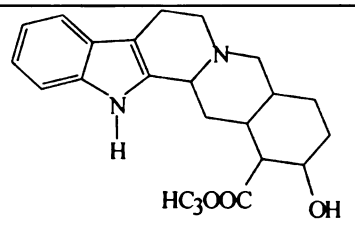

3.2 Results

3.2.1 Norepinephrine Oxidation Current

Well-defined cyclic voltammetric *i-E* curves were observed for NE in Krebs' buffer at all three microelectrode types (100 mV/s). Steady-state or near steady-state curves were observed with $E_{1/2}$ values of 213 ± 4 mV for the P-55 carbon fiber, 174 ± 7 mV for the T-650 carbon fiber, and 370 ± 10 mV for the diamond microelectrode. The least positive $E_{1/2}$ was seen for the more microstructurally-disordered carbon fiber with a more positive value observed for the more ordered fiber. Raman spectroscopic I_D (1350 cm^{-1})/I_G (1580 cm^{-1}) band intensity ratios confirmed the degree of microstructural order. The results indicate that the greater the fraction of exposed edge plane at the sp^2 carbon electrodes, the faster the electrode reaction kinetics are for this molecule [162, 179-181]. The $E_{1/2}$ for diamond was *ca.* 200 mV more positive than the values for the carbon

fibers. This is because the NE oxidation reaction kinetics are generally more sluggish at diamond. We suppose the sluggish kinetics are due to weak adsorption on the H-terminated, sp^3-bonded carbon surface [150]. Unlike the carbon fibers, the diamond microelectrode (as prepared) possesses few carbon-oxygen functionalities and no extended π-electron system. Dipole-dipole, ion-dipole and π-π interactions between polar molecules and the hydrogen-terminated diamond surface are either very weak or non-existent.

3.2.2 Electrochemical Activity of the Drugs at Carbon Fiber and Diamond Microelectrodes

Figure 3.1 shows cyclic voltammetric *i-E* curves for 0.1 mM concentrations of each drug in Krebs' buffer (100 mV/s). Data are presented for P-55 (Fig 3.1A and B) and T-650 (Fig 3.1C and D) carbon fiber, and diamond (Fig 3.1E and F) microelectrodes. Background voltammetric *i-E* curves in the absence of the drugs are also presented, for comparison. For the P-55 carbon fiber, quantifiable oxidation currents are apparent for yohimbine, prazosin and UK 14,304. The nominal $E_{1/2}$ or $E_{p/2}$ values were 779 ± 12, 848 ± 10 and 969 ± 6 mV, respectively. The peak or pseudo-limiting currents increased in the following order: yohimbine < UK 14,304 < prazosin. The current variations are due either to a different number of electrons transferred for each molecule and or to an electrochemically-active area that is distinct for each. A low oxidation current is seen for capsaicin with a nominal $E_{1/2}$ of 639 ± 16. Identical responses are seen for idazoxan and cocaine with both exhibiting no electrochemical activity below

900 mV. Above this potential though, there is anodic current associated with oxidation of the drug. PPADS had no electrochemical activity at this electrode over the entire potential range probed.

Quantifiable oxidation currents are also seen for yohimbine, prazosin and UK 14,304 at the T-650 fiber. The nominal $E_{1/2}$ values were 772 ± 12, 870 ± 17 and 953 ± 9 mV, respectively. The peak or pseudo-limiting oxidation currents increase in the following order: yohimbine < prazosin < UK 14,304. This is different from the order with the P-55 fiber. There is again a small oxidation current for capsaicin starting at ca. 700 mV. As was the case for the P-55 fiber, cocaine and idazoxan have no electrochemical activity below 900 mV. Above this potential, there is net oxidation current for both. PPADS exhibited no electrochemical activity over the entire potential range probed.

For the diamond microelectrode, well-defined oxidation currents are apparent for yohimbine, UK 14,304 and prazosin with nominal $E_{1/2}$ values of 713 ± 13, 827 ± 2 and 952 ± 4 mV, respectively. The peak or limiting oxidation currents increase in the following order: yohimbine < UK 14,304 < prazosin. A noteworthy difference for diamond, as compared to the carbon fibers, is the presence of two oxidation peaks for yohimbine and prazosin. This could be due to a different reaction mechanism at diamond or to the same reaction occurring at two distinctly-different sites on the electrode. Oxidation current is seen for capsaicin albeit at a significantly lower magnitude than for the other three drugs. The nominal $E_{1/2}$ was 624 ± 21 mV. Similar responses are seen for cocaine and idazoxan with both exhibiting no electrochemical activity below 1000 mV. Above this potential, there

is some net oxidation current. PPADS exhibited no electrochemical activity over the entire potential range probed.

3.2.3 Effect of Capsaicin and Prazosin Exposure on Norepinephrine Detection

Figure 3.2 shows cyclic voltammetric *i-E* curves for 0.020 mM NE, 0.020 mM NE + 0.10 mM capsaicin or prazosin, and 0.020 mM NE after drug washout for the P-55 (Fig 3.2A and B), T-650 (Fig 3.2C and D) and diamond (Fig 3.2E and F) microelectrodes. In all cases, the drug concentration was 5x greater than the NE concentration. Comparison of Figure 3.2A and B reveals that exposure to capsaicin caused no change in either the $E_{1/2}$ or the limiting oxidation current for NE at the more microstructurally-ordered carbon fiber. Figure 3.3A and B summarize the change in half-wave potential, $\Delta E_{1/2}$, and limiting current ratio, I_{ratio}, for all three electrodes brought about by drug exposure. Capsaicin exposure caused little change in the electrode response for NE. In the presence of the drug, however, the NE oxidation current was totally suppressed (Fig 3.2A). This means that an *in vitro* measurement of NE with this carbon fiber would be complicated in the presence of this drug. Prazosin exposure produced no change in $\Delta E_{1/2}$ (10.8 $\pm$ 6.9 mV) but the limiting current was reduced as I_{ratio} was 0.68 $\pm$ 0.12* (Fig 3.3A and B). In the presence of this drug, the NE oxidation current was nearly abolished. This means that NE monitoring in the presence of this drug would be problematic with this carbon fiber.

Figure 3.1. Cyclic voltammetric *i-E* curves for drugs at carbon fiber (P55, T650) and diamond microelectrodes: (A) capsaicin, prazosin, UK 14,304 and yohimbine, and (B) idazoxan, PPADS and cocaine at the P55 carbon fiber; (C) capsaicin, prazosin, UK 14,304 and yohimbine and (D) idazoxan, PPADS and cocaine at the T650 carbon fiber; and (E) capsaicin, prazosin, UK 14,304 and yohimbine and (F) idazoxan, PPADS and cocaine at the diamond microelectrode. All curves were acquired in Krebs solution at a scan rate of 0.1 V/s. The concentration of each drug was 0.1 mM.

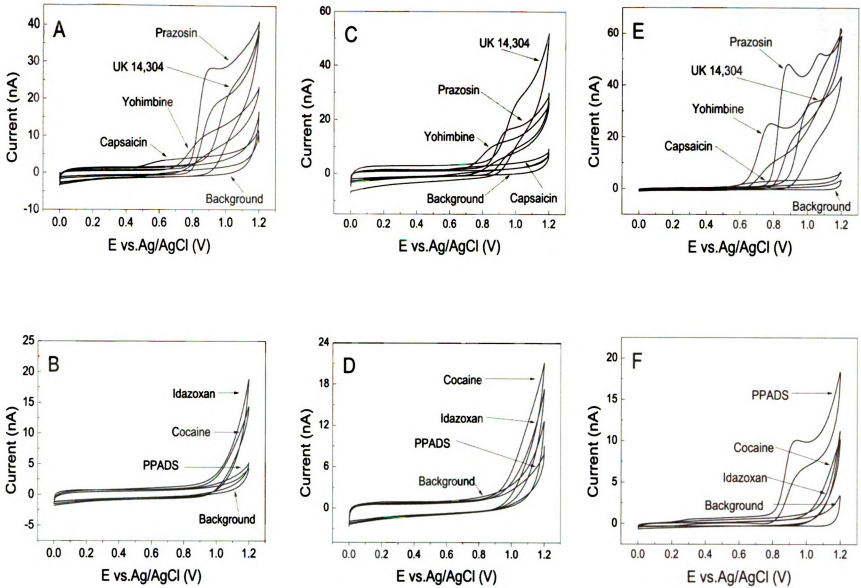
A
Prazosin
UK 14,304
Yohimbine
Capsaicin
Background
Current (nA)
E vs.Ag/AgCl (V)
C
UK 14,304
Prazosin
Yohimbine
Background
Capsaicin
Current (nA)
E vs.Ag/AgCl (V)
E
Prazosin
UK 14,304
Yohimbine
Capsaicin
Background
Current (nA)
E vs.Ag/AgCl (V)
B
Idazoxan
Cocaine
PPADS
Background
Current (nA)
E vs.Ag/AgCl (V)
D
Cocaine
Idazoxan
PPADS
Background
Current (nA)
E vs.Ag/AgCl (V)
F
PPADS
Cocaine
Idazoxan
Background
Current (nA)
E vs.Ag/AgCl (V)

Figure 3.2. Cyclic voltammetric *i-E* curves for NE at (A and B) P55 and (C and D) T650 carbon fiber and (E and F) diamond microelectrodes with and without capsaicin and prazosin. All curves were acquired in Krebs solution at a scan rate of 0.1 V/s. The concentration of NE was 0.02 mM and the concentration of each drug was 0.1 mM.

A
NE
NE after Capsaicin
NE with Capsaicin
Capsaicin
Current (nA)
E vs.Ag/AgCl (V)
B
Prazosin
NE with Prazosin
NE
NE after Prazosin
Current (nA)
E vs.Ag/AgCl (V)
C
NE with Capsaicin
NE after Capsaicin
NE
Capsaicin
Current (nA)
E vs.Ag/AgCl (V)
D
NE with Prazosin
NE after Prazosin
NE
Prazosin
Current (nA)
E vs.Ag/AgCl (V)
E
NE
NE after Capsaicin
NE with Capsaicin
Capsaicin
Current (nA)
E vs.Ag/AgCl (V)
F
NE with Prazosin
Prazosin
NE after Prazosin
NE
Current (nA)
E vs.Ag/AgCl (V)

The same general trends were observed for the T-650 carbon fiber (Fig 3.2C and D). Exposure to capsaicin had only a minor effect on the electrode response for NE. The electrode response was not significantly affected by drug exposure in terms of $E_{1/2}$ ($\Delta E_{1/2}$= -11.3 ± 2.7) but there was minor attenuation of the limiting current (I_{ratio}= 0.86 ± 0.02*) (Fig 3.3A and B). In the presence of the drug though there was attenuation of the NE oxidation current but not total suppression as was the case for the P-55 fiber. $E_{1/2}$ shifted by *ca.* 32 mV and I_{ratio} decreased by 25%. Exposure to prazosin had a negligible effect on the NE voltammetric response ($\Delta E_{1/2}$ = 4.3 ± 1.2 and I_{ratio} = 0.88 ± 0.08) (Fig 3.3A and B). In the presence of the drug, the NE voltammetric response was significantly attenuated as $E_{1/2}$ shifted positive by 45 mV and the limiting current decreased by 86%. A well-defined prazosin oxidation peak is evident at *ca.* 900 mV with no difference in the current magnitude in the presence or absence of NE. This means that only the drug is being oxidized at these positive potentials, and not NE.

For the diamond microelectrode, a well-defined voltammetric response is seen for NE before and after exposure to capsaicin (Fig 3.2E). There was little change in either $E_{1/2}$ or the limiting oxidation current after drug exposure and washout ($\Delta E_{1/2}$ = 14.0 ± 11.1 and I_{ratio} = 0.94 ± 0.03) (see Fig 3.3A and B). In the presence of capsaicin, the $E_{1/2}$ for NE oxidation shifted positive by some 200 mV but the limiting current remained unchanged. This is different from the near total suppression seen for the P-55 carbon fiber. A well-defined voltammogram was observed for NE prior to exposure to prazosin (Fig 3.2F). After drug exposure

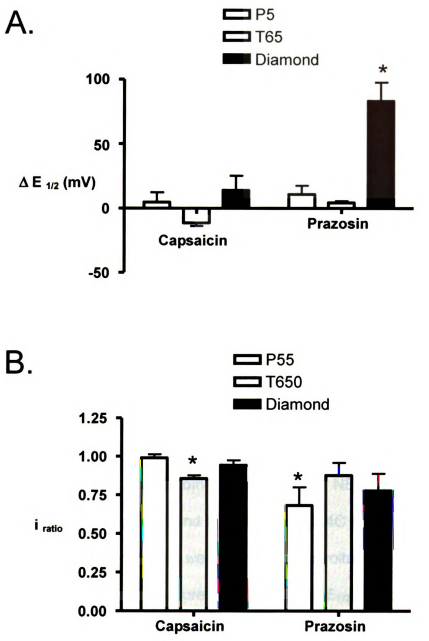

Figure 3.3. Plots of the cyclic voltammetric $\Delta E_{1/2}$ and limiting current ratio, I_{ratio} ($=I_{after\ drug}/I_{initial}$), after drug exposure (capsaicin and prazosin) and washout at the three microelectrode types. Statistical analysis was based on n = 3. *Represents a significantly different value from the control (before drug exposure) as assessed using the standard t-test, $P<0.05$.

and washout, there was a significant positive shift in $E_{1/2}$ and a slight attenuation in the limiting current. $\Delta E_{1/2}$ increased by 83.2 ± 14.3* and I_{ratio} decreased to 0.78 ± 0.11* (Fig 3.3A and B). In the presence of the drug, the NE oxidation current was quite suppressed A low and slowly increasing oxidation current is seen for NE between 400 and 800 mV (Fig 3.2F). The oxidation peak potential for the drug was unaffected by the presence of NE but the oxidation peak current was larger indicating that both the drug and NE undergo oxidation at these potentials. Clearly, a measurement of NE would be complicated in the presence of prazosin using this microelectrode.

3.2.4 Effect of Exposure to UK 14,304 and Yohimbine on Norepinephrine Detection

Figure 3.4 shows cyclic voltammetric *i-E* curves for 0.020 mM NE, 0.020 mM NE + 0.10 mM UK 14,304 or yohimbine, and 0.020 mM NE after drug exposure and washout using P-55 (Fig 3.4A and B), T-650 (Fig 3.4C and D) and diamond (Fig 3.4E and F) microelectrodes. A well-defined cyclic voltammogram was observed for NE before UK 14,304 exposure (Fig 3.4A). The $E_{1/2}$, *ca.* 200 mV, and limiting current, *ca.* 5 nA, were not significantly altered by drug exposure. For example, $\Delta E_{1/2}$ and I_{ratio} were -5.1 ± 11.4 mV and 0.89 ± 0.10, respectively (Fig 3.5A and B). In the presence of UK 14,304, the NE voltammetric response was quite suppressed though as $E_{1/2}$ shifted positive by 140 mV and the limiting current was reduced by 50%. As is seen in Fig 3.4A, a slowly increasing NE oxidation current was recorded between 300 and 900 mV in the presence of the drug, at

which point drug oxidation commenced. The oxidation current for UK 14,304 in the presence of NE was identical in position and magnitude to the current response in the presence of just the drug. This indicates that only UK 14,304 is being oxidized at these potentials and not NE. After exposure to yohimbine (Fig 3.4B), the $E_{1/2}$ for NE oxidation was unchanged ($\Delta E_{1/2}$ = 4.3 ± 12.2 mV) but the limiting current was significantly reduced (I_{ratio} = 0.85 ± 0.03*) (Fig 3.5A and B). As was the case for UK 14,304, the NE oxidation current was suppressed in the presence of yohimbine. For example, $E_{1/2}$ shifted positive by over 140 mV and the limiting current decreased by ca. 50%. A broadly increasing oxidation current was observed for NE in the presence of the drug, as was the case for UK 14,304. No steady-state limiting current was reached over this potential range and the current was significantly less than the control. The oxidation peak potential for yohimbine was unchanged but the current magnitude increased in the presence of NE indicating that both the drug and NE are oxidized at these potentials. Using this carbon fiber, measurements of NE in the presence of these two drugs would be complicated because of response attenuation.

A well-defined cyclic voltammogram was seen for NE using the T-650 carbon fiber before exposure to UK 14,304 (Fig 3.4C). After exposure of the T-650 carbon fiber to UK 14,304, the $E_{1/2}$, *ca.* 180 mV and limiting current, *ca.* 10 nA, were unchanged. For example, the nominal $\Delta E_{1/2}$ value was actually shifted negative by -14.7 ± 0.3* mV (easier to oxidize NE!) but I_{ratio} remained statistically unchanged at 0.94 ± 0.11 (Fig 3.5A and B). In the presence of UK 14,304, the oxidation current for NE was largely unaffected. The $E_{1/2}$ was shifted slightly

Figure 3.4. Cyclic voltammetric *i-E* curves for NE at (A and B) P55 and (C and D) T650 carbon fiber and (E and F) diamond microelectrodes with and without UK 14,304 and yohimbine. All curves were acquired in Krebs solution at scan rate of 0.1 V/s. The concentration of NE was 0.02 mM and the concentration of each drug was 0.1 mM.

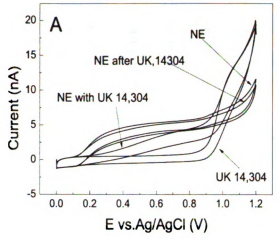
A
NE
NE after UK,14304
NE with UK 14,304
UK 14,304
Current (nA)
E vs.Ag/AgCl (V)

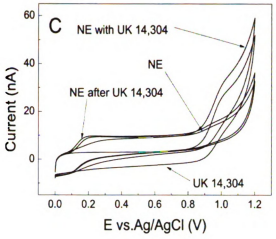
C
NE with UK 14,304
NE
NE after UK 14,304
UK 14,304
Current (nA)
E vs.Ag/AgCl (V)

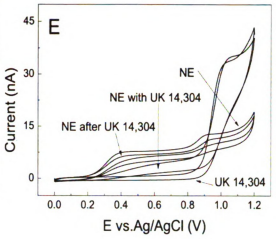
E
NE
NE with UK 14,304
NE after UK 14,304
UK 14,304
Current (nA)
E vs.Ag/AgCl (V)

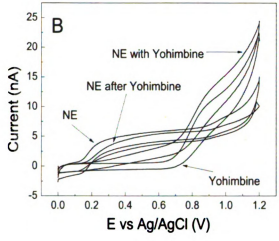
B
NE with Yohimbine
NE after Yohimbine
NE
Yohimbine
Current (nA)
E vs Ag/AgCl (V)

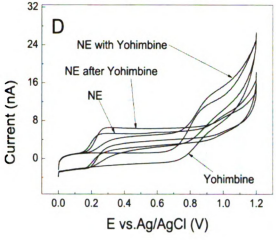
D
NE with Yohimbine
NE after Yohimbine
NE
Yohimbine
Current (nA)
E vs.Ag/AgCl (V)

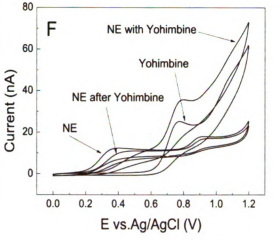
F
NE with Yohimbine
Yohimbine
NE after Yohimbine
NE
Current (nA)
E vs.Ag/AgCl (V)

positive but an unchanged limiting current of *ca.* 10 nA was reached prior to the onset of drug oxidation at *ca.* 900 mV. Little change in the NE voltammetric response was observed after yohimbine exposure and washout (Fig 3.4D). For example, the nominal $\Delta E_{1/2}$ and I_{ratio} values were -4.3 ± 9.5 mV and 0.97 ± 0.11, respectively (Fig 3.5A and B). In the presence of the drug, there was a positive shift in the $E_{1/2}$ and a decrease in the limiting current, but NE was detectable with this carbon fiber. The $E_{1/2}$ shifted positively by 38 mV and the limiting current decreased by 38%. The onset of the oxidation current for yohimbine remained the same in the presence of NE, *ca.* 800 mV, but the oxidation current was slightly increased indicating that both NE and the drug are oxidized at these positive potentials.

Exposure of the diamond microelectrode to UK 14,304 caused no change in $E_{1/2}$ or the limiting current (Fig 3.4E). For example, the nominal $\Delta E_{1/2}$ and I_{ratio} values were 15.3 ± 11.9 mV and 0.85 ± 0.02*, respectively (Fig 3.5A and B). In the presence of UK 14,304, the oxidation current response for NE was strongly affected. A broadly increasing oxidation current, significantly reduced in amplitude compared to the control, was observed commencing at *ca.* 350 mV. The current rise continued until 850 mV at which point oxidation of the drug commenced. The oxidation peak position and current for UK 14,304 were unchanged in the presence of NE indicating that only the drug is oxidized at these positive potentials. After exposure to yohimbine and washout, a positive shift in $E_{1/2}$ was observed with a significantly decreased limiting current. For example, the nominal $\Delta E_{1/2}$ and I_{ratio} values were 37.0 ± 8.6 mV and 0.81 ± 0.05*,

respectively (Fig 3.5A and B). In the presence of yohimbine, the NE oxidation current was suppressed as a broadly increasing current was seen beginning at 350 mV that continued until *ca.* 650 mV, at which point oxidation of the drug commenced. The NE oxidation current was significantly less than the control until 600 mV was reached. The yohimbine oxidation peak potential was unchanged in the presence of NE but the oxidation current magnitude was significantly increased indicating that both NE and the drug are oxidized.

3.2.5 Effect of Electrode Exposure to Cocaine, Idazoxan, and PPADS on Norepinephrine Detection

Figure 3.6 shows cyclic voltammetric *i-E* curves for 0.02 mM NE, 0.02 mM NE + 0.1 mM cocaine, idazoxan or PPADS, and 0.02 mM NE after drug washout on P-55 (Fig 3.6A, B and C), T-650 (Fig 3.6D, E and F) and diamond (Fig 3.6G, H and I) microelectrodes. It is clear that neither cocaine, idazoxan nor PPADS are electrochemically active at any of the three microelectrodes at potentials below 800 mV where NE is detected. Interestingly, diamond is the only microelectrode at which a well-defined oxidation peak is seen for PPADS with a nominal $E_{1/2}$ of 881 $\pm$ 10 mV. Importantly, for all three microelectrodes, the NE voltammetric response in terms of $E_{1/2}$ and the limiting current was largely unaffected by PPADS, idazoxan and cocaine. Furthermore, NE could be reliably detected in the presence of these drugs. There was no significant change in $\Delta E_{1/2}$ or decrease in I_{ratio} for any of the drugs at any of the three microelectrodes. The only major difference for the three microelectrodes was the oxidation peak at 900 mV for the

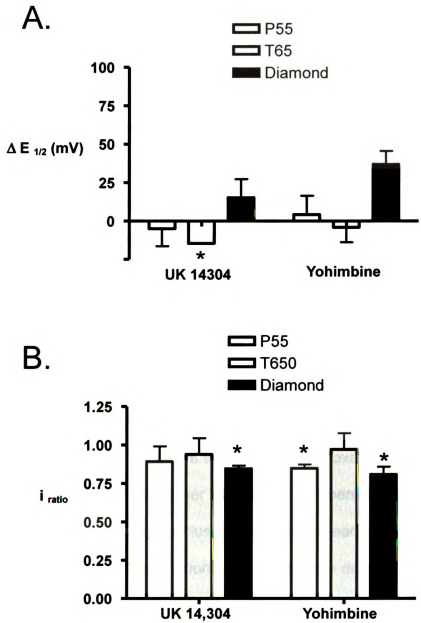

Figure 3.5. Plots of the cyclic voltammetric $\Delta E_{1/2}$ and limiting current ratio, I_{ratio} (= $I_{after\ drug}/I_{initial}$), after drug exposure (UK 14,304 and yohimbine) and washout at the three microelectrode types. Statistical analysis was based on n = 3. *Represents a significantly different value from the control (before drug exposure) as assessed using the standard t-test, $P<0.05$.

drug at diamond, and the increased current at this potential is the presence of NE. The latter indicates that both the drug and NE are oxidized at these potentials.

3.3 Discussion

The key observations from this work are (i) the differential electrochemical activity of some of the drugs at sp^2-bonded carbon fiber and sp^3-bonded diamond microelectrodes, and (ii) the effect some of the drugs have on the voltammetric response for NE depending on the microelectrode type and microstructure. The first aim of this work was to determine if any of the drugs exhibit electrochemical activity at potentials less than 800 mV vs. Ag/AgCl; potentials where NE is detected. For example, the $E_{1/2}$ for NE oxidation at the two carbon fibers is near 200 mV and at the diamond microelectrode is near 400 mV. Therefore, significant drug oxidation currents below 800 mV could pose an interference for NE detection. Figure 3.1 shows that cocaine, idazoxan and PPADS exhibit little electrochemical activity at either of the carbon fibers or diamond at potentials less than 800 mV. Similar conclusions have been reached previously for cocaine [177]. Clearly, the electrooxidation kinetics for some drugs, like PPADS, are more rapid at diamond based on the less positive $E_{1/2}$. This is in contrast to the more sluggish electrode kinetics for NE oxidation at diamond. This is a nice example showing that not all redox reactions are kinetically slower at diamond as compared to sp^2 carbon fiber electrodes. Studies of the drug oxidation reaction mechanisms and understanding the reasons for the differences in oxidation reaction kinetics at the different electrodes will be the subject of future research.

Figure 3.6. Cyclic voltammetric *i-E* curves for NE at (A, B and C) P55 and (D, E and F) T650 carbon fiber, and (G, H and I) diamond microelectrodes with and without cocaine, idazoxan and PPADS. All curves were acquired in Krebs solution at a scan rate of 0.1 V/s. The concentration of NE was 0.02 mM and the concentration of each drug was 0.1 mM.

A
NE with Cocaine
NE after Cocaine
NE
Cocaine
Current (nA)
E vs. Ag/AgCl (V)
B
NE with Idazoxan
NE
NE after Idazoxan
Idazoxan
Current (nA)
E vs. Ag/AgCl (V)
D
NE with Cocaine
NE
NE after Cocaine
Cocaine
Current (nA)
E vs.Ag/AgCl (V)
E
NE with Idazoxan
NE
NE after Idazoxan
Idazoxan
Current (nA)
E vs.Ag/AgCl (V)
G
NE with Cocaine
Cocaine
NE after Cocaine
NE
Current (nA)
E vs.Ag/AgCl (V)
H
NE with Idazoxan
Idazoxan
NE after Idazoxan
NE
Current (nA)
E vs.Ag/AgCl (V)

Figure 3.6. (continued)

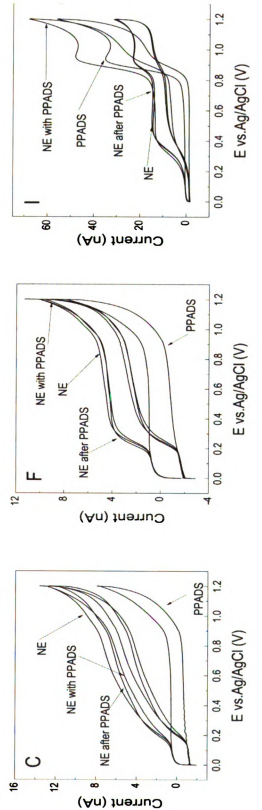

At this time, we speculate that the less positive $E_{1/2}$ for PPADS at diamond may be due to more favorable interaction of the molecule with the hydrophobic sp^3-bonded carbon surface. Importantly though, oxidation of PPADS, idazoxan and cocaine at all three microelectrodes occurs well positive of the potentials used for NE detection, so they present no direct interference. Furthermore, the voltammetric response for NE oxidation, both in terms of the $E_{1/2}$ and limiting current, was largely unaffected by exposure to any of these drugs. This is apparent from the cyclic voltammetric curves presented in Figure 3.6 and the data summary in Table 3.2. *NE can be reliably detected with both carbon fiber and diamond microelectrodes in the presence of any one of these drugs.*

More significant effects were seen for UK 14,304 and yohimbine in terms of drug electrochemical activity and changes in the voltammetric response for NE. Both drugs are electrochemically active at the carbon fiber and diamond microelectrodes. A well-defined oxidation peak is seen for UK 14,304 at all three microelectrodes with an $E_{1/2}$ of *ca.* 950 mV, as shown in Figure 3.1. There were no significant differences in the electrode-reaction kinetics at any of the three microelectrodes based on the similarity of the $E_{1/2}$ values. After drug exposure and washout, the most positive shift in $E_{1/2}$ for NE oxidation was seen for the diamond microelectrode. This is evident from the data in Figures 4 and 5, and Table 3.3. At most though, $E_{1/2}$ shifted only by 15 mV and I_{ratio} decreased only by 15%; both relatively minor changes. Greater adsorption of this drug on the low oxygen, sp^3-bonded carbon surface may be the reason for the positive shift in the NE oxidation $E_{1/2}$. Importantly, the original NE voltammetric response could be

regained after a 20 min soak of the diamond microelectrode in clean 2-propanol. This indicates that any kind of drug-surface interaction is relatively weak in strength and is chemically reversible. For UK 14,304, the oxidation current for NE in the presence of the drug was quite suppressed at the more microstructurally-ordered carbon fiber (P-55) and diamond microelectrodes. The NE oxidation current slowly increased with potential and never reached a steady state prior to the onset of drug oxidation. The current magnitude in the presence of the drug, even at potentials as positive of 0.6 V, was significantly less for these two microelectrodes than the values in the absence of the drug. Furthermore, there was no additional current for NE oxidation at the potentials where the drug is oxidized. These observations are consistent with there being a competitive interaction between the drug and NE for sites on the surface where the oxidation reaction can take place. The fact that the oxidation current maximum for the drug was the same in the presence of NE suggests that, if there is competition for sites, the drug preferentially interacts with these sites. These sites are apparently not exclusively associated with the edge plane regions based on the data for the more microstructurally-disordered carbon fiber (T-650). In the presence of UK 14,304 at this microelectrode, there was a slight shift in the NE oxidation $E_{1/2}$ but a stable limiting current was reached that was the same magnitude as that recorded in the absence of the drug. This could mean that NE is preferentially interacting with the edge plane sites while the drug is interacting more with the basal plane sites of the sp^2 carbon electrodes. Clearly, for this microelectrode, sites are available for the oxidation of both compounds. *For NE measurements in*

Table 3.2. Summary of cyclic voltammetric $\Delta E_{1/2}$ and I_{ratio} values for NE oxidation in the absence of different drugs.

*Represents a statistically different value as compared to the control (before drug measurement) using Student t-test. $P < 0.05$. $I_{ratio} = I_{after\ drug}/I_{initial}$.

Drug	P55		T650		Diamond	
	$\Delta E_{1/2}$ (mV)	I ratio	$\Delta E_{1/2}$ (mV)	I ratio	$\Delta E_{1/2}$ (mV)	I ratio
Capsaicin	4.8 ± 7.6	0.99 ± 0.02	-11.3 ± 2.7	0.86 ± 0.02 *	14.0 ± 11.1	0.94 ± 0.03
Prazosin	10.8 ± 6.9	0.68 ± 0.12 *	4.3 ± 1.2	0.88 ± 0.08	83.2 ± 14.3 *	0.78 ± 0.11
UK 14,304	-5.1 ± 11.4	0.89 ± 0.10	-14.7 ± 0.3 *	0.94 ± 0.11	15.3 ± 11.9	0.85 ± 0.02 *
Yohimbine	4.3 ± 12.2	0.85 ± 0.03 *	-4.3 ± 9.5	0.97 ± 0.11	37.0 ± 8.6	0.81 ± 0.05 *
Cocaine	2.0 ± 9.2	1.36 ± 0.13 *	-11.8 ± 2.3 *	1.23 ± 0.23	-12.0 ±7.1	0.99 ±0.06
Idazoxan	-2.0 ± 7.2	0.84 ± 0.04 *	-8.5 ± 2.1	1.09 ± 0.11	-7.3 ± 7.9	0.89 ± 0.03
PPADS	0.7 ± 4.8	1.00 ± 0.06	-22.0 ± 8.6	0.99 ± 0.03	0.7 ± 4.7	0.99± 0.04

the presence of UK 14,304, the T-650 carbon fiber would provide the best performance.

For yohimbine, the most significant changes in the NE voltammetric response were also seen for the diamond microelectrode. The drug was electroactive at all three microelectrode types with an $E_{1/2}$ between 0.7 and 0.8 V, as seen in Figure 3.1. The least positive $E_{1/2}$ was observed for diamond,. This means that the electrode reaction kinetics for this drug are most rapid at diamond, possibly because of stronger molecular interaction with the surface. After drug exposure and washout, the NE oxidation $E_{1/2}$ for the two carbon fibers was unaffected but I_{ratio} for the more microstructurally-ordered carbon fiber (P-55) was reduced by 15%. This is seen in Figure 3.5 and Table 3.3. In contrast, $E_{1/2}$ for NE oxidation at diamond was shifted significantly positive and I_{ratio} was reduced by 19%. In the presence of the drug, the trends for NE oxidation were similar to those observed for UK 14,304. At the more microstructurally-ordered carbon fiber (P-55) and the diamond microelectrode, the oxidation current for NE only gradually increased with potential, never reaching a steady state prior to the onset of drug oxidation. There was, however, additional current at both microelectrodes for NE oxidation at the potentials where the drug is oxidized. Again these observations may mean that there is competitive interaction between the drug and NE for sites on the surface where the oxidation reaction can occur. Again, these sites do not appear to be exclusively the edge plane regions based on the data for the more microstructurally-disordered carbon fiber (T-650). In the presence of yohimbine at this microelectrode, there was a slight shift in the NE

oxidation $E_{1/2}$ and a limiting current was reached that was the same magnitude as that recorded in the absence of the drug. *For NE release measurements in the presence of yohimbine, the T-650 carbon fiber would provide the best performance.*

The two drugs that produce the most complications for NE detection at all three microelectrodes are capsaicin and prazosin. Capsaicin is easily oxidized at all three microelectrodes near the potentials at which NE is detected. The oxidation $E_{1/2}$ values were in the 0.55 to 0.65 V range with the least positive $E_{1/2}$ seen for the microstructurally-disordered T-650 carbon fiber. After drug exposure and washout, the $E_{1/2}$ and limiting current were largely unchanged from the control values for all three microelectrodes, as seen in Figures 2 and 3, and Table 3.3. The greatest reduction in I_{ratio} of 14 % was seen for the T-650 carbon fiber. These results indicate that any interaction of the drug with these three microelectrodes is relatively weak and reversible. However, in the presence of the drug, near total suppression of the NE oxidation current was seen for the microstructurally-ordered P-55 carbon fiber. For the T-650 carbon fiber and diamond microelectrodes in the presence of the drug, the NE oxidation $E_{1/2}$ shifted positive but nearly the same limiting current was reached. Prazosin was also electrochemically active at all three microelectrodes with an $E_{1/2}$ value ranging between 0.82 to 0.87 V. After drug exposure and washout, the NE oxidation $E_{1/2}$ shifted slightly positive but there was a significant reduction in I_{ratio} of 32% for the P-55 carbon fiber. Small positive shifts in $E_{1/2}$ for NE oxidation were seen for the T-650 carbon fiber and diamond microelectrodes after drug

exposure and washout with reductions in I_{ratio} of 12 and 22%, respectively. In contrast with the data for capsaicin, the results for prazosin indicate that any interaction of the drug with these three microelectrodes is stronger and less reversible. *Most important, in the presence of the drug, the NE oxidation current was nearly totally suppressed for all three microelectrodes.*

Finally, two redox waves for NE were often observed at the diamond microelectrodes with $E_{1/2}$ values of ca. 0.4 and 0.9 V. In contrast, only one redox wave was seen at both carbon fibers. Our current supposition is that these two peaks represent oxidation of NE at two distinct sites on the diamond microelectrode. Not all diamond microelectrodes exhibit two peaks but the batch used for this work did. The presence of the second peak seems to be connected with the deposition conditions and post-deposition treatment. Ongoing work will hopefully reveal the origin of this higher potential oxidation peak.

3.4 Conclusion

The key findings from the work can be summarized as follows:

1. The oxidation of PPADS, idazoxan and cocaine at all three microelectrodes occurs well positive of the potentials used for NE detection, so they present no direct interference. Furthermore, the voltammetric response for NE oxidation, both in terms of the $E_{1/2}$ and limiting current, was largely unaffected by exposure to any of these drugs. NE can be reliably detected with both carbon fiber and diamond microelectrodes in the presence of any one of these three drugs.

2. The oxidation of UK 14,304 and yohimbine at all three microelecrodes occurs at potentials positive of where NE is detection, so they present no direct interference. The voltammetric response for NE oxidation at all three microelectrodes was not significantly affected by drug exposure. Minor shifts and $E_{1/2}$ and reductions in limiting current were seen, but all effects were reversed by soaking the microelectrodes in clean 2-propanol. In the presence of UK 14,304 and yohimbine, significant response attenuation was seen for NE oxidation under these test conditions at the P-55 and diamond micrelectrodes. Minor effects were observed for the T-650 carbon fiber. For NE release measurements in the presence of UK 14.304 or yohimbine, the T-650 carbon fiber provides the best performance.

3. The two drugs that produce the most complications for NE detection at all three microelectrodes are capsaicin and prazosin. Capsaicin was oxidized, although low in current, at all three microelectrodes at the potentials where NE is detected. Prazosin was not so it poses no direct interference. Exposure to both capsaicin caused some minor alterations in the voltammetric response for NE but these effects could be fully reversed by soaking the microelectrodes in clean 2-propanol. Only partial response recovery was seen after 2-propanol soak. Detection of NE in the presence of capsaicin is possible using all three microelectrodes but near total suppression of the oxidation current is observed for prazosin at all three. Measurements of NE release with any of the three microelectrodes would be complicated in the presence of prazosin.

The results demonstrate that when drugs are used in electrochemical

studies of neuroeffector transmission, one should carefully assess the electrochemical activity of the particular drug at the recording microelectrode and how exposure to the drug affects the microelectrode response (*i.e.*, sensitivity) for the neurotransmitter of interest. Future work will involve studies of the oxidation reaction mechanism of some of the electroactive drugs.

CHAPTER 4

TEMPERATURE-RELATED DIFFERENCES IN SYMPATHETIC NEUROEFFECTOR TRANSMISSION TO MESENTERIC ARTERIES AND VEINS

4.1 Introduction

Sympathetic nerves control arterial and venous tone. Arteries are resistance while veins are capacitance vessels [87, 89]. The venous system contains 70% of the total blood volume, with most of this in small veins and venues. Mesenteric veins (MV) differ markedly from mesenteric arteries (MA) in their contractile [8, 47] and electrical [88, 91] response to sympathetic nerve stimulation.

There are major differences between MA and MV neuroeffector transmission. First, adenosine 5'-triphosphate (ATP) and norepinephrine (NE) are the primary neurotransmitters released by sympathetic nerves supplying small MA [90], while NE is the primary vasoconstrictor released by perivenous nerves in rat [31, 33, 34]. Second, excitatory junction potentials mediated by ATP acting at P2X receptors are recorded from arteries but not veins [88, 89, 182] Third, the depolarization produced by repetitive nerve stimulation is proportionally greater in MV than MA [88]. Finally, NE release from sympathetic nerves in rat MV exceeds release in MA even though the density of sympathetic nerves in MV is lower than that in MA [47, 91].

The efficiency of neuromuscular transmission in blood vessels can be affected by several factors that allow the strength of junctional communication to

be regulated. Prejunctional receptors are important in this regard [61]. The prejunctional α_2-adrenergic receptors (α_2ARs) mediate NE release as part of an important negative feedback mechanism [29, 34, 91, 127, 183]. The role of α_2ARs in MA and MV is controversial. In rats, α_2ARs regulate NE release through negative feedback in MA more so than in MV [34, 91, 131]. However, there is also work demonstrating that α_2AR-mediated neuromodulation plays a greater role in canine MV than MA [32]. On the other hand, the termination of transmitter actions at the neuroeffector junction depends on removal (NE reuptake) and extracellular metabolism [74, 75]. The degree to which NE clearance depends on these processes varies and may also vary between arteries and veins [91, 124].

Temperature variation has been used to probe molecular mechanisms controlling transmitter release and clearance in the central and peripheral nervous systems [152]. At low temperature, the kinetics of reactions in sympathetic nerve terminals are reduced (e.g., slow activation of Na^+ channels or depression of voltage-dependent Ca^{2+} channels) [124, 184]. Since NE release is a multi-step process, one way to test the hypothesis that there are fundamental differences in NE release and clearance mechanisms in arteries and veins is to study the temperature-dependence of NE overflow.

Because NE can be oxidized via a 2 electron / 2 proton redox reaction, it can be detected electrochemically as an oxidation current [129, 185], This is accomplished using differential pulse amperometry or continuous amperometry with carbon fiber microelectrodes to study NE release and clearance in blood

vessels maintained *in vitro* [130-133]. This technique measures the diffusive overflow of NE from multiple neuroeffector junctions in the vicinity of the recording electrode. The overflow depends on the mechanistic and kinetic aspects of release and clearance. It is by far the best available method to study the nerve stimulation-induced release of endogenous NE. Its high sensitivity and fast response time allow measurements in real time to be made. In other words, the time course of NE concentrations at the blood vessel surface can be probed locally.

In this study, continuous amperometry was employed to investigate NE levels *in vitro* at the adventitial surface of isolated rat MA and MV. A diamond microelectrode was employed for detection due to its excellent response sensitivity and reproducibility compared to a carbon fiber microelectrode [127, 167, 186]. The magnitude of the NE oxidation current detected is governed by the complex interplay between release and clearance [124]. We used temperature as a probe to test the hypothesis that NE release and clearance at sympathetic neuroeffector junctions at rat MA and MV are differentially regulated.

4.2 Results

4.2.1 Sodium and Calcium Channel Function on NE Release at MA and MV

Electrical stimulation evokes neurotransmitter NE release from sympathetic nerves and NE can be detected directly by electrochemical methods. The oxidation current measured at 700 mV (*vs.* Ag/AgCl reference, 3M KCl) is directly related to the concentration of endogenous NE at the blood vessel surface [127,

128, 130]. After release from the nerve terminals, some NE molecules bind with presynaptic receptors, some of them diffuse across the synaptic junction and bind at specific receptors on the nearby vascular smooth muscle cells, and a large faction gets cleared by neuronal reuptake. The remainder diffuses away from the release sites. The latter is what is detected by the recording microelectrode. Evidence that the current was caused by NE oxidation came from measurements using a sodium channel antagonist, tetrodotoxin (TTX) [91]. In our study, we use 10 Hz for tissue nerve stimulation since it is at the half maximum stimulation frequency response curve and thus more sensitive to detect the differences between groups [91]. TTX (0.3 μM) blocked stimulation evoked oxidation currents in arteries and veins (Fig. 4.1A).

We used the calcium channel blocker, $CdCl_2$, to inhibit NE release during nerve stimulation 1B). Representative tracings show the inhibition caused $CdCl_2$ (30 μM) on NE release in MA and MV (Fig. 4.1B). The NE oxidation current was inhibited by 50% in artery and by 75% in the vein. The release of NE in MV was more sensitive to inhibition by $CdCl_2$ compared to MA as the pEC_{50} in MV was 6.5 ± 0.2 and in MA this value was 4.8 ± 0.9 ($P < 0.01$).

4.2.2 Temperature Dependent NE Oxidation Currents from MA and MV

Figure 2A and B display representative NE oxidation current transients for MA and MV at 37 and 28 °C, respectively. At 37 °C, the current amplitude for MV (13.7 pA) is greater than that for MA (10.3 pA). At 28 °C, the current amplitude for both MA and MV decreased to around 5 pA. The fractional decrease in current

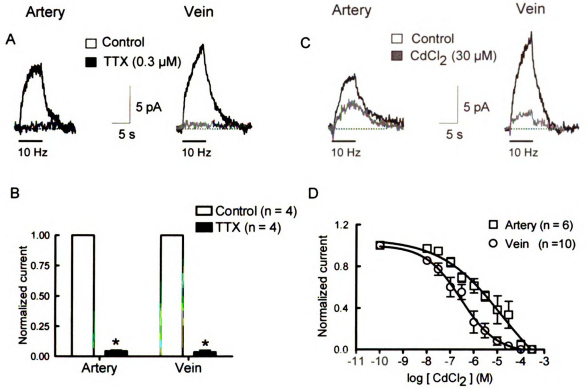

Figure 4.1 (A) NE oxidation currents recorded from a MA and MV in the absence and presence of TTX. TTX completely blocked the stimulation evoked oxidation current. (B) Pooled data from experiments illustrated in "A" showing the TTX blocks stimulation evoked oxidation currents. *indicates significantly different from control ($P < 0.05$). (C) NE oxidation currents from a MA and MV in the absence and presence of $CdCl_2$, a calcium channel blocker. (D) $CdCl_2$ concentration response curve for inhibition of NE oxidation current evoked by electrical stimulation. Veins were more sensitive to the inhibitory effects of $CdCl_2$ compared to arteries. Data are mean ± S.E.M.

was greater for MV. Figure 1C is a plot of the maximum oxidation currents for MA and MV as a function of temperature. There is a temperature dependence on the current overflow from both vessel types but the temperature sensitivity is greater for MV. At all temperatures, overflow at MV exceeded that at MA except at 28 °C. At 37 °C, the NE current for MV is 1.6 times greater than for MA. The temperature coefficient Q_{10} is a measure of the rate of change of a biological or chemical system as a consequence of increasing the temperature by 10° C. It can be calculated by the following equation,

$$Q_{10} = \left(\frac{R_2}{R_1}\right)^{\frac{10}{T_2 - T_1}}$$

with R is the rate, the current amplitude in our case, and T is the temperature in celsius degrees or kelvins. The calculated Q_{10} values for MA and MV were 2.0 ± 0.2 and 3.1 ± 0.4, respectively ($P < 0.05$). The larger Q_{10} value indicates that NE release and or clearance in MV have are more temperature sensitive than in MA.

The total charge passed during the NE measurement (Q), was calculated by integrating the current/time profile and is related to the number of electrons transferred per molecule (n) and the number of moles of NE oxidized (N) through Faraday's law, Q = nFN, where F is the Faraday constant (96,500 C mol^{-1}). The number of NE molecules detected at 37°C in MA was 2.2 (± 0.19) × 10^8 and 6.9 (± 0.25) × 10^8 in MV. We plotted the number of NE molecules detected as the function of the temperature for both MA and MV. The number of molecules detected increased with the temperature and followed the same trend as the

peak current vs. temperature plots.

The current measured reflects NE overflow from nearby varicosities. During the 6 s stimulation period, NE accumulates in the neuroeffector junction with a fraction diffusing to the microelectrode. The increase in oxidation current is related to the junctional concentration. As indicated above, the junctional concentration is controlled by the amount of NE released during nerve stimulation, offset by the amount cleared by neuronal reuptake or the amount bound to nerve terminal or smooth muscle receptors. The rate of change of the NE current reflects NE release kinetics off-set by the clearance kinetics [187]. The rates of NE release and clearance were quantitatively different for MA and MV at the different temperatures. The representative curves shown in Fig. 4.2A and B illustrate that the rise of the oxidation current for MV is much steeper than that for MA at 37 °C. Furthermore, the rates of the current rise and decay time were temperature sensitive. The 10 - 90% rise slope, rise time and decay time of the NE oxidation current at 37 and 28 °C are shown in Fig. 4.3. The rate of current rise was significantly faster in MV than in MA at 37 °C. This difference diminished at 28 °C. The peak NE current was larger in MV so although the rate of rise was faster in MV than MA, the time to peak current was the same for both blood vessels at 37 °C (Fig. 4.3B). At 28 °C, NE oxidation currents peaked prior to the end of the stimulation period so the current rise times in MA and MV were significantly less compared to that at 37 °C. Current decay times were longer in MV compared to MA both temperatures. The current decay represents NE clearance by re-uptake, metabolism and diffusion.

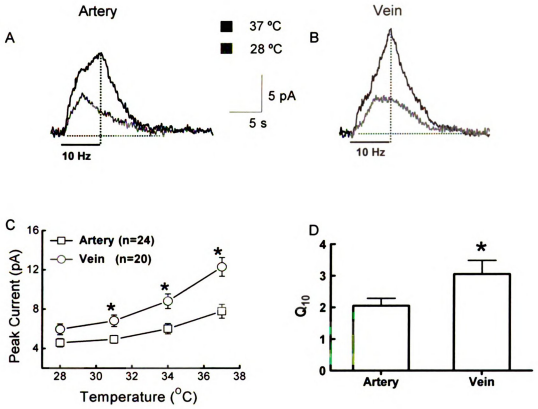

Figure 4.2 NE oxidation currents recorded from a MA (A) and MV (B) at 37 °C (black trace) and 28 °C (grey trace). The oxidation current continued to increase in MA and MV at 37 °C throughout the stimulus train. At 28 °C the current began to decline in MA while it was sustained in MV. The bar under the current traces represent the period of nerve stimulation (60 pluses with a 0.5 ms pulse width). (C) Plot of the temperature dependence of peak current amplitude in MA and MV. The peak current amplitude in MV is more temperature dependent. (D) Q_{10} values for NE current amplitudes. Data are mean ± S.E.M. * represents significant difference from MA, $P < 0.05$

4.2.3 Effect of Temperature on the Regulation of NE Release by Prejunctional α_2 ARs

The α_2AR antagonist, idazoxan (1μM), was employed to study its effect on the temperature dependence of NE release from periarterial and perivenous sympathetic nerves. Idazoxan increased oxidation currents recorded from MA at both 37 and 28 °C. At 37 °C, the current increased in amplitude throughout the period of stimulation in the absence and presence of idazoxan. However, at 28 °C in the absence of idazoxan, the current peaked and began to decay during the stimulus train while in the presence of idazoxan the current continued to increase thoughout the stimulus train (Fig. 4.4A). Although the oxidation currents were smaller at 28 °C compared to 37 °C, idazoxan did not change the time course or peak amplitude of the current in MV at either temperature (Fig. 4.4B). There was a 2-fold increase in the oxidation current for MA in the presence of the drug at all temperatures (Fig. 4.4C). Idazoxan didn't change the Q_{10} for the MA peak current (Table 4.1). Idazoxan did not change oxidation current amplitude at any temperature in MV (Fig. 4.4D).

Figure 4.5 shows the 10-90% rise slope (A,B), rise time (C,D) and decay time (E,F) for MA and MV at 37 and 28 °C in the absence (control) and presence of idazoxan. Idazoxan increased the rate of rise of the oxidation current in MA, but not MV, at 37 and 28 °C. The current rise time was not changed by idazoxan in MA or MV at 37 °C; however, the current rise time was increased significantly by idazoxan in MA at 37 but not 28 °C (Fig. 4.5 C,D). Idazoxan did not affect current decay time in MA and MV at either temperature (Fig. 4.5 E,F).

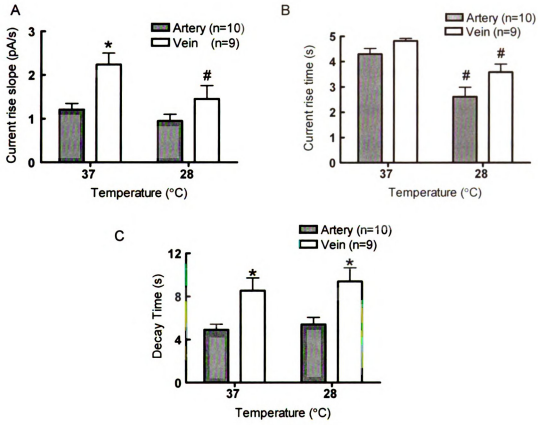

Figure 4.3 Comparison of the time profiles of NE oxidation currents in MA and MV at 37 and 28 °C. (A) 10 to 90% rise slope of the NE oxidation current is greater for MV compared to MA at 37 °C but not 28 °C, (B) The time to peak NE oxidation current is significantly greater at 37 than 28 °C for both MA and MV, (C) the 10 to 90% decay time of NE oxidation current is much longer for MV than for MA at both 37 °C and 28 °C. Data are mean ± S.E.M. *indicates significantly different from MA; # indicates significantly different from 37 °C, $P < 0.05$.

both 37 and 28 °C. At 37 °C, the current increased in amplitude throughout the period of stimulation in the absence and presence of idazoxan. However, at 28 °C in the absence of idazoxan, the current peaked and began to decay during the stimulus train while in the presence of idazoxan the current continued to increase thoughout the stimulus train (Fig. 4.4A). Although the oxidation currents were smaller at 28 °C compared to 37 °C, idazoxan did not change the time course or peak amplitude of the current in MV at either temperature (Fig. 4.4B). There was a 2-fold increase in the oxidation current for MA in the presence of the drug at all temperatures (Fig. 4.4C). Idazoxan didn't change the Q_{10} for the MA peak current (Table 4.1). Idazoxan did not change oxidation current amplitude at any temperature in MV (Fig. 4.4D).

Figure 4.5 shows the 10-90% rise slope (A,B), rise time (C,D) and decay time (E,F) for MA and MV at 37 and 28 °C in the absence (control) and presence of idazoxan. Idazoxan increased the rate of rise of the oxidation current in MA, but not MV, at 37 and 28 °C. The current rise time was not changed by idazoxan in MA or MV at 37 °C; however, the current rise time was increased significantly by idazoxan in MA at 37 but not 28 °C (Fig. 4.5 C,D). Idazoxan did not affect current decay time in MA and MV at either temperature (Fig. 4.5 E,F).

4.2.4 Function of Pertussis Toxin Sensitive G Protein in MA and MV

We used pertussis toxin (PTX) to examine the function of G_i/G_o protein which couples to the presynaptic α_2AR. MA and MV were incubated in 3 µg/ml PTX while control groups were incubated in OPTI-MEM medium [188]. The NE

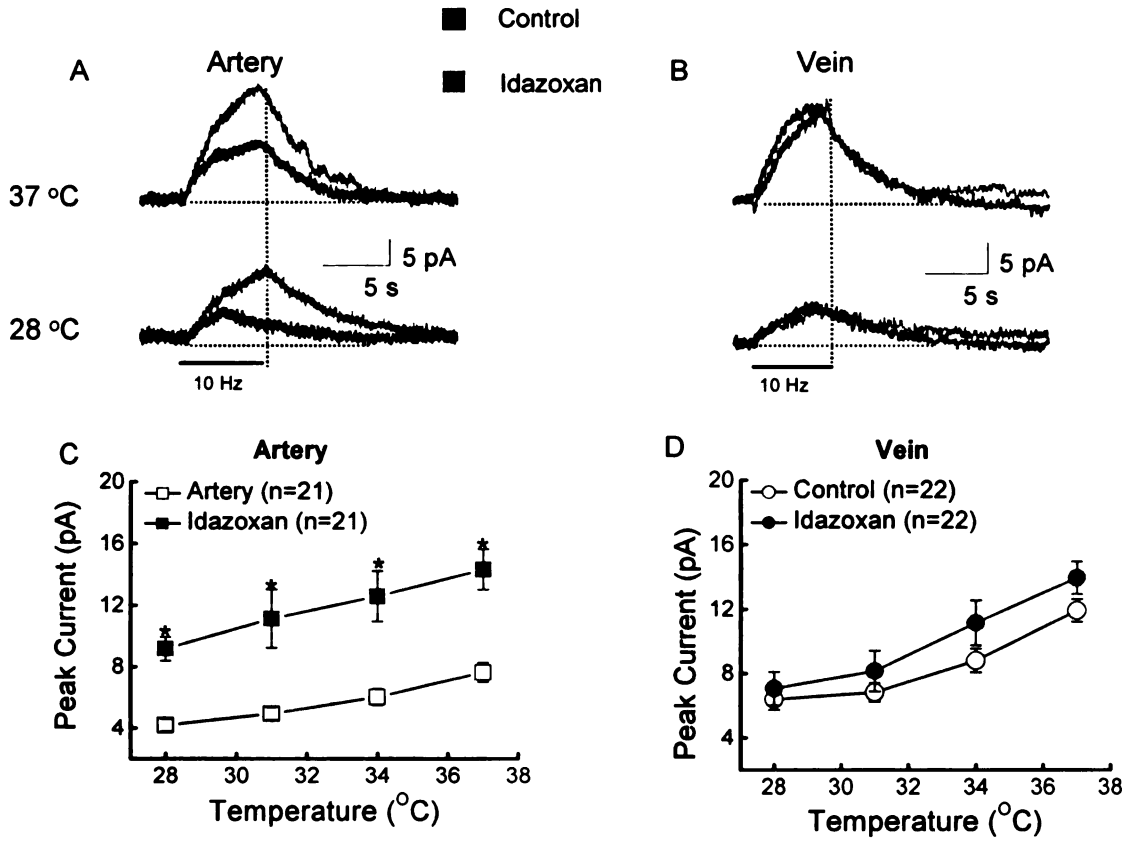

Figure 4.4 Effect of the α_2AR blocker, idazoxan, NE oxidation current from MA and MV at different temperatures. (A) NE oxidation current traces from a MA in the absence and presence of idazoxan (1 μM) at 37 and 28 °C. At 37 °C, idazoxan increases peak currents but the time to peak current is similar. At 28 °C, idazoxan increases peak current and time to peak current as the current amplitude increases throughout the train of stimulation in the presence of the antagonist. (B) Idazoxan does not alter NE oxidation currents in MV at 37 or 28 °C. Bars under the current traces represent the period of nerve stimulation (60 pluses with a 0.5 ms pulse width). Pooled data for NE oxidation current at different temperature with and without idazoxan for MA (C) and MV (D). Data are mean ± S.E.M.; *indicates significant difference from control, $P < 0.05$.

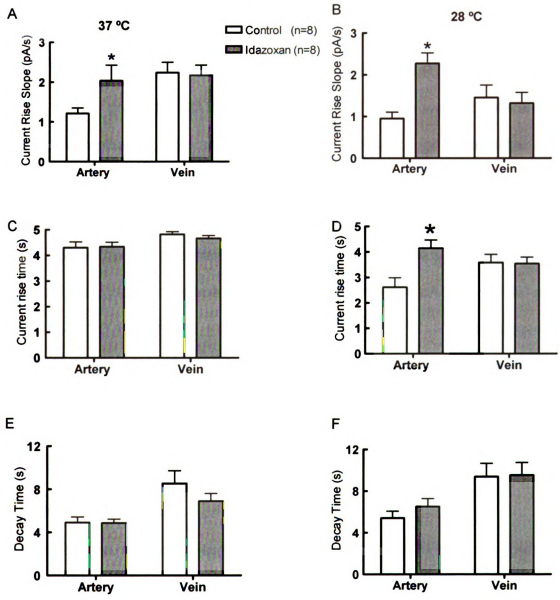

Figure 4.5 Time course of NE oxidation currents in MA and MV at 37 and 28 °C with and without idazoxan. (A) 10 to 90% rise slope of NE oxidation current is significantly increased by idazoxan (1 μM) in MA but not MV at 37 °C and at 28 oC (B). (C) The 10 to 90% rise time of NE oxidation current was unaffected by idazoxan at 37 °C in MA and MV but idazoxan increased the current rise time at 28 °C for MA but not MV (D). Idazoxan did not change the 10 to 90% decay time of NE oxidation currents in MA or MV at 37 °C (E) and 28 °C (F). Data are mean ± S.E.M. and * represents significant difference from control, $P < 0.05$.

current amplitudes were significantly increased for MA at both 37 and 28 °C after PTX treatment compared to control (Fig. 4.6A), but not for MV (Fig. 4.6 B). α_2AR blocker, idazoxan (1 μM), increased NE current for both the PTX treatment group and the control group for MA at both 37 and 28 °C. There was no difference in the current amplitude before and after idazoxan application for MV at either 37 or 28 °C. PTX didn't change the Q_{10} for the peak current for either MA or MV (Table 1). The current rise slope, rise time, and decay time after PTX treatment for MA and MV follow the similar pattern as the data shown in Fig. 4.5. Specifically, PTX increased the current rise slope from 1.4 ± 0.2 to 2.1 ± 0.4 pA/s ($P < 0.05$) at 37 °C and from 1.0 ± 0.3 to 1.8 ± 0.1 pA/s ($P < 0.05$) at 28 °C. PTX prolonged the current decay time from 2.4 ± 0.4 to 3.8 ± 0.3 s ($P < 0.05$) at 28 °C but not at 37 °C. PTX didn't change the current rise slope, rise time and decay time for MV and current decay time for MA at either temperature.

4.2.5 Effect of Temperature on NE Reuptake

After release, approximately 90% of the NE is cleared from the neuroeffector junction by the NET [74]. Cocaine (10 μM) was used for NET blockade. Cocaine significantly increased the maximum oxidation current at MA at all temperatures with the largest increase of 80% at 37 °C (Fig. 4.7 A,C). Cocaine increased the Q_{10} value for peak currents in MA from 2.0 ± 0.2 to 2.7 ± 0.3 ($P < 0.05$) (Table 4.1). Maximum currents in MV were not affected by cocaine at any temperature (Fig. 4.7 B,D).

Cocaine increased the rate of current rise in MA at both 37 (Fig. 4.8 A) and

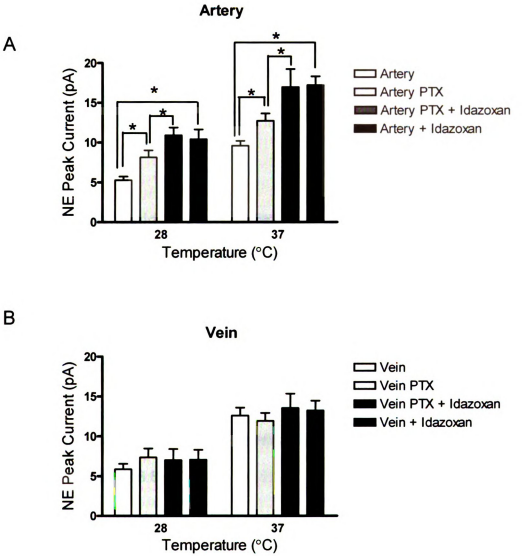

Figure 4.6 Effect of G_i/G_o protein blocker, pertussis toxin (PTX, 3 μg/ml), on inhibition of NE release in MA (A) and MV (B) at 37 and 28 °C. PTX increased NE current in MA at both 37 and 28 °C but not in MV. α_2AR blocker, idazoxan (1 μM), increased NE current for MA in both PTX treatment group and control group at both 37 and 28 °C. Idazoxan didn't increase the current amplitude for MV in either group at any temperature. Data are mean ± S.E.M. and *indicates a significant difference between two groups, $P < 0.05$.

28 °C (Fig. 4.8B), with the greater increase at 37 °C. There was no change in the rise slope for MV at any temperature in the presence of cocaine. Cocaine also increased the total rise time of the oxidation current in MA at 28 °C but not in MV (Fig. 4.8 D) Cocaine also prolonged current decay time in MA but not MV at 37 and 28 °C (Fig. 4.8 E and F).

4.2.6 Effect of Guanethidine on NE Release

In order to test if there is difference in the availability of NET in MA and MV, guanethidine was employed. Guanethidine is taken up by NET to the nerve endings [189]. It inhibits NE release and causes NE depletion by inhibition of the Na^+ATPase dependent pump. Guanethidine inhibits NE in a concentration dependent way, which is shown in Fig. 4.9. The release of NE in MV was more sensitive to inhibition by guanethidine compared to MA with the pEC_{50} for MV of 7.3 ± 0.3 and for MA of 6.8 ± 0.08 ($P < 0.01$).

4.3 Discussion

4.3.1 Temperature-dependence of NE Oxidation Currents Recorded from MA and MV

We verified that focal electrical stimulation of MA and MV evokes a neurogenic oxidation current. This conclusion is supported by the observation that the oxidation currents were blocked completely by the sodium channel blocker, tetrodotoxin, indicating a requirement for axonal action potentials. We also showed that the oxidation currents were inhibited in a concentration

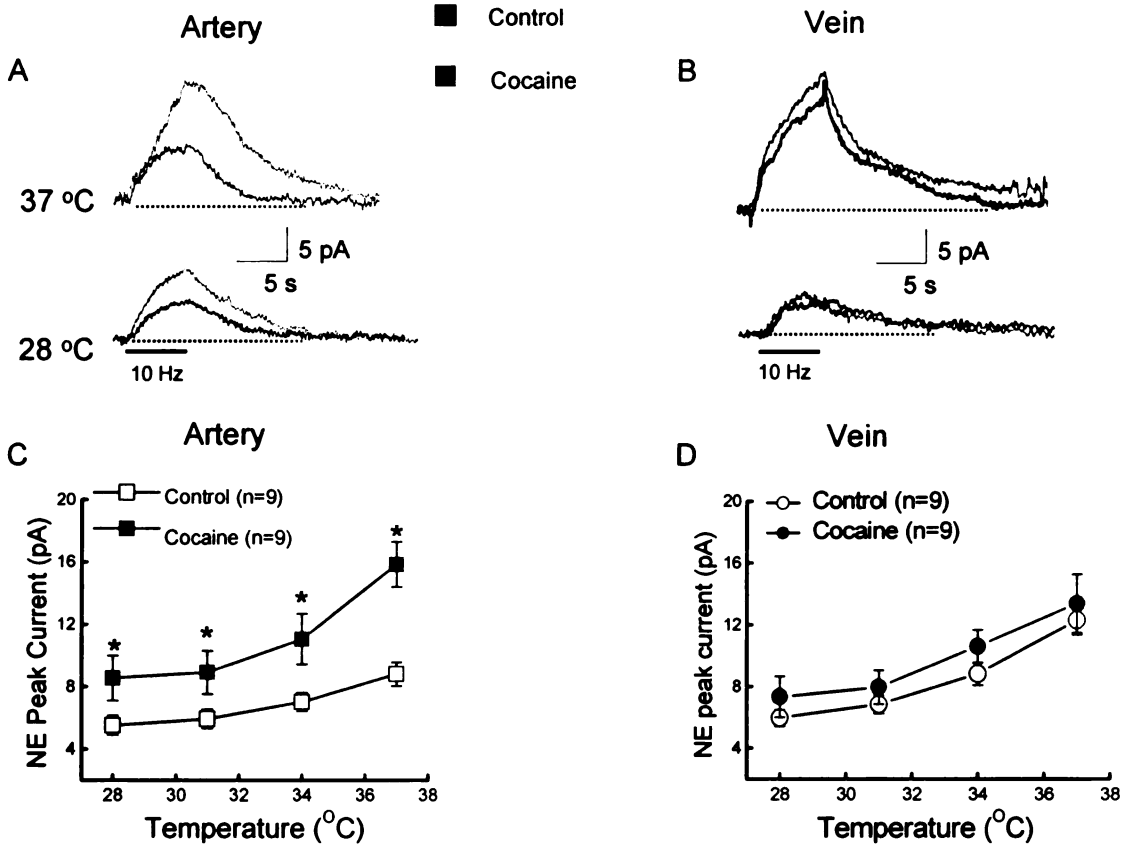

Figure 4.7 Effect of cocaine (10 μM) on NE oxidation currents in MA and MV. Representative recordings of oxidation currents in MA (A) and MV (B) at 37 and 28 °C. Bars under the current tracings represent the period of nerve stimulation (60 pluses with a 0.5 ms pulse width). Cocaine increases peak oxidation currents in MA at both temperatures. Oxidation currents in MV are unaffected by cocaine. (C) Pooled data for effects of temperature and cocaine on oxidation currents in MA and in MV (D). Data are mean ± S.E.M. and *indicates a significant difference from control, $P < 0.05$.

Figure 4.8. Comparison of the time course for NE oxidation currents from MA and MV at 37 °C and 28 °C with and without cocaine (10 μM). The 10 to 90% current rise slope of NE oxidation current increased significantly after treatment of cocaine in MA at both 37 °C (A) and 28 °C (B). Cocaine did not affect the time course of the current in MV at either temperature. (C) The 10 to 90% current rise time was not affected by cocaine treatment for both MA and MV at 37 °C (C) but increased at MA at 28 °C (D). The 10 to 90% decay time of the NE oxidation current was prolonged in MA but not MV at 37 °C (E) and 28 °C (F). Data are mean ± S.E.M. and *indicates significantly different from control, $P < 0.05$.

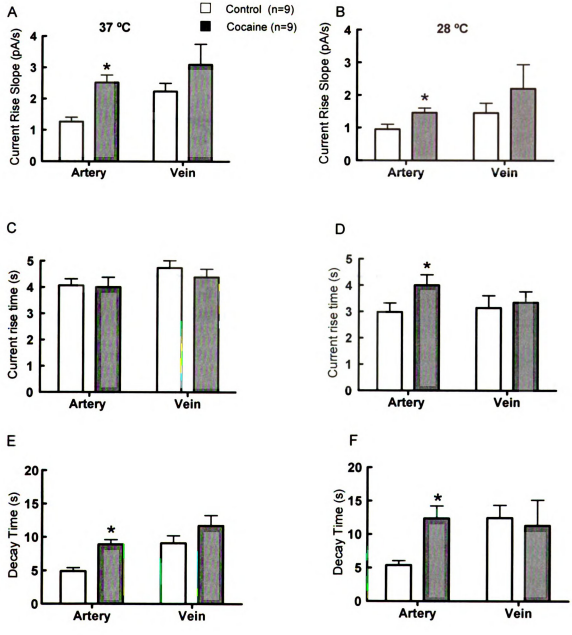
A
37 °C
Control (n=9)
Cocaine (n=9)
Current Rise Slope (pA/s)
Artery
Vein
B
28 °C
Current Rise Slope (pA/s)
Artery
Vein
C
Current rise time (s)
Artery
Vein
D
Current rise time (s)
Artery
Vein
E
Decay Time (s)
Artery
Vein
F
Decay Time (s)
Artery
Vein

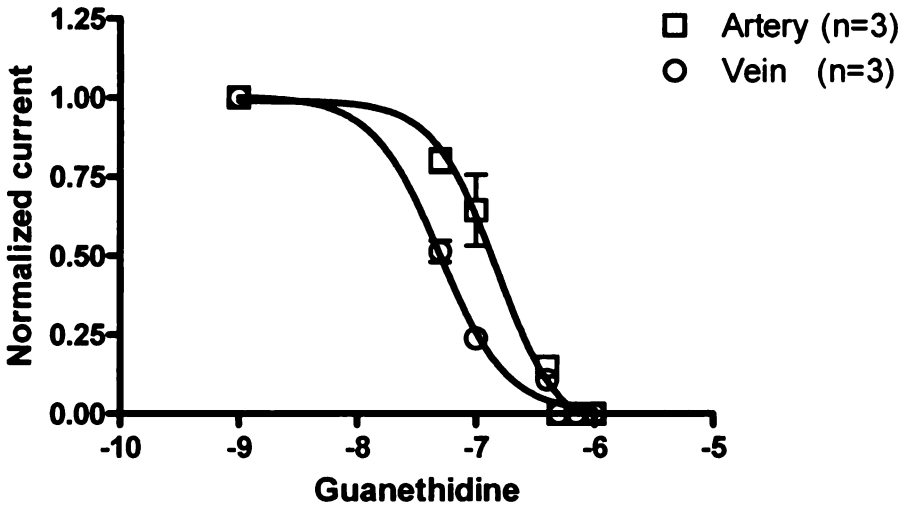

Figure 4.9 Guanethdine concentration response curve for inhibition of NE current in MA and MV at 37 °C. MV is more sensitive to the inhibition effect of guanethidine. Data are mean ± S.E.M.

dependent manner by the non-selective calcium channel blocker, $CdCl_2$. A novel finding was that the oxidation currents recorded from MV were more sensitive to $CdCl_2$ induced inhibition than those recorded from MA. This result is consistent with the overall conclusion that regulation of NE release from periarterial and perivenous nerves is different but the mechanism responsible for this difference is not clear. Recent studies [190] have shown that may be differential calcium channel subtype expression by periarterial and perivenous sympathetic nerves at least in dog. Similar differences in calcium channel expression in rat MA and MV might explain the increased $CdCl_2$ sensitivity of NE release from perivenous sympathetic nerves.

Temperature variation has been used to probe molecular mechanisms controlling transmitter release and clearance in the central and peripheral nervous systems [152]. As neurotransmitter release is a multi-step process, it is not surprising that synaptic transmission would be markedly altered by even small temperature changes. For example, small changes in temperature can alter synaptic vesicle movements and can change the dynamics of vesicle release responsible for synaptic plasticity in the central nervous system [153-155]. These studies revealed that treatments which increase synaptic efficacy reduce the temperature sensitivity of synaptic transmission. Increased synaptic efficacy is associated with an increased vesicle number and/or an increase in the content of synaptic vesicles that are replenished after release. Thus, temperature sensitivity would be a useful tool to probe physiological differences in the mechanisms controlling release and clearance of NE from periarterial and

perivenous nerves.

We estimate that reducing the temperature from 37 to 28 °C, would decrease the peak current by ~10% due to temperature-dependent changes in the NE diffusion coefficient [170, 191, 192]. However, NE oxidation currents decreased by more than 40% in MA and MV when reducing the temperature from 37 to 28 °C. This means that the decrease in current is caused primarily by alterations in the NE release and clearance mechanisms rather than by reduced diffusion.

Small arteries such as those studied here are resistance blood vessels that deliver oxygenated blood to tissues. Small veins are capacitance blood vessels which store blood and carry oxygen poor blood away from tissues. Based on these different hemodynamic functions, it might be expected that arteries and veins would be regulated differently by the sympathetic nervous system. Furthermore, different subsets of sympathetic nerves supply MA and MV [87]. There are also functional differences between sympathetic nerves supplying MA and MV. In small MA from rats, (≤300 μm), like those studied here, ATP and NE are co-transmitters [31, 33], while in rat mesenteric veins, NE is the dominant neurotransmitter [34]. This profile differs somewhat in guinea pig mesenteric arteries and veins where purinergic neurotransmission is more prominent in veins [31, 47].

Several factors influence NE signaling: the amount of NE released, binding to pre and post-junctional receptors, clearance by neuronal and extraneuronal reuptake, diffusion, and metabolism [74, 124]. At 37 °C, peak NE

currents were larger in MV compared to MA. However, there was a decline in the peak NE current between 28 and 37 °C in MA at MV and this decline was larger in MV compared to MA. At lower temperatures, altered ion channel function, reduced enzyme activity and alterations in vesicle mobility and fusion with the presynaptic membrane could all contribute to reduced NE release [124]. Each could contribute to the different temperature dependence of NE overflow from MA and MV. We investigated the function of sodium and calcium channels in MA and MV (Fig. 4.1). NE oxidation currents were equally sensitive to TTX suggesting that temperature-dependent changes in sodium channel function do not make a major contribution to the difference in temperature sensitivity of MA and MV. However, the release of NE in MV is more sensitive to the calcium channel blocker $CdCl_2$ compared to MA. Temperature dependent changes in action potential propagation or calcium channel function are probably not a major factor accounting for the temperature dependent NE current difference between MA and MV. If this was the case, NE oxidation currents should be equally affected by temperature reductions. Furthermore, studies in adrenal chromaffin cells have shown that temperature dependent reductions in calcium signals can not account for differences in vesicle mobilization [193].

4.3.2 Function of α_2 ARs in MA and MV

Prejunctional α_2ARs couple to $G_{i/o}$ proteins that link to the inhibition of adenylate cyclase and N- and P/Q-type calcium channels and activation potassium channels [61]. NE release from sympathetic nerves is partly

controlled by α_2 ARs, which provide negative feedback to inhibit NE release. The absence or inhibition of autoreceptor function would lead to greater NE release and larger oxidation currents. Blockade of α_2ARs using idazoxan increased the NE oxidation current at all temperatures for MA, but produced no change in current amplitude for MV (Fig. 4.4). The rate limiting step for α_2AR mediated autoinhibition of NE release is the time required for sufficient build up of the NE concentration at the receptors during a train of stimulation [124]. In our study, there was sufficient time (6s) for the accumulation of NE at α_2ARs, at least in MA, as indicated by the increase in oxidation current caused by idazoxan through the temperature range studied. It is also likely that sufficient NE would be available to activate prejunctional α_2ARs on perivenous nerves but oxidation currents recorded from MV were unaffected by idazoxan at any temperature. Sympathetic nerves supplying MV do express functional α_2ARs as exogenously applied α_2AR agonists inhibit NE oxidation currents in these blood vessels [91]. G_i/G_o protein blockade by PTX failed to increase the NE current demonstrating the presynaptic G_i/G_o protein, which couples to α_2ARs, does not function as effectively in MV compared to that in MA. However, the increase of NE current caused by PTX in MA was smaller compared to the increase caused by idazoxan. The extra current increase caused by idazoxan could be due to the blockade of the low affinity intrajunctional buffering sites, which bind NE and re-release it at a later time [124]. It may also be due to the low efficiency of the drug itself, or an insufficient tissue incubation period with PTX, since the effect of PTX inhibition on neurotransmitters release is temperature and time dependent [194]. Nonetheless,

our work suggests that with the same PTX treatment, the function of G_i/G_o proteins in MV is not as effective as that in MA. Taken together, these data suggest that NE release is not tightly regulated by endogenous NE acting presynaptic α_2AR in rat MV. It is possible that the prejunctional α_2AR on perivenous nerve endings is not accessible to endogenously released NE. Alternatively, the lower density of sympathetic nerve fibers supplying MV may reduce the opportunity for lateral inhibition by NE released from adjacent varicosities [124].

An interesting finding from the present work is that the increase in NE oxidation current caused by idazoxan was augmented in MA at 28 °C. After α_2AR blockade in MA, the peak NE current increased 83% at 37 °C but 102% at 28 °C; the current rise slope increased 69% at 37 °C but 122% at 28 °C. In addition, at 28 °C, the NE oxidation current peaked and began to decline prior to the end of the stimulus train but in the presence of idazoxan, the current increased throughout the train. There are two potential explanations for these results. First, sympathetic nerve endings, like other nerves, contain a readily releasable pool and a reserve pool of synaptic vesicles. The reserve pool is mobilized during trains of stimulation and helps to maintain NE release during bursts of action potentials [124]. In our studies, a large amount of NE may be released from the readily releasable and reserve pools of NE at 37 °C, but only a small fraction binds to α_2ARs. This would produce minimal feedback inhibition. However, at 28 °C, less NE is released from both pools of transmitter and a larger fraction of NE binds to the α_2AR producing more efficient autoinhibition. It

is also possible that the presynaptic α_2AR binding affinity for NE is greater at 28 °C than at 37 °C. Previous work showed that cooling augments postjunctional α_2AR, but not α_1AR, function on vascular smooth muscle in rat tail arteries and canine veins [158, 195, 196].

4.3.3 Low Efficiency of NE Transporter in MV

NET is a monoamine transporter that transports around 90% of the NE released from sympathetic nerves back into nerve terminals [75]. NET can be blocked by cocaine and NET function is regulated by several neurotransmitters, temperature, peptides, psychostimulant drugs, ionic environment, nucleotides and various pathological conditions [76]. Vanhoutte and co-workers reported that, in canine cutaneous veins, cooling reduced NE uptake [195] and Yamamoto et al. [156] came to the same conclusion with rat mesenteric arteries. In our studies, cocaine increased the peak NE current in MA but not MV at all temperatures studied and cocaine increased the Q_{10} for the peak NE current in MA. The NET expressed in HEK 293 cells has a Q_{10} value of 2.5 for transport of the fluorescent dye, ASP+ [197], so it would be anticipated that NET would function more efficiently at 37 °C vs. 28 °C. This may be why the NE current increased markedly at 37 °C where NET would be most effective at clearing NE. This would account for the increased Q_{10} value for the peak NE current in the presence of cocaine.

Cocaine also increased the current rise slope for MA at 37 and 28 °C indicating that NET clears NE even as it is being released. However, Venton *et*

al monitored the actions of cocaine on dopamine release in the striatum of anesthetized mice and they concluded that cocaine also enhanced dopamine release by mobilizing a synapsin-dependent reserve pool of dopamine-containing synaptic vesicles [198]. We can not exclude the possibility that the increased rise slope of the NE current is partly due to increased NE release caused by cocaine. The NE current rise slope, peak current or current decay were not altered in MV at any temperature by cocaine indicating that NET does not make a major contribution to NE clearance in rat MV even though NET expression can be detected in these blood vessels [34]. Guanethidine inhibited NE release through NET and therefore the complete inhibition of NE release by guanethdine in MV (Fig. 4.9) also support that MV express NET, however, NET may not be positioned to clear endogenously released NE or the low density of varicosities in MV prevents lateral clearance by varicosities adjacent to those that release NE.

The NE current decay time was increased by cocaine in MA at 37 and 28 °C and cocaine treatment removed the difference in the temperature sensitivity of NE currents between MA and MV (Fig. 4.8). This result indicates that NET is an important factor accounting for MA *vs.* MV differences in temperature sensitivity. Taken together, our study indicates that NET plays an important role in NE clearance in MA but NE is mainly cleared by diffusion and possibly metabolism in MV.

4.3.4 NE Vesicle Pools at Sympathetic Nerve Endings

Sympathetic nerve endings, like other nerve endings, contain two vesicle pools: the reserve pool and the readily releasable pool [124]. The readily releasable pool is composed of docked vesicles that are depleted during high frequency stimulation. The readily releasable pool is maintained by vesicle recycling and refilling from the reserve pool [199]. Our data show that at 28 °C, the NE current in MA, but not MV, declines prior to the end of the stimulus train. This may be due to a small readily releasable pool or slow mobilization of the reserve pool at low temperature in individual varicosities. Ultrastructural studies have revealed the sympathetic nerve varicosities can form specialized neuromuscular junctions in submucosal arterioles and mesenteric veins [12-14]. These junctions have active zones with synaptic vesicle clusters and there is no obvious difference between individual neuroeffector junctions or in junctional density in arteries or veins. This suggests that the difference in temperature sensitivity of peak NE oxidation currents is related to differences in release and clearance mechanisms within individual neuroeffector junctions.

It is possible that the readily releasable pool is larger in MV but the reserve pool of vesicles is further away from the active zone in perivenous compared to periarterial nerves. Therefore, NE release from perivenous sympathetic nerves is greater than from periarterial nerves at 37 °C, but at lower temperatures, the transport rate of reserve vesicles to the release sites is slow, leading to a reduction in NE release from perivenous nerves and the current is comparable to that at MA. This proposal is consistent with data obtained in adrenal chromaffin cells where it was shown that refilling of the readily releasable pools is more

efficient at physiological temperatures [193]. At room temperature, the release of catecholamines from the reserve pool is delayed compared to that at 37 °C and this difference is attributed to a decline in temperature-dependent mobilization of the reserve pool of vesicles [200]. The rate of vesicle pool depletion is also slowed at a synapse in the CNS at physiological temperatures due to an acceleration of vesicle recruitment to release sites [201].

4.4 Summary and conclusions

Our work demonstrates that NE release and clearance from rat periarterial and perivenous sympathetic nerves are regulated differently. This difference is based largely on the function of prejunctional α_2ARs and NET but may also include different function or expression of calcium channels. These differences revealed the greater temperature sensitivity of NE overflow from sympathetic nerves in MV compared to MA. It is possible that there are also MA-MV differences in the content and recycling dynamics of NE containing vesicles in periarterial and perivenous sympathetic nerves. These differences in neuroeffector transmission may contribute to the different hemodynamic functions of mesenteric arteries and veins.

CHAPTER 5

IMPAIRED ADRENERGIC NEUROTRANSMISSION TO MESENTERIC ARTERIES BUT NOT VEINS IN DOCA-SALT HYPERTENSIVE RATS

5.1 Introduction

The sympathetic nervous system innervating the splanchnic circulation plays an important role in blood pressure regulation [7]. Mesenteric arterial resistance vessels (MA) and mesenteric venous capacitance vessels (MV) in the splanchnic circulation are particularly important [168]. MA and MV are densely innervated by sympathetic nerves, which release norepinephrine (NE) ,adenosine–triphosphate (ATP) and neuropeptide Y (NPY) [202]. NE mediates a constriction via binding with α_1-adrenergic receptors, while ATP causes constriction by binding to P2X receptors on the postjunctional smooth muscle cells. While NE and ATP are the main neurotransmitters for vasoconstriction in MA, NE is the dominant neurotransmitter in MV in rats [31, 33, 203]. The venous system contains ≈ 70% of the total blood volume, most in the small veins and venules, and has been shown to be important in the development of hypertension [95, 204, 205]. MV are also more sensitive to sympathetic activation than MA and perivenous sympathetic nerves release more NE upon nerve stimulation [88, 89].

The release of NE from peripheral nerves depends on the influx of Ca^{2+} through voltage dependent Ca^{2+} channels. Ca^{2+} stimulates migration, fusion and exocytosis of synaptic vesicles [51]. After being released, 90% of the NE is

recaptured into the nerve terminal by the NE transporter (NET) [76]. Prejunctional regulation of NE release occurs via binding of NE to α_2-adrenergic autoreceptors (α_2AR) on sympathetic nerve endings [35]. It could also be regulated by the ATP hydrolysis product, adenosine binding with prejunctional adenosine A1 autoreceptors to inhibit NE release through negative feedback [29, 30]. Both of these receptors are coupled to pertussis-toxin sensitive second messenger systems which inhibit neurotransmitter release in part by inhibiting Ca^{2+} channels and in part by inhibiting adenylate cyclase [61]. Previous work suggested that NE release in MA and MV is regulated differently by prejunctional α_2AR and adenosine A1 receptors.

Elevated sympathetic nerve activity which results in increased NE level occurs in human hypertension and various animal models of hypertension, such as deoxycorticosterone acetate (DOCA)-salt and spontaneously hypertensive rats [18, 34, 75, 206]. However, the mechanisms that lead to impaired regulation of NE in hypertension are not clear. The altered NE regulation in DOCA-salt hypertension is closely related with the activity of sympathetic nerve firing rate, prejunctional Ca^{2+} channels, autoreceptors and NET uptake [59, 75, 79, 207]. However, the results with the function of these receptors in DOCA-salt rats are controversial. For example, both impaired [23, 208] and unaltered [67] prejunctional α_2AR in the isolated MA have been reported. Moreover, few detailed studies of the mechanisms underlying increases in sympathetic input to veins have been done in hypertension [8, 34, 209]. Since NE release and clearance is a multi-step biochemical process, one manipulation to probe the

altered mechanisms of NE release and clearance in DOCA-salt hypertension is through the study of the temperature dependence of NE overflow. Temperature has large effects on enzyme kinetics, plasma membrane fluidity, synaptic transmission and vascular function [159]. Importantly, temperature variation has been used for many years as an experimental tool for probing the molecular mechanisms underlying neurotransmitter release in the nervous system [152, 154, 155, 195].

Continuous amperometry with a carbon fiber microelectrode has been used to detect the nerve stimulation-induced endogenous NE [127, 175, 187]. At a potential of 500 mV, NE can be detected as an oxidation current, as co-transmitters ATP and NPY are non-electroactive at this potential. This technique allows measurement of NE very near the release sites in real time and in response to stimulation parameters that closely mimic endogenous sympathetic nerve activity. The amount of NE measured at the microelectrode is determined by the amount of NE released offset by reuptake and diffusion. And since the microelectrode is so close to the NE release sites, NE release and clearance kinetics can be studied. Similar observations have previously been made for NE-induced electrochemical signals recorded at the adventitial surface of the rat tail artery [128, 137].

In the present work, continuous amperometry with a carbon fiber microelectrode was used to detect nerve stimulation induced endogenous NE from sympathetic nerves supplying rat MA and MV *in vitro*. We used temperature as a probe to study the release and clearance mechanisms of NE and how these

mechanisms are altered in DOCA-salt hypertensive rats. The study evaluated the effect of prejunctional Ca^{2+} channel, α_2AR and NET blockade on NE release and clearance in sham and DOCA-salt MA and MV. We tested the hypothesis that impaired prejunctional α_2AR and NET are involved in the altered regulation of NE in synaptic transmission in DOCA-salt hypertension.

5.2 Results

5.2.1 Sham and DOCA-salt rats

Mean systolic blood pressures for sham and DOCA-salt rats were 121 ± 5 mmHg (n=56) and 198 ± 7 mmHg (n=52), respectively ($P < 0.05$). The mean body weights of sham and DOCA-salt rats were 400 ± 10 g and 321 ± 12 g, respectively ($P < 0.05$).

5.2.2 Temperature dependence of NE oxidation currents

Representative tracings of NE oxidation currents, elicited by 10 Hz trains of focal nerve stimulation, at MA and MV from sham and DOCA-salt rats are shown in Fig. 5.1. The oxidation currents were normalized to the basal level before nerve stimulation at 37 and 28 °C (Fig. 5.1). The current progressively increased during the stimulation period of 6 s. During this period, multiple action potentials likely occur that cause NE to build up in the neuroeffetor junction faster than NE can be cleared by the NET. At 37 °C, the oxidation current recorded in DOCA-salt MA was larger than that recorded from sham MA (13.1 pA *vs.* 10.2 pA). Furthermore, the temporal rise in the oxidation current occurred faster in DOCA-salt MA than in

sham MA. At 28 °C, NE current from both sham and DOCA-salt MA decreased to around 5 pA, and therefore the relative current decrease was greater in DOCA-salt MA. However, there were no differences in the amplitude of oxidation currents recorded for sham and DOCA-salt MV at any temperature. These data are summarized in Fig. 5.2 A and B. There was a temperature dependent increase in NE current in all blood vessels. Significant differences in peak oxidation current are seen at 37 and 34 °C for DOCA-salt MA compared to sham MA. At 37 °C, the NE current in DOCA-salt MA was around 1.3 times greater than sham MA while they were comparable at 28 °C, suggesting the overflow of NE from DOCA-salt MA is more temperature-sensitive than in sham MA. The temperature coefficient, Q_{10}, was the ratio of response amplitudes measured over a 10 °C change in temperature. The calculated Q_{10} values are summarized in Table 5.1. The Q_{10} values for DOCA-salt MA is significantly greater than sham MA (2.8 ± 0.2 *vs.* 2.0 ± 0.2, $P < 0.05$), which indicate that NE release and/or clearance in DOCA-salt MA has greater temperature sensitivity than that for sham MA.

5.2.3 Kinetics of NE oxidation currents at different temperatures

The measured oxidation current results from diffusional escape of some fraction of the total NE molecules released at nearby neuroeffector junctions. The early rise of current is controlled by the release kinetics (number of firing events, concentration of NE per firing event, etc.). The current decay is controlled largely by the clearance kinetics (reuptake). The current transient near the peak is

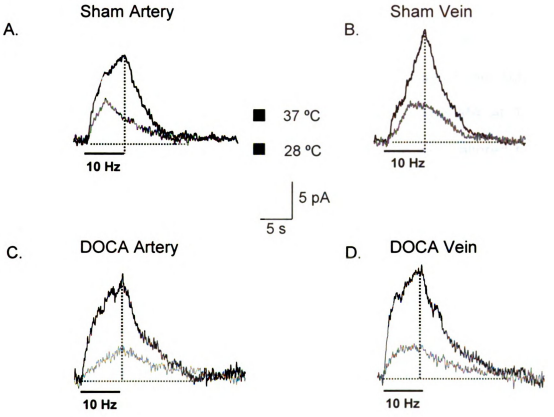

Figure 5.1 *In vitro* continuous amperometric recordings of NE oxidation currents from sham MA (A) and MV (B), and DOCA-salt MA (C) and MV (D) at 37 °C (black trace) and 28 °C (grey trace). NE oxidation currents were evoked by 10 Hz stimulus trains and the bar under the current traces represents the period of nerve stimulation (60 pluses with a 0.5 ms pulse width).

controlled by a combination of the release kinetics offset by the clearance kinetics. Current rising slope (rate of rise), rise time, and decay time have been used to access the neurotransmitter release and clearance kinetics [91, 187]. The representative tracings in Fig. 5.1 illustrate that the rise of the oxidation current for DOCA-salt MA is much faster than that for sham MA at 37 °C. Furthermore, the rates of the current rise and decay time were altered by the temperature. Fig. 5.3 shows plots of current rise slope (A), rise time (B), and decay time (C) for MA and MV from control and DOCA-salt rats at 37 and 28 °C. At 37 °C, the NE current rise slope in DOCA-salt MA was significantly greater than that in sham MA, but not at 28 °C. The current rise slope for both sham and DOCA-salt MV was greater than sham MA at 37 °C but there was no significant difference in the rise slope between sham and DOCA-salt MV. There were no significant differences in the current rise time among these blood vessels at 37 °C. At 28 °C, the current rise time was decreased compared to that at 37 °C for each type of the blood vessel, however, the rise time in sham MA is significantly lower compared to other types of blood vessels. The clearance of NE was significantly slower in DOCA-salt MA compared to sham MA at 37 °C, but not at 28 °C. There was no difference of NE clearance kinetics between sham and DOCA-salt MV at either temperature. Together with the temperature dependent NE peak oxidation currents, these data indicate that sympathetic neurotransmission to MA is disrupted in DOCA-salt hypertension.

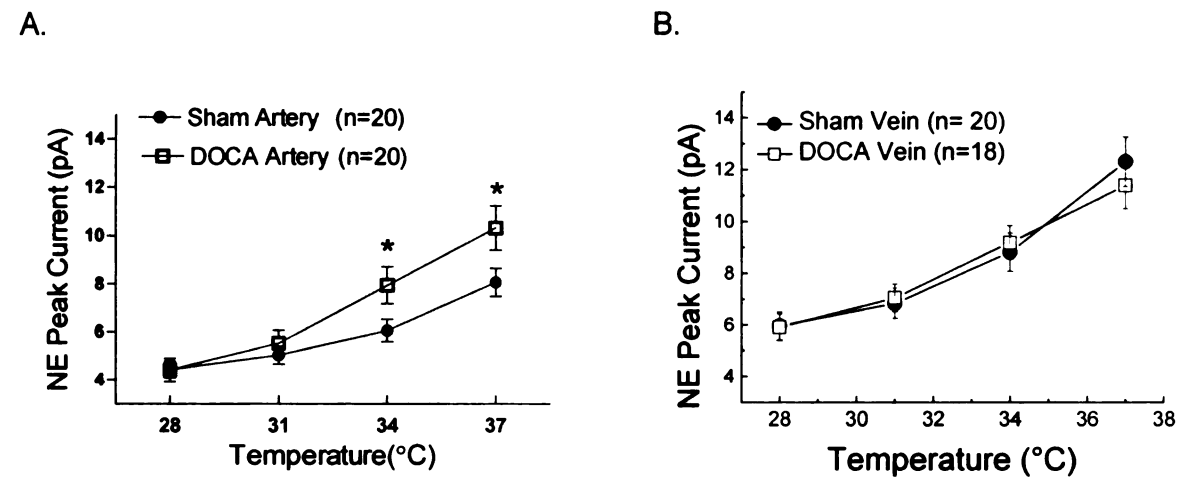

Figure 5.2 Temperature effects on NE maximum oxidation current evoked by focal electric stimulation at MA (A) and MV (B) from sham and DOCA-salt rats. The peak current amplitude in DOCA-salt MA is more steeply temperature dependent. Data are mean ± S.E.M. and * indicates significantly different from sham MA, $P < 0.05$.

5.2.4 Prejunctional α_2 adrenergic receptors function in DOCA-salt rats

The prejunctional α_2 adrenergic receptor (α_2 AR) regulates NE release from sympathetic nerves through a negative feedback mechanism [59, 60]. Therefore, we used the α_2 AR antagonist, idazoxan (1 μM), to investigate prejunctional α_2 AR function in DOCA-salt MA and MV. As shown in Fig. 5.4, idazoxan increased the peak oxidation current almost two-fold in sham MA at all temperature, but this effect was not as prominent in DOCA-salt MA. Idazoxan increased the peak NE current by 83% at 37 °C but 102% at 28 °C in sham MA indicating that prejunctional α_2AR can bind with NE more efficiently at 28 °C to regulate NE release. Although there were significant peak current increases in DOCA-salt MA after α_2AR blockade, the increases were much less than that occurred at the same temperature in sham MA, e.g. 30% increase at 37 °C and 51% increase at 28 °C (Fig. 5.4A and B). The data suggest that prejunctional α_2 ARs function is impaired in DOCA-salt MA. Idazoxan did not increase the NE peak current significantly in sham and DOCA-salt MV at any temperature (Fig. 5.4C and D). Idazoxan didn't change the Q_{10} for peak current for any type of blood vessel (Table 5.1).

Figure 5 shows the 10-90% rise slope (A,B), rise time (C,D) and decay time (E,F) for sham and DOCA-salt MA and MV at 37 and 28 °C in the absence (control) and presence of idazoxan. Idazoxan increased rise slope of the current in sham MA, but not DOCA-salt MA, and sham and DOCA-salt MV, at 37 and 28 °C. The current rise time was not changed by idazoxan in any blood vessel at 37 °C; however, the current rise time was increased significantly by idazoxan in

Figure 5.3. Comparison of the time course of NE oxidation current between sham and DOCA-salt MA, and sham and DOCA-salt MV at 37 and 28 °C. (A) the 10 to 90% rise slope of NE oxidation current is significantly lower in sham MA compared to DOCA-salt MA, sham MV and DOCA-salt MV at 37 °C but not at 28 °C, (B) the 10 to 90% rise time of NE oxidation current is decreased significantly by temperature from 37 to 28 °C for all types of tissues with the sham MA has the maximum decrease; and the rise time for sham MA is significantly lower than DOCA-salt MA, sham and DOCA-salt MV at 28 °C (C) the 10 to 90% decay time of NE oxidation current was much less in sham MA than in DOCA-salt MA at 37 °C but not 28 °C; the current decay time was longer in sham and DOCA-salt MV than sham MA at both 37 °C and 28 °C. Data are mean ± S.E.M. and * represents significantly different from 37 °C; # represents significantly different from sham MA, $P < 0.05$.

A.

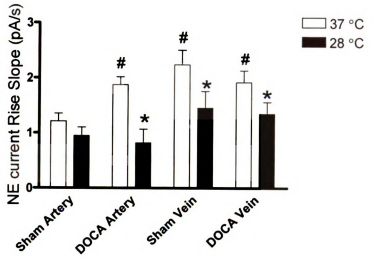
37 °C
28 °C
NE current Rise Slope (pA/s)
0
1
2
3
#
*
Sham Artery
DOCA Artery
Sham Vein
DOCA Vein

B.

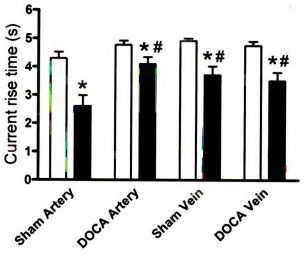
Current rise time (s)
0
1
2
3
4
5
6
*
*#
Sham Artery
DOCA Artery
Sham Vein
DOCA Vein

C.

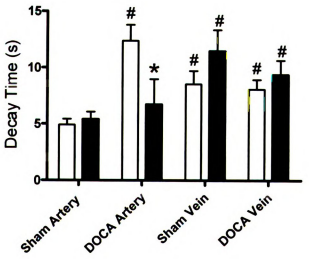
Decay Time (s)
0
5
10
15
#
*
Sham Artery
DOCA Artery
Sham Vein
DOCA Vein

sham MA at 28 °C (Fig. 5C,D). Idazoxan did not affect current decay time in any types of blood vessels at either temperature (Fig. 5E,F) suggesting that prejunctional α_2ARs do not contribute to NE clearance.

5.2.5 Function of pertussis toxin (PTX) sensitive G protein in DOCA-salt rats

The α_2AR is G_i/G_o protein coupled receptor. PTX was used to examine the function of G_i/G_o protein. Peak NE oxidation currents were significantly increased after PTX incubation at 37 and 28 °C for sham MA but not DOCA-salt MA, sham and DOCA-salt MV (Fig. 5.6). After α_2AR blockade by 1 μM idazoxan, the peak currents increased for control and PTX treatment groups from sham MA (Fig. 5.6A). The peak current was increased by idazoxan only in the control group from DOCA-salt MA at both temperatures, which is consistent with the result shown in Fig. 5.4. There were no differences in the oxidation current before and after idazoxan application for sham and DOCA-salt MV at either 37 or 28 °C. PTX didn't change the Q_{10} for the NE current for any type of blood vessel (Table 1). The oxidation current rise slope, rise time and decay time after PTX incubation were similar to the data shown in Fig. 5.5. PTX only increased the current rise slope for sham MA from 1.4 ± 0.2 to 2.1 ± 0.4 pA/s ($P < 0.05$) at 37 °C and from 1.0 ± 0.3 to 1.8 ± 0.1 pA/s ($P < 0.05$) at 28 °C. The current rise time was prolonged from 2.4 ± 0.4 to 3.8 ± 0.3 s ($P < 0.05$) at 28 °C but not at 37 °C for sham MA. The current rise slope and rise time didn't change for DOCA-salt MA and sham and DOCA-salt MV. PTX didn't change the current decay time for any

Q10	Sham Artery	DOCA Artery	Sham Vein	DOCA Vein
Control	2.0 ± 0.2	2.8 ± 0.2 *	3.1 ± 0.4 *	2.7 ± 0.2 *
Idazoxan	1.7 ± 0.2	2.6 ± 0.3	3.3 ± 0.7	3.0 ± 0.2
Cocaine	2.7 ± 0.3 #	2.3 ± 0.4	3.0 ± 0.4	2.4 ± 0.2
PTX	1.9 ± 0.2	2.9 ± 0.4	2.9 ± 0.4	2.5 ± 0.3

Table 5.1 Q_{10} values for sham and DOCA-salt MA and MV with different treatments. Data are mean ± S.E.M. *indicates significantly different from sham MA; # indicates significantly different from control, $P < 0.05$.

type of blood vessel.

5.2.6 NET Function in MA and MV from DOCA-salt rats

NE is cleared by NET and/or diffusion away from the junction. To test NET function in DOCA-salt MA and MV, I measured the temperature dependent NE current after the blockade of NET by cocaine (10 μM). Fig. 5.7 shows peak oxidation currents before and after cocaine. Cocaine increased the NE current in sham MA at all temperatures withaa maximum increase of 81% from 8.8 to 15.9 pA at 37 °C. The current was increased significantly for DOCA-salt MA at 28 and 31 °C, while there was very little increase at 37 °C. NE current from sham and DOCA-salt MV were not significantly changed by cocaine at any temperature. Cocaine significantly increased the Q_{10} for sham MA and the difference in Q_{10} between sham and DOCA-salt MA disappeared (Table 1). This result indicates that NET is one of the important factors that contribute to the different temperature sensitivity of NE overflow between sham and DOCA-salt MA.

NE current rise slopes were increased by cocaine at 37 and 28 °C, with a greater increase at 37 °C for sham MA (Fig. 5.8A and B). Cocaine increased the current rise slope at 28 but not 37 °C for DOCA-salt MA. The current rise time was also increased for sham MA at 28 °C. NET blockade didn't affect the current rise slope and rise time in MV from sham and DOCA-salt rats. Since cocaine inhibits NET function, the remaining NE can only been cleared by diffusion which slows NE clearance kinetics. So there was prolonged NE current decay time in sham MA at 37 and 28 °C and in DOCA-salt MA at 28 °C. Cocaine did not

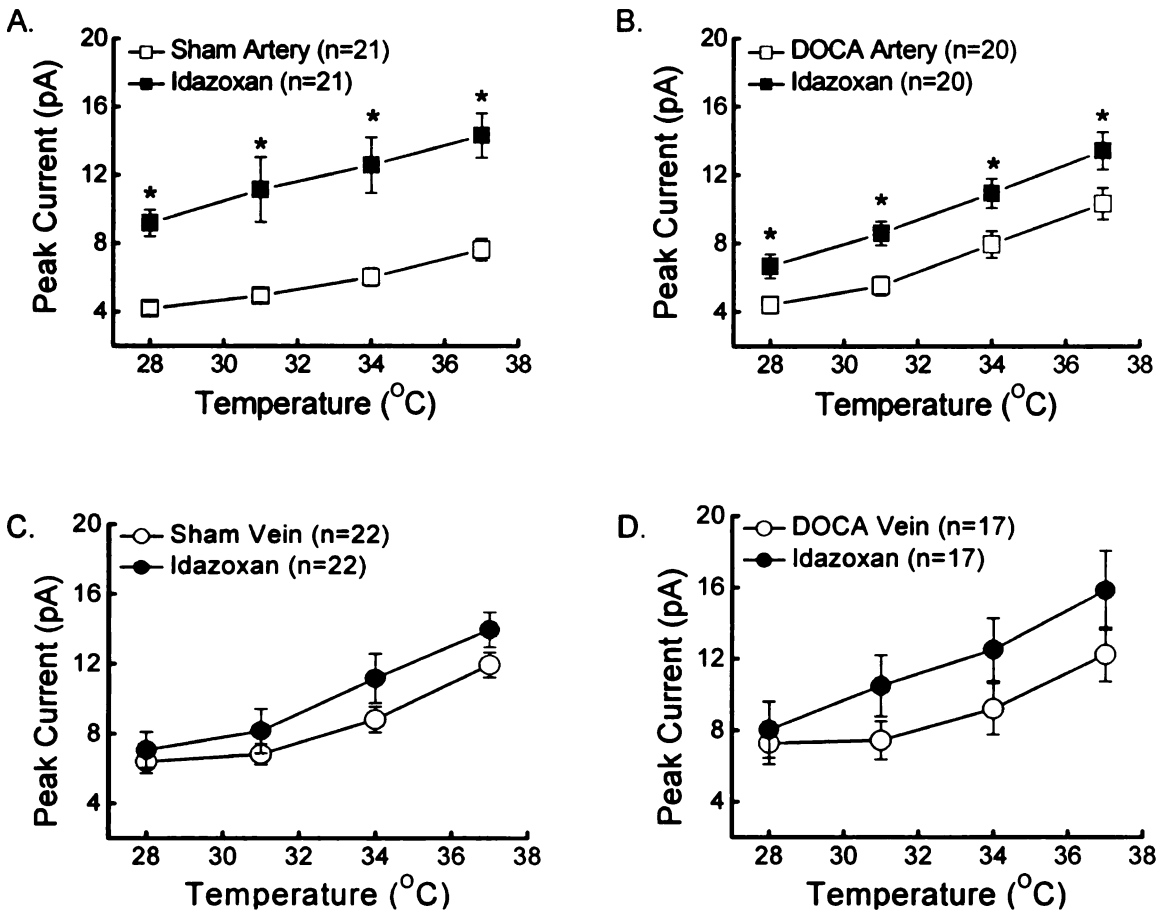

Figure 5.4 Effect of α_2AR antagonist, idazoxan (1 μM), on temperature dependent NE oxidation current at different temperatures. Idazoxan increased peak NE current more than two fold for sham MA (A) and around 30% for DOCA-salt MA at different temperatures (B). There was no change in NE current at sham MV (C) and DOCA-salt MV (D) after idazoxan treatment. Data are shown as mean ± S.E.M. and * represents significant different from control, $P < 0.05$.

change the current decay time in sham and DOCA-salt MV suggesting that NE clearance from the neuroeffector junction in MV is mainly by diffusion.

5.2.7 Ca^{2+} channel function is not altered in DOCA-salt MA

Miledi and Katz first discovered that neurotransmission was dependent on Ca influx into prejunctional terminals [51]. Depolarization-evoked entry of Ca^{2+} into nerve terminals plays a key role in triggering NE release during trains of stimulation of sympathetic nerves [174]. The role of Ca^{2+} sensitivity on adrenergic neurotransmission from sympathetic nerves was compared between sham and DOCA-salt MA since the differences were all found in MA. $CdCl_2$, a Ca^{2+} channel blocker, was applied y (10^{-8} – 10^{-4} M) at 37 °C and caused a concentration-dependent inhibition of peak NE amplitude (Fig. 5.9). $CdCl_2$ concentration response curves were not different between DOCA-salt and sham MA (pEC_{50} was 5.2 ± 0.3 and 5.0 ± 0.2, respectively, $P > 0.05$). $CdCl_2$ (100 mM) completely inhibited NE release.

5.3 Discussion

5.3.1 Temperature sensitive NE current in MA and MV from control and DOCA-salt rats

NE, ATP and NPY are co-transmitters released from sympathetic nerve endings supplying MA and MV. There is increased sympathetic nerve activity in DOCA-salt hypertension, which is associated with elevated plasma NE levels [34, 208, 210]. We, therefore, investigated the NE release and clearance

Figure 5.5 Comparison of the time course of NE oxidation currents from sham and DOCA-salt MA and MV at 37 and 28 ºC with and without idazoxan. The 10 to 90% rise slope of NE oxidation current was significantly increased after the treatment of idazoxan for sham MA at both 37 ºC(A) and 28 ºC (B); idazoxan increased 10 to 90 % current rise time significantly only at 28 ºC for sham MA (C and D); the 10 to 90% decay time of NE current did not change after the treatment of idazoxan at 37 ºC (E) and 28 ºC (F) for any type of tissues. Data are mean ± S.E.M. and * represents significant difference from control, $P < 0.05$.

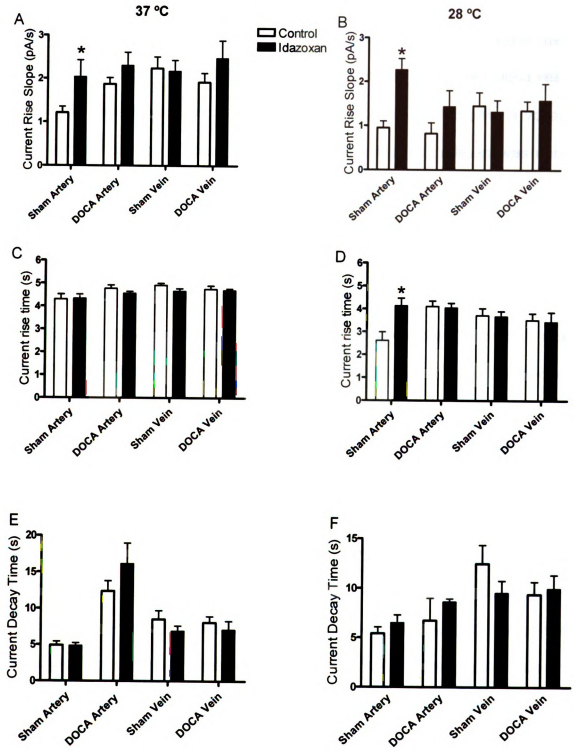
A
37 °C
Control
Idazoxan
Current Rise Slope (pA/s)
Sham Artery
DOCA Artery
Sham Vein
DOCA Vein
B
28 °C
C
Current rise time (s)
D
E
Current Decay Time (s)
F

mechanisms and how DOCA-salt hypertension differentially alters transmission to MA and MV. NE was measured *in vitro* as an oxidation current using continuous amperometry. Both NE oxidation current and the elicited blood vessel constriction were blocked completely by tetrodotoxin (TTX, 0.3 μM), a voltage-gated sodium channel blocker. This demonstrates that NE release was nerve-mediated. We also confirmed that the drugs used in this study (e.g., idazoxan, cocaine and $CdCl_2$) are electrochemically-inactive at carbon fiber microelectrodes at the potential where NE is detected. Therefore, they do not influence the reproducibility and stability of the NE measurement [186].

NE currents were temperature dependent for MA and MV from both sham and DOCA-salt hypertensive rats. This could be due to the effect of temperature on biological phenomena and, in particular, on enzyme kinetics, plasma membrane state, and synaptic transmission [211]. Dunn and Mercier have confirmed that decreasing temperature reduced the number of quanta of transmitter released per nerve impulses [212]. Our results indicated that at 37 °C, nerve stimulation evoked greater NE overflow in DOCA-salt compared to sham MA. However, this difference between sham and DOCA-salt MA decreased at lower temperatures and was abolished at 28 °C. NE overflow in DOCA-salt MA shows greater temperature sensitivity than sham MA. Increased NE overflow could be due to increased release of NE from sympathetic nerve terminals, impaired function of prejunctional autoreceptors, reduced clearance or extracellular enzyme metabolism. The altered mechanisms of NE release and clearance in DOCA-salt MA have a greater impact on NE regulation at 37 but not

28 °C. This point has been further confirmed by the fact that a greater current rise slope and prolonged decay time were observed for DOCA-salt MA, compared to sham MA only at 37 °C, which illustrates a faster release and slower clearance of NE regulation at DOCA-salt MA.

Dunn has pointed out in their work that the reduction in quantal content with temperature is probably the result of reduced calcium influx through voltage-gated calcium channels in the synaptic terminals [212]. Calcium passage through the pore-forming region of an open calcium channel has little temperature sensitivity [213]. Morris and Clarke pointed out that this high temperature-sensitivity of calcium channels resulted from coupling to multiple metabolic events [214]. Because neurotransmitter release is closely related with the function of calcium channels, we thus investigated the function of calcium channels in sham and DOCA-salt MA. However, my data show that $CdCl_2$ blocks NE release equally well in sham and DOCA-salt MA at 37 °C. Herein, the prejunctional differences related to NE release and clearance in sham and DOCA-salt MA is not due to the function of calcium channels.

Despite the focus on arteries, the role played by veins in the development of hypertension is important. Previous work has shown that there is increased sympathetically-mediated venoconstriction in hypertension [96, 97]. Mean circulatory filling pressure (MCFP) can provide a good estimate of overall circulatory capacitance or compliance, properties determined for the most part by the smooth muscle tone of veins when combined with measurements of blood volume [215]. Although MCFP cannot be measured directly in humans, it is

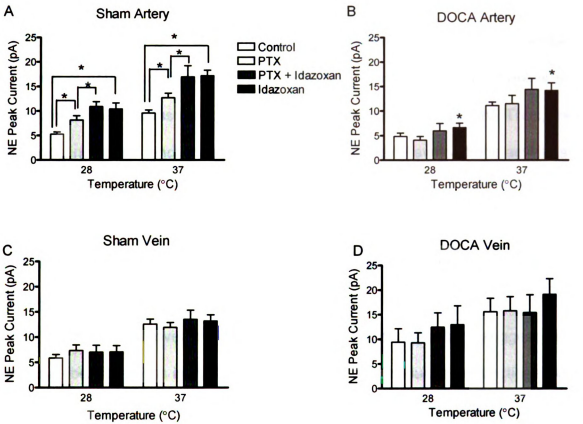

Figure 5.6 Effects of pertussis toxin (PTX, 3 μg/ml) on NE release at sham and DOCA-salt MA and MV. After 2h tissue incubation in PTX, NE maximum current was significantly increased at sham MA (A) but not DOCA-salt MA, sham and DOCA-salt MV (B, C and D). For comparison, we also blocked α_2AR function by idazoxan for the control and PTX treatment groups. Both NE current and current rise slope were increased significantly by idazoxan for sham control and PTX treatment groups (A) but the increase was very little in DOCA-salt MA control group (B). There was no current increase in sham and DOCA-salt MV groups (C and D). This represents that the function of G_i/G_o which couples to α_2AR is impaired in DOCA-salt MA and G_i/G_o does not function in sham and DOCA-salt MV as well as in sham MA. The current increased by idazoxan plus PTX was significantly greater than that caused by PTX alone for sham MA. Data are mean ± S.E.M. with * represents significant difference, $P < 0.05$.

increased in hypertension models, including DOCA-salt hypertension in rats [216-218]. This may be due to increased sympathetic activity [98], increased efficiency of neurotransmission [96] or both. My work indicates that there is no change in NE neurotransmission in DOCA-salt compared to sham MV. Thus, the difference in venous function is probably due to increased sympathetic activity at postjunctional but not prejunctional sites.

5.3.2 Impaired prejunctional α_2 adrenergic receptors function in DOCA-salt MA but not MV

The increased overflow of NE and current rise slope both suggest that there may be alterations in the local mechanisms that modulate prejunctional NE release. Previous work demonstrated that the release of NE from sympathetic nerves supplying MA is tightly related with the regulation by prejunctional α_2AR through a pertussis toxin-sensitive negative feedback mechanism [35, 60]. Importantly, impaired prejunctional α_2AR function is associated with hypertension in animals [7, 23, 59, 64] and humans [65, 66]. However, the function of α_2AR in DOCA-salt rats is controversial. Both impaired [23, 59] and unaltered [67] α_2AR autoreceptors in the isolated MA have been reported. Our work indicates that after the blockade of prejunctional α_2AR with its antagonist, idazoxan, peak NE current amplitude increased almost 2-fold in sham MA but much less increase occurred in DOCA-salt MA at any temperature. This is consistent with studies showing that another α_2AR antagonist, yohimbine, failed to increase the NE levels in the DOCA-salt mesenteric vasculature [23, 208]. The current rise slope

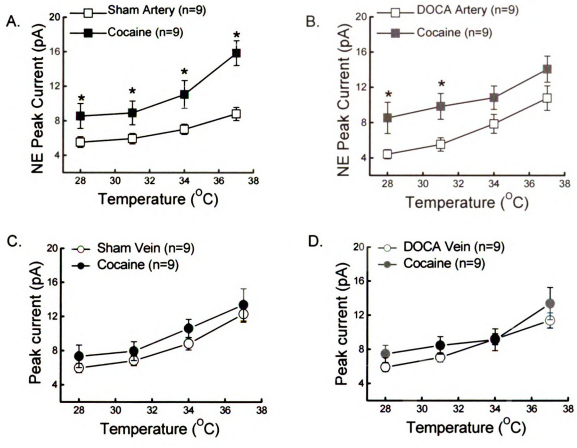

Figure 5.7 Effect of NE transporter blocker, cocaine (10 μM), on temperature dependent NE oxidation current. Oxidation current was significantly increased from sham MA at every temperature (A) but only at low temperatures from DOCA-salt MA (B). No current increase was observed at sham MV (C) and DOCA-salt MV (D). Data are shown as mean ± S.E.M. and * represents significant difference from control, $P < 0.05$.

was lower in sham MA than DOCA-salt MA at 37 °C. This may be due to the inhibition effect of prejunctional α_2AR on the release of NE after NE concentration at the neuroeffector junction accumulated to a certain degree. The current rise slope increased after α_2AR blockade significantly in sham MA but not in DOCA-salt MA indicating that NE release is regulated by prejunctional α_2AR but this regulation is impaired in DOCA-salt MA. However, the slow increase of the NE current in sham MA could be due to slow diffusion of NE from the junction to the electrode or NE diffusion could be delayed by NE binding with a low affinity binding site in or near the junction. There may be a low affinity intrajunctional NE binding site that does not play a role in activation of the smooth muscle but slows NE diffusion and thereby maintains the NE concentration at near smooth muscle receptors [124]. Furthermore, the effects of idazoxan could not be accounted for changes in NE clearance as this agent had no effect on the current decay time, which is consistent with previous work [91, 187]. I demonstrated previously that the prejunctional α_2AR response was augmented at 28 °C. After α_2AR blockade in sham MA, the peak NE current and the current rise slope increased more at 28 °C than that at 37 °C. In addition, the NE current reaches the maximum prior to the end of the stimulus train at 28 °C. However, after α_2AR blockade by idazoxan, the current increased until the stimulation stops for sham MA. This also suggests that α_2AR inhibit NE release more efficiently at 28 °C. The enhanced α_2AR function at 28 °C could be due to a higher percentage of NE binding with α_2AR, or a higher binding coefficient [158, 195, 196]. In DOCA-salt MA, the current rise time decreased very little from 37 to 28 °C and it failed to increase after α_2AR

Figure 5.8 Comparison of the time course of NE oxidation currents from sham and DOCA-salt MA and MV at 37 and 28 °C with and without cocaine. The 10 to 90% rise slope of NE oxidation current was increased significantly after the treatment of cocaine for sham MA at both 37 °C (A) and 28 °C (B) and for DOCA-salt MA at 28 °C. Cocaine increased the 10 to 90 % current rise time significantly only at 28 °C for sham MA (C and D); the 10 to 90% decay time of NE current was prolonged in sham MA at both 37 °C (E) and 28 °C (F); and it was prolonged in DOCA-salt MA at 28 °C only. Data are mean ± S.E.M. and * represents significant difference from control, $P < 0.05$.

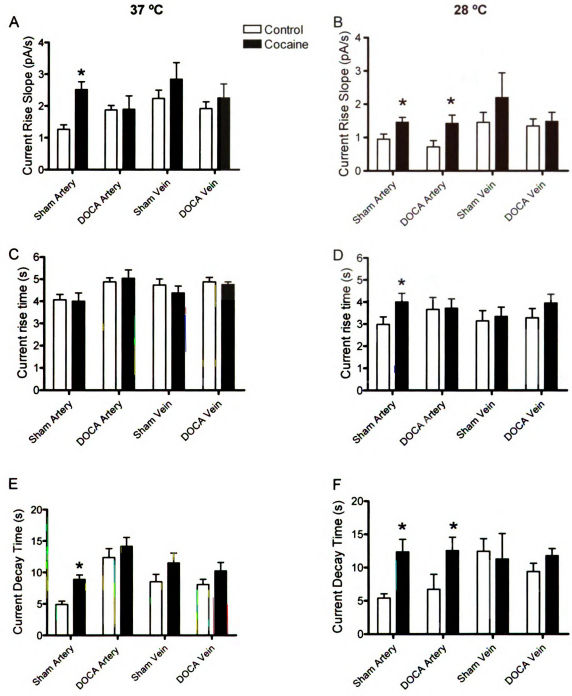
37 °C
28 °C
Control
Cocaine
A
B
C
D
E
F
Current Rise Slope (pA/s)
Current rise time (s)
Current Decay Time (s)
Sham Artery
DOCA Artery
Sham Vein
DOCA Vein
*

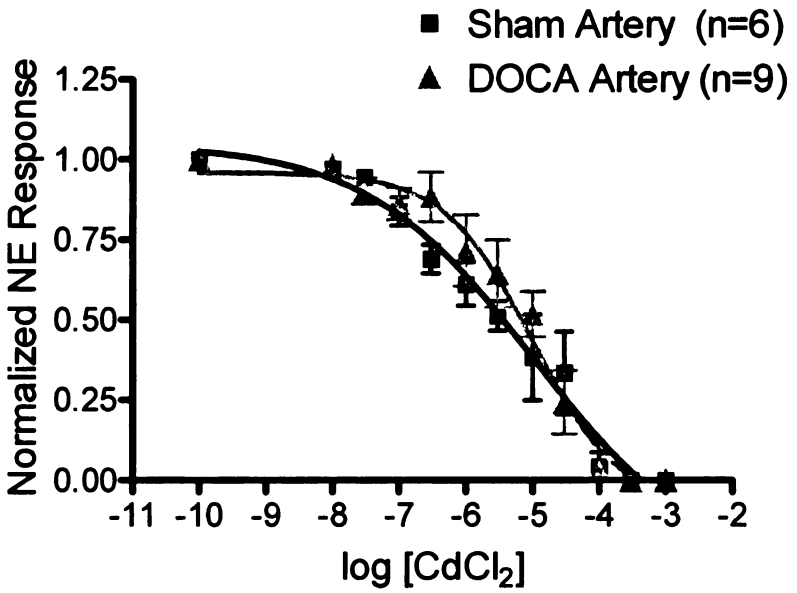

Figure 5.9 Concentration response curves for Ca channel blocker $CdCl_2$ on NE inhibition were not different between sham and DOCA-salt MA. Data are mean ±S.E.M.

blockade at 28 °C, suggesting that the NE release from sympathetic nerve terminals is not tightly regulated by the α_2AR. Furthermore, it is known that in sham MA, ATP is the main neurotransmitter causing arterial constriction, while NE is the dominant neurotransmitter in the DOCA-salt MA. It has been reported that ATP in the sympathetic nerve terminal is easier to be depleted in DOCA-salt MA [63]. Our data suggest that NE is resistant to depletion, which might be a compensatory mechanism to maintain vascular tone in DOCA-salt MA.

Prejunctional α_2ARs couple to pertussis toxin (PTX) sensitive G_i/G_o proteins to inhibit release of neurotransmitter by opening K^+ channels, blocking voltage-dependent Ca^{2+} channels and inhibiting adenylate cyclase. The impaired function of prejunctional α_2AR in DOCA-salt MA may be due either to receptor down regulation or the impaired signaling pathway to the autoreceptors. We used PTX to inhibit G_i/G_o protein function. PTX failed to increase the NE current in DOCA-salt MA demonstrating that the prejunctional G_i/G_o protein which couples to α_2ARs does not function effectively compared to that in sham MA. Taken together, my data suggest that NE release is not tightly regulated by endogenous NE acting presynaptic α_2AR in DOCA-salt MA which may be due to the less functional G_i/G_o protein. This alteration may be related with the increased level of reactive oxygen species which can cause protein and tissue damages [219].

In contrast to MA, there is neither significant peak NE current increase, nor the current rise slope increase after prejunctional α_2AR blockade in sham and DOCA-salt MV. This result is consistent with the study showing no significant increase in NE release after yohimbine application in portal veins from DOCA-salt

rats [59]. PTX treatment failed to induce the NE current increase in MV. These data suggest that NE release is less regulated by prejunctional α_2AR in MV, although MV does express α_2AR [91]. This may be due to the low density of prejunctional α_2AR, or the α_2AR in MV is not close enough to the NE release sites at the sympathetic nerve terminals. However, cooling did not augment the function of prejunctional α_2AR in MV as compared to sham MA (Fig. 5.4). This suggests it is more likely that the prejunctional α_2AR in MV locate at some distance away from the NE release sites. At 37 °C, there is more NE released and a small portion can diffuse away to activate the prejunctional α_2AR, so the peak NE current increases after α_2AR blockade, though not significantly. However, at 28 °C, NE release is decreased and little NE can diffuse to activate prejunctional α_2AR. So no increase in peak NE current was observed in sham and DOCA-salt MV although the binding of NE with prejunctional α_2AR became more efficiently at low temperature.

5.3.3 Dysfunction of NET in DOCA-salt MA but not MV

NET removes NE from the neuroeffector junction once it is released from the nerve terminal [220]. Reduced reuptake may explain the elevated NE in DOCA-salt hypertension and human essential hypertension [77, 78]. However, unaltered neuronal reuptake of NE in DOCA-salt hypertensive rats [79, 80] and enhanced NE neuronal uptake in chronic hypertension model and spontaneously hypertensive rats arteries [81, 82] have been reported also. Our study demonstrates that there is a dysfunction of NET and the reuptake of NE is

reduced in DOCA-salt MA. After block NET function, peak NE current increased markedly at all temperatures with the greatest increase at 37 °C in sham MA. This suggests that NET function is reduced at low temperature, which is consistent with previous work showing that cooling can depress the extraneuronal uptake of NE in vascular smooth muscle [156, 158]. The reduced function of NET to increase NE amplitude might help to compensate for reduced synaptic transmission at low temperature and thus maintain the NE concentration at the smooth muscle receptors. However, the increased peak current and prolonged current decay time were only seen at low temperature in DOCA-salt MA after NET blockade suggesting the reduced function of NET. At 37 °C, there were excessive NE released, so the dysfunctional NET uptake NE less efficiently. While at lower temperature, there were less NE being released so NET can bind with NE and function relatively efficient to uptake NE. NET can clear NE before it diffuses to the microelectrode and this leads to the increased current rise slope for MA at 37 and 28 °C and increased current rise time at °C after NET blockade. Cocaine also increased the Q_{10} for the peak NE current in sham MA which is then similar to that for DOCA-salt MA. Thus, NET is one of the important factors that accounts for the temperature dependent sensitivity of NE overflow but this function is impaired in DOCA-salt MA.

There was no change in the peak NE current, current rise slope, current rise time, and decay time after NET blockade in sham and DOCA-slat MV. This could be due to either low density of NET at the nerve endings or NET is localized far away from the NE release sites to clear NE, although MV does

express NET in sympathetic ganglia [34]. Our result reveals that NE clearance seems to be mainly by diffusion instead of uptake through NET in sham and DOCA-salt MV.

5.4 Conclusion

The present work demonstrates that, the overflow of NE display greater temperature sensitivity in DOCA-salt MA than sham MA and NE transporter account for this difference. Presynaptic α_2AR and NE transporter play a greater role in regulating NE release and clearance at the neuroeffector junction in sham MA than in MV. These mechanisms have been altered in DOCA-salt MA but not MV. The elevated NE overflow from perivascular sympathetic nerves in DOCA-salt MA is likely due to impaired G_i/G_o protein coupled presynaptic α_2-adrenergic autoreceptors, and NE transporters, but not presynaptic calcium channels.

CHAPTER 6

O_2^- INTERACTS WITH PERTUSSIS TOXIN-SENSITIVE G-PROTEINS TO DISRUPT α_2 ADRENERGIC RECEPTOR FUNCTION INSYMPATHETIC NERVES SUPPLYING MESENTERIC ARTERIES IN DOCA-SALT HYPERTENSION

6.1 Introduction

Under physiological conditions, reactive oxygen species (ROS) act as signaling molecules regulating the growth and function of vascular smooth muscle cells [103]. Enhanced production of ROS and a decrease in the antioxidant reserve in plasma and tissues were reported in hypertensive animals and human [116]. The major ROS resulting from oxidative stress are superoxide anion, hydrogen peroxide, hydroxyl radical and peroxynitrite ($\cdot O_2^-$, H_2O_2, $OH\cdot$, $ONOO\cdot$). It has been found that in the deoxycorticosterone acetate (DOCA)-salt, the genetic SHR, the Dahl-salt sensitive and the angiotensin-induced models of hypertension in rats, that a progressive increase of $\cdot O_2^-$ production in vascular and cardiac tissue occurs during the development of hypertension [106-108, 221]. $\cdot O_2^-$ is at the origin of the cascade leading to the formation of most ROS. It is a free radical species, which is usually short-lived due to its rapid reduction by superoxide dismutase (SOD) to hydrogen peroxide and then catalyzed to H_2O and O_2. [101].

NADPH oxidase is the major source of $\cdot O_2^-$ in the vasculature [222]. $\cdot O_2^-$ and NADPH oxidase activity are increased in DOCA-salt hypertension including

in the sympathetic nervous system [106, 223]. There are functional changes in the sympathetic nervous system in DOCA-salt hypertensive rat, including the increased sympathetic nerve activity and enhanced release of norepinephrine (NE) [18, 34]. ROS affect sympathetic nervous system function. H_2O_2 can activate the protein kinase C pathway causing facilitation of NE release from nerve terminals [224]. In addition, $\cdot O_2^-$ can reduce the effect of NO, which modulates NE release through a negative feedback mechanism [225]. A previous study revealed that ROS can cause enhanced production of inositol triphosphate and reduced production of cyclic GMP in cultured vascular smooth muscle cells [101]. Nishida *et al* revealed that a pertussis toxin-sensitive G protein is the target of ROS [115]. However, Giniatullin *et al* showed that the depressant effect of H_2O_2 on acetylcholine release was pertussis toxin-insensitive, ruling out Gi/o-protein dependent cascades [226]. In addition to the increased level of NADPH oxidase, SOD activity was reduced in DOCA-salt rats which can also cause increased levels of $\cdot O_2^-$ [106].

The effects of antioxidant treatment on ROS levels have been studied in animal models of hypertension. Some studies have shown that inhibition of ROS generation with apocynin (a NADPH oxidase inhibitor) and radical scavenging with antioxidants or SOD mimetics, such as tempol (4-hydroxy-2,2,6,6-tetramethylpiperidinyloxy), decrease blood pressure and prevent development of hypertension in most hypertensive models [222, 227, 228]. However, other studies have shown that acute treatment with antioxidants, such as ascorbic acid, do not decrease blood pressure in hypertensive patients [229] or in DOCA-salt

rats [113]. Long-term treatment of hypertensive patients with ascorbic acid can reduce systolic blood pressure [230]. In the adult hypertensive SHR model, chronic treatment with the antioxidants, melatonin or N-acetyl-cysteine, were found to reduce blood pressure, heart rate and circulating NE levels [120]. The effect of tempol on NE secretion, sympathetic nerve activity, and blood pressure regulation may be in part dependent and in part independent of NO [105, 113].

In DOCA-salt rats, there is increased plasma NE levels due, in part, to the impaired function of prejunctional α_2AR, which contributes to the increased sympathetic nerve activity [23, 64]. Although the precise effects of increased ROS in sympathetic nervous system are unknown, it is possible that ROS signaling can impair the nerve terminal and thereby cause increased release of NE. To test the hypothesis that ROS may raise sympathetic nervous system activity and impair the function at the neuroeffctor junction, I evaluated the effects of the NADPH oxidase inhibitor, apocynin, and SOD mimetic, tempol, on blood pressure and NE release from DOCA-salt MA. I also examined the function of $G_{i/o}$ protein, which couples to the prejunctional α_2AR. NE release was measured locally at the blood vessel surface *in vitro* using continuous amperometry with a microelectrode. NE concentration changes with time were recorded as an oxidation current in these studies.

6.2 Results

6.2.1 Sham and DOCA-salt rats

Mean systolic blood pressures for sham and DOCA-salt rats were 121 ± 5

mmHg (n=56) and 198 ± 7 mmHg (n=52), respectively ($P < 0.05$). The mean body weights of sham and DOCA-salt rats were 400 ± 10 g and 321 ± 12 g, respectively ($P < 0.05$)

6.2.2 Impaired function of prejunctional α_2AR in DOCA-salt MA

NE is released from sympathetic nerve endings innervating MA and MV [67]. Nerve stimulation-induced NE release can be detected as an oxidation current by continuous amperometry with a carbon fiber microelectrode [127, 187]. The oxidation current measured reflects the extracellular concentration of NE at the artery surface, which equals the amount of NE released offset by neuronal reuptake and diffusion. There is increased NE release in DOCA-salt MA [34, 59]. Representative NE time profiles before and after α_2AR blockade by idazoxan (1 μM) at sham and DOCA-salt MA are shown in Fig. 6.1A. The bars under the traces represent the period of nerve stimulation. The focal nerve stimulation produced significantly greater NE overflow for DOCA-salt than for sham MA as shown in Fig. 6.1B. The rise of the current was also much steeper for DOCA-salt MA as shown in Fig. 6.1C. Previously, we showed that this is at least partially due to the impaired α_2AR function (Chapter 5). In order to examine the function of α_2AR, we applied the antagonist, idazoxan, and measured the NE current again. The oxidation current was significantly increased by *ca.* 79% in sham MA while only *ca.* 25% in DOCA-salt MA. Similarly, the current rise slope was increased significantly by *ca.* 67% in sham MA but only *ca.* 22% in DOCA-salt MA. Idazoxan itself does not contribute to the increase of the oxidation current [186].

So these results illustrate that the function of prejunctional α_2ARs is impaired in DOCA-salt MA.

6.2.3 Chronic apocynin and tempol treatment lowers blood pressure of DOCA-salt rats

DOCA-salt rats were separated into three groups: DOCA-salt control group, apocynin-treated group and tempol-treated group. Blood pressure was recorded for 2 control days and 24 treatment days. There was a significant interaction between treatment and blood pressure ($P < 0.05$). The mean arterial blood pressure (MAP) was plotted as a function of time: control, treatment day 18 and treatment day 24 in Fig. 6.2. No difference was found in MAP among three groups in the control period. MAP for three groups increased over 24 treatment days but it was significantly lowered by apocynin and tempol treatment compared to DOCA-salt control group, especially on day 18. However, by the end of the study, the MAP from the apocynin and tempol group was not significantly different from that of the DOCA-salt group on day 24.

6.2.4 Apocynin and tempol treatment reduce NE release and restore α_2ARs function in DOCA-salt MA

Previous studies on the kinetics of neurotransmitter release have shown that the release of ATP and NE is frequency dependent and at lower stimulation frequency (up to 8 Hz), NE is released in very small amounts compared with ATP [91, 231]. In other words, the portion of NE released from sympathetic

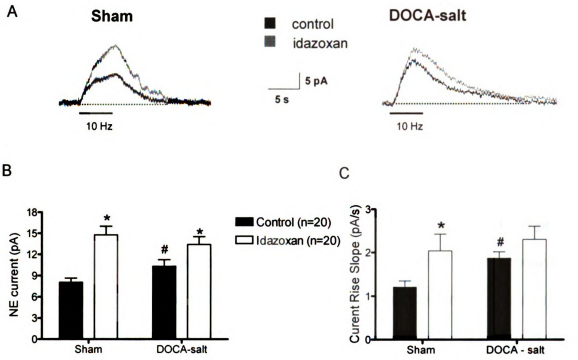

Figure 6.1 (A) Representative recordings of *in vitro* continuous amperometric measurement of NE oxidation currents from sham and DOCA-salt MA before (black trace) and after (grey trace) the blockade of presynaptic α_2AR using 1 μM idazoxan. NE oxidation currents were evoked by a 10 Hz stimulus train and the bar under the current traces represents the period of nerve stimulation (60 pluses with a 0.5 ms pulse width). Statistical results for NE current (B) and 10-90% NE current rise slope (C) from sham and DOCA-salt MA demonstrate that the NE level is higher and α_2AR function is impaired in DOCA-salt MA. Data are means ± S.E.M. with * represents significant difference from control, and # represents significant difference from sham MA, $P < 0.05$.

nervous system may vary by stimulation frequency. Therefore, the effect of antioxidant treatment on sympathetic nerve function was studied by endogenous NE measurement at different stimulation frequencies. On the 24th day of the chronic antioxidant treatment, the rats were sacrificed and the mesenteric tissue was taken out for measurement. Representative NE oxidation current profiles before and after α_2AR blockade from the DOCA-salt, apocynin and tempol groups are shown in Fig. 6.3 A and B. Apocynin and tempol decreased the peak current significantly at all stimulation frequencies with the most prominent difference occurring at 2 and 5 Hz for apocynin and tempol treatment groups (Fig. 6.3C). And the current rise slopes, which were partially determined by presynaptic α_2AR function, were significantly reduced by apocynin and tempol at 10 and 20 Hz, probably due to restored function of α_2ARs.

Idazoxan (1 μM) was used to investigate the function of prejunctional α_2ARs. Idazoxan increased NE peak current 2-fold in the apocynin and tempol treatment groups at stimulation frequencies ≤ 10 Hz and *ca.* 1.5 fold at 20 Hz. Oxidation currents recorded for DOCA-salt MA were increased by idazoxan only at stimulation frequencies ≤ 10 Hz with smaller increases than that occurring in antioxidant treatment groups. Idazoxan failed to increase NE current at 20 Hz for DOCA-salt MA. Oxidation current rise slopes were increased by idazoxan at stimulation frequencies ≤ 10 Hz in apocynin and tempol treatment groups but there was no change in the DOCA-salt group. Both the differences in peak current and current rise slopes among three groups were abolished after the blockade of α_2AR. Taken together, these data support a role for oxidative stress

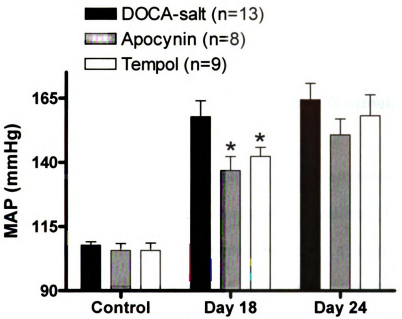

Figure 6.2 Mean arterial pressure (MAP) for chronic antioxidant treatment for DOCA-salt rats *in vivo* study. MAP increased for the three groups with time. It decreased in response to chronic antioxidant treatment with apocynin (grey bar) and tempol (open bar) compared to DOCA-salt controls, particullaly on day 18. Two-way ANOVA indicates there is significant difference for the MAP among three groups with time ($P < 0.05$). Data are means ± S.E.M. and * indicates significant difference compared to DOCA-salt controls by Newman-Keuls post hoc test, $P < 0.05$.

in the impairment of α_2AR which leads to the increase in NE release and the rate of release in DOCA-salt MA. α_2AR function was restored, at least in part, after chronic antioxidant treatment at sympathetic nerve endings.

6.2.5 Impaired function of pertussis toxin sensitive G protein in DOCA-salt MA

Previous studies revealed that ROS, mainly O_2^-, produce membrane protein and lipid damage disrupting intra and intercellular signaling [101]. Since the prejunctional α_2AR is a G-protein coupled receptor, it is possible that the increased ROS target G_i/G_o proteins and, therefore, cause impaired signaling pathway to α_2AR. To test this, I incubated sham and DOCA-salt MA in 3 μg/ml pertussis toxin (PTX) to examine the function of G_i/G_o protein [188]. Both the NE peak current and current rise slope from PTX incubated sham MA were significantly increased compared to control incubated tissue (Fig. 6.4 A and C). However, there was no difference in either the oxidation peak current or the current rise slope in DOCA-salt MA after PTX incubation compared to control (Fig. 6.4 B and D). These observations demonstrate that the function of G_i/G_o protein coupled to prejunctional α_2AR is impaired in DOCA-salt MA. For comparison, idazoxan (1 μM) was used to investigate the function of prejunctional α_2AR in control and PTX incubated tissues. Marked increases in both NE peak current current and current rise slope were observed in sham incubated MA but very little increase in DOCA-salt tissues (Fig. 6.4). However, the increase of current caused by PTX is less than those caused by idazoxan alone and PTX plus

Figure 6.3. Effects of chronic antioxidant treatment, apocynin and tempol, on the release of NE and prejunctional α_2AR function at the sympathetic nerve endings. Representative traces of NE oxidation current from DOCA-salt control (black), apocynin (dark grey) and tempol (light grey) groups before (A) and after (B) the blockade of prejunctional α_2AR using 1 μM idazoxan. NE oxidation currents were evoked by 10 Hz stimulus trains (60 pluses, 0.5 ms pulse width). The maximum NE current (C) and 10-90% current rise slope (E) were significantly decreased in apocynin and tempol groups compared to DOCA-salt controls. The differences in NE maximum current (D) and 10-90% current rise slope (F) disappeared after the blockade of prejunctional α_2AR by idazoxan. This indicates that the differences among three groups were partially caused by α_2AR and the function of α_2AR was restored by chronic apocynin and tempol treatment. Data are mean ± S.E.M. and * represents significant difference from DOCA-salt control by one-way ANOVA with Newman-Keuls post hoc test, $P < 0.05$.

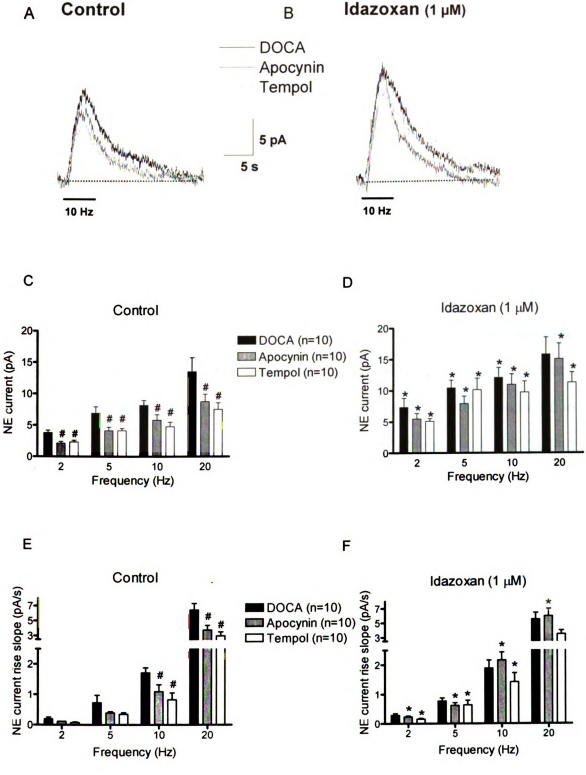
A
Control
B
Idazoxan (1 μM)
DOCA
Apocynin
Tempol
5 pA
5 s
10 Hz
10 Hz
C
Control
D
Idazoxan (1 μM)
DOCA (n=10)
Apocynin (n=10)
Tempol (n=10)
NE current (pA)
Frequency (Hz)
E
Control
F
Idazoxan (1 μM)
NE current rise slope (pA/s)
Frequency (Hz)

idazoxan. Taken together, these results suggest that the tissue incubation in the medium itself did not change the function of presynaptic α_2AR. It is the impaired function of G_i/G_o protein coupled to α_2AR in the DOCA-salt MA that made the difference in NE overflow compared to sham MA.

6.3 Discussion

The results confirm previous observations regarding differences in sympathetic neurotransmission to MA from sham and DOCA-salt rats. Specifically, the results demonstrate that endogenous NE release from DOCA-salt MA, evoked by nerve stimulation, is significantly greater than that from sham MA [34]. The prejunctional autoreceptor regulates NE release through negative feedback and it has been established that the function of prejunctional α_2AR is impaired in human hypertension [65, 66] and many animal hypertension models, including SHR and DOCA-salt rats [7, 59]. It is therefore likely that the elevated NE overflow and the increased rising slope of the current in DOCA-salt MA are partially due to the impaired function of prejunctional α_2AR. The present study was designed to investigate the role of oxidative stress on the elevated NE release in DOCA-salt MA and if the sympathetic neurotransmission at the neuroeffector junction is impaired by oxidative stress.

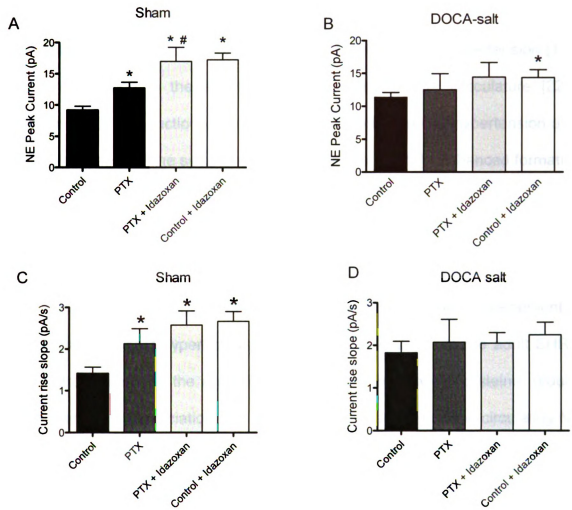

Figure 6.4 Effects of pertussis toxin (PTX, 3 μg/ml) on NE release at sham and DOCA-salt MA. After 2h tissue incubation in PTX, NE maximum current and 10-90% NE current rise slope were significantly increased at sham MA (A and C) but not DOCA-salt MA (B and D). For comparison, we also blocked α_2AR function by idazoxan for the control and PTX treatment groups. Both NE current and current rise slope were increased significantly by idazoxan for sham control and PTX treatment groups (A and C) but the increase was very little in DOCA-salt MA (B and D). This represents that the function of G_i/G_o which couples to α_2AR is impaired in DOCA-salt MA. The current increased by idazoxan plus PTX was significantly greater than that caused by PTX alone for sham MA. Data are means ± S.E.M. with * represents significant difference from control, and # represents significant difference from PTX incubated MA, $P < 0.05$.

Many studies have raised the possibility that an enhanced production of ROS, especially $\cdot O_2^-$, may be involved in the development of hypertension [101, 116]. In addition to the effects of ROS directly on the vasculature [222], augmented $\cdot O_2^-$ production contributes to the development of hypertension also through activation of the sympathetic nervous system [227]. Enhanced formation of $\cdot O_2^-$ results from increased NADPH oxidase activity, and reduced SOD activity occurs in DOCA-salt rats [106, 228]. Inhibition of ROS generation with apocynin, an NADPH oxidase inhibitor, and radical scavenging with antioxidants or SOD mimetics, like tempol, can decrease blood pressure and prevent development of hypertension in most hypertensive models [111, 227, 232]. In the adult SHRs, chronic treatment with the antioxidants, melatonin or N-acetyl-cysteine, reduce blood pressure in association with a reduction in heart rate and in circulating NE [120]. It therefore likely that $\cdot O_2^-$ level is increased in DOCA-salt rats and antioxidant treatment can lower the NE release at the sympathetic nerve endings. For that reason, we focused this study on the role played by antioxidant, apocynin and tempol on the recovery effect in sympathetic neurotransmission in the DOCA-salt hypertension, with specific attention to NE bioavailability.

My results confirm that oxidative stress is involved in the changes that occur in sympathetic neurotransmission in DOCA-salt hypertension. Specifically, I show that chronic treatment of antioxidants, apocynin and tempol, reduced blood pressure in a time dependent manner, especially at day 18. Although there was no significant difference of MAP from apocynin and tempol group compared to DOCA-salt group at the end of the study, the chronic antioxidant treatment is a

time course response and the fact that blood pressure for an extended period would minimize chronic injury caused by accumulation of O_2^- during the course of the study. In order to verify that, at day 24, the effectiveness of antioxidant treatment on sympathetic nerve was assessed by measuring dihydroethidium (DHE) intensity, a marker of superoxide level in the sympathetic ganglia. The DHE staining of inferior mesenteric ganglia was reduced by ca. 50% in apocynin and tempol treated group compared to DOCA-salt control group [233]. This confirms that although the MAP didn't change at the 24^{th} day, the antioxidant treatment lowered the superoxide level in DOCA-salt rats in the overall treatment period. Furthermore, the nerve stimulation induced release of NE was significantly decreased in the apocynin and tempol groups while the function of prejunctional α_2AR was restored compared to DOCA-salt group. And we also demonstrate that the function of pertussis toxin sensitive G_i/G_o protein, which could be the target of ROS [115, 234], is impaired in DOCA-salt rats. These findings are in keeping with the hypothesis that the increased sympathetic nerve activity may due in part to the elevated level of ROS and ROS may alter the sympathetic neuroeffector junction in DOCA-salt hypertensive rats.

DOCA-salt rats have significantly greater mRNA levels of the NADPH oxidase subunit p22phox in the prevertebral sympathetic ganglia than do sham rats, which suggests that NADPH oxidase is increased and is responsible for increased $\cdot O_2^-$ production and possibly contributes to increased blood pressure in the DOCA-salt hypertensive rat [223, 228]. The mechanisms modulating the NADPH oxidase activity in hypertensive rats is still unclear. Some studies

suggest that the local activated renin-angiotensin system and endothelin system in DOCA-salt hypertensive rats might be involved in the higher levels of $\cdot O_2^-$ production [235, 236]. Further studies are needed to verify this hypothesis. In addition to the increased NADPH oxidase activity, a decreased Cu/Zn SOD activity appears to play an important role in the high level of aortic $\cdot O_2^-$ formation in DOCA-salt rats [106]. Apocynin and tempol decreased $\cdot O_2^-$ level by different mechanisms. Apocynin is known as an inhibitor of NADPH oxidase. However, a recent study suggests that apocynin predominantly acts as an antioxidant which works independent of NADPH oxidase [237]. So far, it is not known if this alternative mechanism for apocynin works in the sympathetic neurons. In addition, it is shown that long-term treatment of apocynin can reduce the $\cdot O_2^-$ level and blood pressure, but not the acute treatment in a short time [114]. Tempol works as a SOD mimetic to reduce the $\cdot O_2^-$ level regardless of its origin. Both long term and short term treatment of tempol can lower the blood pressure in DOCA-salt rat [114].

The novel finding in my study is the beneficial effect of chronic antioxidant treatment on the sympathetic nerve function. It is well known that under pathological conditions, ROS has deleterious effect on vasculature, such as impair the endothelium dependent vasorelaxation [104], induce vascular smooth muscle cell growth [238] and activate vasoconstrictory signal transduction pathway [239]. I demonstrate that ROS also act via prejunctional mechanisms that contribute to the elevated sympathetic nervous system activity in DOCA-salt hypertensoin. The restored function of prejunctional α_2AR by chronic apocynin

and tempol treatment groups demonstrates that the impairment of α_2AR may partially caused by the elevated level of ROS. One thing we need to point out that although ROS was shown to increase the entry of Ca^{2+} into myocytes [116], the prejunctional Ca^{2+} channel function equally well in sham and DOCA-salt hypertensive rats MA (Chapter 5). So ROS didn't change the function of prejunctional Ca^{2+} channel. G_i/G_o are target protein of ROS [115] and it has been revealed that oxygen radicals can cause protein damage and degradation [234], as well as protein fragmentation and polymerization [240] by oxidizing the sulfhydryl groups and methionine residues [241]. My study suggests that impaired G_i/G_o proteins, which may be caused by elevated ROS, is part of the reason for the impaired function of prejunctional α_2AR. However, I do expect that after the PTX incubation for sham MA, the increase of NE current should at least equal to the increase that caused by idazoxan, if not more than that (Fig. 6.4). The greater current increase caused by idazoxan could be partially due to its blockade of the low affinity intrajunctional buffering sites which bind NE and re-release it at a later time [124]. It could also be possible that PTX works less efficiently on blocking G_i/G_o proteins, or the tissue incubation in PTX was not sufficient enough [194]. Nonetheless, my work suggests that with the same PTX treatment, the function of G_i/G_o proteins in DOCA-salt MA is significantly lower than that in sham MA. In addition, there may be other vesicle regulating proteins in the sympathetic nerve terminal which are sensitive to ROS. For example, SNAP25, one of three essential fusion proteins, which mediates the ROS-induced impairment of releasing machinery in the central nervous system [226],

may also be a target of ROS in the sympathetic nervous system. Furthermore, there is also study showing that not only are the proteins themselves potential targets, but also interactions between molecules within a signaling complex may be modified by ROS [222].

I do not exclude other possibilities that can lead to increased overflow of NE in DOCA-salt MA, such as impaired function of NE transporter (Chapter 5). It has also been published that nitric oxide (NO) inhibits NE release from sympathetic nerves [242]. The reduction in the bioavailability of NO as a result of elevated oxidative stress contributes to the increase in NE overflow from SHR MA [225]. Many studies have shown that SOD mimetic, tempol, can scavenge $\cdot O_2^-$, increase the bioavailability of NO, which cause vasodilation and thus reduce the blood pressure in SHR and angiotensin II-infused hypertensive rats [243, 244]. However, tempol can directly inhibit peripheral sympathetic nerves, possibly by inhibiting sympathetic neuroeffector transmission; this effect is NO-independent in DOCA-salt hypertensive rats [113]. Similar results have been obtained by Campese and his coworkers [105]. My study supports this idea by showing that tempol restored the function of prejunctional α_2AR which inhibits NE release and thus decreased the peripheral sympathetic nerves activity.

6.4 Summary and conclusions

Our data herein indicate that the increased sympathetic overflow in DOCA-salt MA is partially due to the impaired function of presynaptic α_2AR. Oxidative stress alters the sympathetic neurotransmission in DOCA-salt

hypertensive rats probably by impairing pertussis toxin-sensitive G proteins which couple to α_2AR at the nerve terminal. Chronic treatment with apocynin and tempol reduced oxidative stress, lowered the mean arterial blood pressure and the sympathetic overflow. Chronic antioxidant treatment also has the beneficial effect on the sympathetic nerve function by restoring presynaptic α_2AR function in DOCA-salt MA and thus decreased the overflow of NE. Taken together, these observations strongly suggest that oxidative stress in the cardiovascular system constitutes an important mechanism in the development of hypertension and support a new mechanism for the beneficial effect of antioxidant treatment in hypertension.

CHAPTER 7

CONCLUSIONS

Sympathetic nerves innervating MA and MV play an important role in blood pressure regulation. Alteration in sympathetic nerve function underlies several types of hypertension including DOCA-salt hypertension. NE is the major neurotransmitter in the sympathetic nervous system and elevated plasma NE levels occur in DOCA-salt hypertension in rats. However, how hypertension alters the mechanisms that regulate NE transmission is unclear. A major focus of my thesis work was to test the hypothesis that there are artery-vein differences in NE release and clearance mechanisms and these mechanisms are altered in DOCA-salt hypertensive rats. I also proposed that alterations in sympathetic neurotransmission are associated with oxidative stress. Continuous amperometry with a microelectrode was used to monitor endogenous NE release elicited by focal nerve stimulation, at the adventitial surface of MA and MV from sham and DOCA-salt rats *in vitro.* Measurements were made as a function of temperature from 28 to 37 °C. There are four major conclusions that can be drawn from the results of this work.

I. **The drugs used to study sympathetic neurotransmission can alter the microelectrode response sensitivity and stability. The effects of drugs on microelectrode response sensitivity and stability should be ascertained before making *in vitro* or *in vivo* electrochemical measurements.**

Amperometry coupled with drugs was used to investigate the mechanisms regulating NE release. It is, therefore, of importance to investigate if the drugs are electrochemically active at the electrode potential where NE is detected and if the drug attenuates the electrode response for NE by molecule adsorption and electrode fouling. Carbon fiber (T 650 and P 55 type) and diamond microelectrodes were used for this study. Results revealed that cocaine, idazoxan and PPADS are electrochemically inactive at both microelectrodes at the potentials used to detect NE, and drug exposure has little effect on the NE oxidation current. On the other hand, exposure to capsaicin, prazosin, yohimbine and UK 14,304 produced varying degrees of NE oxidation current attenuation at both microelectrode types. When yohimbine and UK 14,304 are present, NE can be detected but the oxidation current is reduced. Furthermore, detection of NE in the presence of prazosin or capsaicin is complicated by the fact that both drugs are oxidized near the potentials used for NE monitoring.

Carbon fiber and diamond microelectrode has sp^2 and sp^3 bonded carbon surface microstructure, respectively. The influence of drugs on NE detection at these two microelectrodes behaves differently due to the extent of absorption of drug on the microelectrode surface. NE is favorable to react at the more microstructurally-disordered material, like T-650 carbon fiber; and some drug (e.g. PPADS, yohimbine) has more favorable interaction with microstructurally-ordered material, such as P-55 carbon fiber and the hydrophobic sp^3-bonded diamond. Therefore, diamond possesses the superior properties over carbon fiber for biochemical detection due to the weak adsorption of polar biomolecules and

contaminants; on the other hand, for NE measurement in the presence of drug, especially those can strongly adsorb on the electrode surface, the T-650 carbon fiber provides the best performance.

II. NE release and clearance mechanisms are different in sympathetic nerves associated with MA and MV.

Arteries and veins contribute differentially to the hemodynamics. My work reveals that the release and clearance mechanisms of NE from MA and MV are different. Specifically, 1) NE overflow from MV exceeds than that from MA, and it behaves more temperature sensitive compared to MA, 2) NE release in MA is tightly regulated by prejunctional α_2AR but not in MV, possibly due due to the lower expression of G_i/G_o proteins that couple to α_2AR, 3) NE release is more sensitive to calcium channel blockers in MV, 4) NE is cleared by NET from the neuroeffector junction in MA but mainly by diffusion in MV; NET function contributes to the temperature dependent difference in NE overflow between MA and MV, 5) the possible differences may also exist in the content and recycling dynamics of NE vesicles in periarterial and perivenous sympathetic nerves. The key findings are shown in Fig. 7.1.

One interesting finding is that cocaine didn't increase NE oxidation currents in MV, however, guanethidine, a known inhibitor of NE secretion through NET, decreased NE release more in MV than in MA. This may be explained by the reduced opportunity for lateral inhibition by NE released from adjacent varicosities due to the low density of sympathetic nerve fibers supplying MV

(Stjärne and Stjärne, 1995). Future study may focus on ultrastructural studies comparing the subcellular structure of sympathetic varicosities using transmission electron microscopy. These studies may provide insight into the sympathetic nerve terminal, patterns of vesicle distribution, and possibly the NET distribution at the nerve terminals [12, 13].

Although the α_2AR antagonist, idazoxan, failed to induce a significant increase in NE currents in MV, the α_2AR agonist, UK 14,304, inhibited NE currents. This result supports the presence of functional prejunctional α_2ARs in MV [91]. It is possible that α_2ARs on perivenous nerve endings are not be accessible to endogenously released NE. Alternatively there may be several subtypes of prejunctional α_2AR existing at MV, which can be activated by different agonists or blocked by different antagonists. Future studies of prejunctional α_2ARs could focus on specific α_{2A}, α_{2B}, α_{2C}, and α_{2D} subtypes that may selectively inhibit NE release at the sympathetic nerve endings in MV.

The differences in neuroeffector transmission may contribute to the different hemodynamic functions of MA and MV. MV are more sensitive to the vasoconstrictor effects of sympathetic nerve stimulation than MA. Reduced regulation of NE release and clearance by prejunctional α_2AR and NET may maintain venous tone that leads to a redistribution of some stored blood from peripheral veins to the heart and then into the arterial circulation.

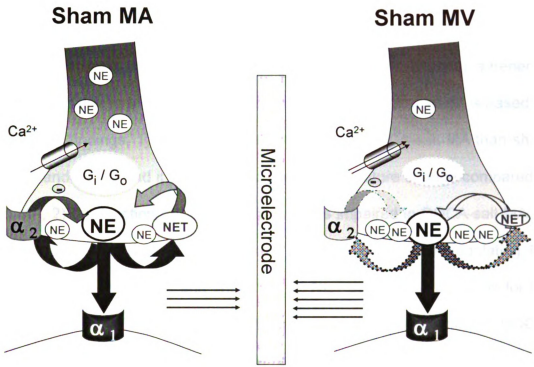

Figure 7.1 Mesenteric artery and vein neuroeffector junctions in normotensive rats. NE is released from sympathetic nerve terminals in response to nerve stimulation and depolarization of the nerve terminal. NE bind with α_1AR post junctionally resulting in constriction of the smooth muscle cell. NE release in MA is tightly regulated by prejunctional α_2AR but not in MV, possibly due due to the lower expression of G_i/G_o proteins that couple to α_2AR. NE release is more sensitive to calcium channel blockers in MV compared to MA. NE is cleared by NET from the neuroeffector junction in MA but mainly by diffusion in MV; NET function contributes to the temperature dependent difference in NE overflow between MA and MV. It is possible that the readily releasable pool at the sympathetic nerve endings is larger in MV but the reserve pool of vesicles is further away from the active zone in perivenous compared to periarterial nerves. These differences lead to the exceeding NE overflow at 37 °C and greater temperature dependent sensitivity in NE overflow from MV than that from MA.

III. There is impaired regulation of NE transmission from sympathetic periarterial nerves in DOCA-salt rats.

Several changes at the neuroeffector junction occur which alter adrenergic neurotransmission to MA in DOCA-salt hypertension. This conclusion is based on the following findings, 1) NE overflow is greater from DOCA-salt MA than sham MA at 37 and 34 °C, and it is more sensitive to temperature change compared to sham MA, 2) the function of prejunctional α_2AR is impaired in DOCA-salt MA; 3) there is no difference in calcium channel function in terms of regulating NE release between DOCA-salt and sham MA, 4) NET dysfunction accounts for the slow clearance of NE at the vicinity of the sympathetic nerve junction in DOCA-salt MA; NET contributes to the NE overflow temperature dependent difference between DOCA-salt and sham MA, 5) there is no difference in NE release and clearance mechanisms between DOCA-salt and sham MV. The key findings are shown in Fig. 7.2.

There are many other factors which contribute to the probability and amount of NE released, since transmission from individual varicosities involves the release of variable size packages of transmitter onto different size receptor patches [245]. One possibility for the increased NE release in DOCA-salt MA is the increased NE bioavailability in the nerve terminal. Other possible mechanisms include changes in the ability of NE to be stored in vesicles or the distribution of readily releasable vesicles docked at the sympathetic nerve endings. Transmission electron microscopy would be able to show the altered distribution or amount of the NE vesicles at the nerve endings in the future study.

Facilitation at the neuroeffctor junction occurs due to increased calcium in nerve terminals in response to trains of stimulation [246]. I expected NE release to be more sensitive to calcium channel blockers in DOCA-salt MA compared to sham MA; however, this was not the case. There are L-, N-, P/Q , R, and T type voltage dependent calcium channels [55], among which, N- and P/Q type play a more prominent role in neurotransmitter release. Therefore, the function of specific N- and P/Q type calcium channels on NE release in DOCA-salt MA may be included in the future study. Another future study targeting the impaired function of NET with knock out animals will also provide insight into the importance of adrenergic neurotransmission in hypertension.

The dysfunction of presynaptic α_2AR and NET but not calcium channels contributes to the impaired adrenergic neurotransmission to MA but not MV in DOCA-salt hypertensive rats. These altered mechanisms on NE release and clearance maintain peripheral arterial tone when coupled with the increased cardiac filling pressure and/or cardiac output caused by increased venous tone causes sustained increases in arterial pressure.

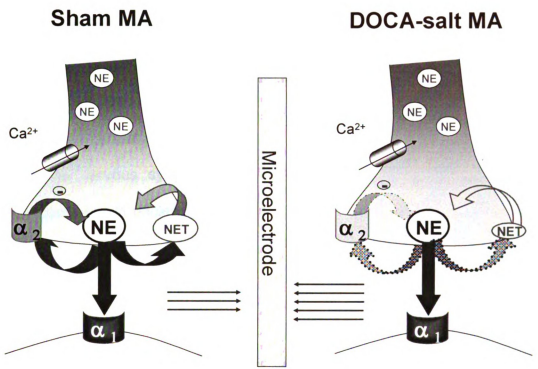

Figure 7.2 Mesenteric artery neuroeffector junctions in control and DOCA-salt rat. In DOCA-salt hypertension, several changes occur to the sympathetic nerve endings which affect neurotransmitter release. Calcium channel remain functional, providing sufficient Ca^{2+} influx for vesicle fusion and neurotransmitter release. However, the function of prejunctional α_2AR and NET are impaired in DOCA-salt MA. NET contributes to the NE overflow temperature dependent difference between DOCA-salt and sham MA. These differences all contribute to the increased NE overflow at 37 °C and greater temperature dependent sensitivity in NE overflow from DOCA-salt MA than that from sham MA.

IV. Reactive oxidative stress impairs the sympathetic nerve function at the neuroeffector junction and its effects contribute to high blood pressure in DOCA-salt hypertensive rats.

ROS are involved in the development of hypertension, partly by increasing peripheral and central sympathetic nerve activity [101]. However, the targets of ROS in the nervous system and how they modulate neurotransmission in hypertension remain unclear. My work demonstrated that increased ROS targets G_i/G_o proteins coupling to prejunctional α_2AR in sympathetic nerve endings leading to impaired neurotransmission and increased blood pressure. Chronic antioxidant treatment lowers blood pressure and restores sympathetic nerve function at the neuroeffector junction in DOCA-salt hypertensive rats. The key findings are summarized in Fig. 7.3. This work reveals a new mechanism for the beneficial effect of antioxidant treatment in hypertension.

Oxygen radicals can cause protein damage and degradation [234], protein fragmentation and polymerization [240] by oxidizing the sulfhydryl groups and methionine residues [241]. ROS may cause damage to the $G_{i/o}$ protein coupling to α_2AR by chemical reaction. α_2AR contains two cysteine residues, which are connected by a disulfide bond and play a role in ligand binding [247]. Thiol group in the cysteine residue can be oxidized by ROS [248], which may be the target of ROS at Gi/o protein. Future work may include the chemical reaction study of how ROS interact with the oxidizable amino acid in the $G_{i/o}$ protein coupling to α_2AR. In addition, there may be other vesicle regulating proteins in the sympathetic nerve terminal which are sensitive to ROS. Such as, SNAP25, which mediates

the ROS-induced impairment of releasing machinery in the central nervous system [226], may also be a target of ROS in the sympathetic nervous system. Additional targets at nerve terminal may also include the NET, which is impaired by ROS [249, 250]. If and how the impaired NET in DOCA-salt hypertensive model is related to increased ROS level can be studied in the future.

ROS, however, may exert their cardiovascular effects through other pathways. For example, ROS can reduce the production and/or availability of NO and results in NO-mediated sympathoinhibitory effects [105]. Future work may also focus on if and how NO in the mesenteric vasculature is decreased by ROS and how this may alter NE release mechanisms in DOCA-salt hypertension.

Although my work suggests that chronic antioxidant treatment lowers sympathetic nerve activity and blood pressure, the cause-effect relationship between oxidative stress and hypertension remains controversial [251]. It may be beneficial to investigate the role of ROS at nerve endings and blood pressure regulation using genetic models to locally deliver a superoxide dismutase gene regulating oxidative stress in a specific target tissue.

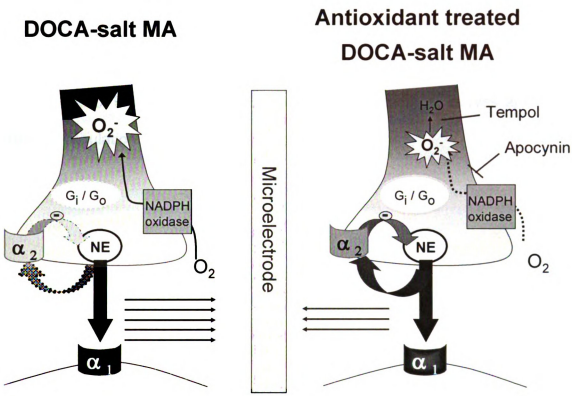

Figure 7.3 Mesenteric artery neuroeffector junctions in DOCA-salt rat with (right) and without (left) antioxidant treatment. There is increased ROS in the DOCA-salt hypertensive rat MA nerve terminals. Increased ROS may target G_i/G_o proteins coupling to presynaptic α_2AR in sympathetic nerve endings leading to impaired neurotransmission and increased blood pressure. Chronic antioxidant treatment, apocynin and tempol, lowers NE release, blood pressure and restores sympathetic nerve function at the neuroeffector junction in DOCA-salt hypertensive rats.

In conclusion, the results of this thesis work extend our knowledge of adrenergic neurotransmission from periarterial and perivenous sympathetic nerves, the role of adrenergic neurotransmission in blood pressure regulation, and the role of ROS in altering NE release from sympathetic nerves and blood pressure regulation.

BIBLIOGRAPHY

1. MacMahon, S., et al., *Blood pressure, stroke, and coronary heart disease. Part 1, Prolonged differences in blood pressure: prospective observational studies corrected for the regression dilution bias.* Lancet, 1990. **335**(8692): p. 765-74.

2. Wong, N., et al., *Inadequate control of hypertension in US adults with cardiovascular disease comorbidities in 2003-2004.* Arch Intern Med. , 2007 **167**(22): p. 2431-6.

3. Anderson, E., et al., *Elevated sympathetic nerve activity in borderline hypertensive humans. Evidence from direct intraneural recordings.* Hypertension, 1989. **14**: p. 177-83.

4. Cowley, A.J., J. Liard, and A. Guyton, *Role of baroreceptor reflex in daily control of arterial blood pressure and other variables in dogs.* Circ Res. , 1973. **32**(5): p. 564-76.

5. Head, G., *The sympathetic nervous system in hypertension: assessment by blood pressure variability and ganglionic blockade.* J Hypertens. , 2003. **21**(9): p. 1619-21.

6. Sinski, M., et al., *Why study sympathetic nervous system?* J Physiol Pharmacol., 2006: p. 79-92.

7. Zugck, C., et al., *Increased cardiac norepinephrine release in spontaneously hypertensive rats: role of presynaptic alpha-2A adrenoceptors.* J Hypertens., 2003. **21**: p. 1363-9.

8. Fink, G.D., R.J. Johnson, and J.J. Galligan, *Mechanisms of increased venous smooth muscle tone in desoxycorticosterone acetate-salt hypertension.* Hypertension, 2000. **35**: p. 464–469.

9. Taylor, P., *The Pharmacological Basis of Therapeutics.* 1990. **Eighth Edition**.

10. Donoso, M., M. Steiner, and J. Huidobro-Toro, *BIBP 3226, suramin and prazosin identify neuropeptide Y, adenosine 5'-triphosphate and noradrenaline as sympathetic cotransmitters in the rat arterial mesenteric bed.* J Pharmacol Exp Ther. , 1997. **282**(2): p. 691-8.

11. Smyth, L.M., L.T. Breen, and V.N. Mutafova-Yambolieva, *Nicotinamide adenine dinucleotide is released from sympathetic nerve terminals via a botulinum neurotoxin A-mediated mechanism in canine mesenteric artery.* Am J Physiol Heart Circ Physiol, 2006. **290**(5): p. H1818-25.

12. Luff, S.E. and E.M. McLachlan, *Frequency of neuromuscular junctions on arteries of different dimensions in the rabbit, guinea pig and rat.* Blood Vessels, 1989. **26**(2): p. 95-106.

13. Klemm, M.F., D.F. Van Helden, and S.E. Luff, *Ultrastructural analysis of sympathetic neuromuscular junctions on mesenteric veins of the guinea pig.* J Comp Neurol, 1993. **334**(1): p. 159-67.

14. Luff, S.E., *Ultrastructure of sympathetic axons and their structural relationship with vascular smooth muscle.* Anat Embryol (Berl), 1996. **193**(6): p. 515-31.

15. Shoukas, A.A. and H.G. Bohlen, *Rat venular pressure-diameter relationships are regulated by sympathetic activity.* Am. J. Physiol., 1990. **259**: p. H674-80.

16. Ozono, K., Z. Bosnjak, and J. Kampine, *Effect of sympathetic tone on pressure-diameter relation of rabbit mesenteric veins in situ.* Circ Res. , 1991. **68**(3): p. 888-96.

17. Esler, M., *Sympathetic nervous system: contribution to human hypertension and related cardiovascular diseases.* J Cardiovasc Pharmacol., 1995. **26**: p. S24-8.

18. Bouvier, M. and J.d. Champlain, *Increased apparent norepinephrine release rate in anesthetized DOCA-salt hypertensive rats.* Clin Exp Hypertens A. , 1985. **7**(11): p. 1629-45.

19. Ekas, R.J. and M. Lokhandwala, *Sympathetic nerve function and vascular reactivity in spontaneously hypertensive rats.* Am J Physiol. , 1981. **241**(5): p. R379-84.

20. Fried, G., *Small noradrenergic storage vesicles isolated from rat vas deferens--biochemical and morphological characterization.* Acta Physiol Scand Suppl. , 1980. **493**: p. 1-28.

21. Stjärne, L. and P. Astrand, *Relative pre- and postjunctional roles of noradrenaline and adenosine 5'-triphosphate as neurotransmitters of the sympathetic nerves of guinea-pig and mouse vas deferens.* Neuroscience, 1985. **14**(3): p. 929-46.

22. de Champlain, J., *Pre- and postsynaptic adrenergic dysfunctions in hypertension.* J Hypertens Suppl. , 1990. **8**(7): p. S77-85.

23. Luo, M., et al., *Impaired function of alpha2-adrenergic autoreceptors on sympathetic nerves associated with mesenteric arteries and veins in*

DOCA-salt hypertension. Am. J. Physiol. Heart Circ. Physiol., 2004. **286**: p. H1558–H1564.

24. Knowles, J., *Enzyme-catalyzed phosphoryl transfer reactions.* Annu. Rev. Biochem. , 1980. **49**: p. 877–919.

25. Burnstock, G., *Purinergic nerves.* . Pharmacol Rev. , 1972. **24**: p. 509–581.
26. Fields, R.D. and G. Burnstock, *Purinergic signalling in neuron–glia interactions.* Nat Rev Neurosci., 2006. **7**: p. 423–436.

27. Fredholm, B., et al., *Nomenclature and classification of purinoceptors.* Pharmacol Rev 1994. **2**: p. 143–156.

28. Sperlágh, B., et al., *Co-release of endogenous ATP and [3H]noradrenaline from rat hypothalamic slices: origin and modulation by alpha2-adrenoceptors.* Neuroscience., 1998. **82**: p. 511-20.

29. Todorov, L.D., et al., *Neuronal release of soluble nucleotidases and their role in neurotransmitter inactivation.* Nature, 1997. **387**: p. 76-79.

30. Westfall, D., L. Todorov, and S. Mihaylova-Todorova, *ATP as a cotransmitter in sympathetic nerves and its inactivation by releasable enzymes.* J Pharmacol Exp Ther., 2002. **303**(2): p. 439-44.

31. Bobalova, J. and V.N. Mutafova-Yambolieva, *Corelease of endogenous ATP and NA in guinea-pig vein exceeds corelease in mesenteric artery.* Clin. Exp Pharmacol. Physiol., 2001. **28**: p. 397-401.

32. Bobalova, J. and V.N. Mutafova-Yambolieva, *Presynaptic a_2-adrenoceptor-mediated modulation of adenosine 5 triphosphate and noradrenaline corelease: differences in canine mesenteric artery and vein.* J. Auton. Pharmacol., 2001. **21**: p. 47-55.

33. Burnstock, G. and P. Sneddon, *Evidence for ATP and noradrenaline as cotransmitters in sympathetic nerves.* Clin. Sci., 1985. **68**: p. 89s-92s.

34. Luo, M., et al., *Differential alterations in sympathetic neurotransmission in mesenteric arteries and veins in DOCA-salt hypertensive rats.* Auton. Neurosci., 2003. **104**: p. 47-57.

35. Langer, S.Z., *Presynaptic regulation of the release of catecholamines.* Pharmacol Rev. , 1980. **32**(4): p. 337-62.

36. Elsner, D., et al., *Postsynaptic alpha 1- and alpha 2-adrenergic receptors in adrenergic control of capacitance vessel tone in vivo.* Hypertension, 1986. **8**(11): p. 1003-14.

37. Lundberg, J., et al., *High levels of neuropeptide Y in peripheral noradrenergic neurons in various mammals including man.* Neurosci Lett., 1983. **42**(2): p. 167-72.

38. Morris, M., et al., *Region-specific neuropeptide Y overflows at rest and during sympathetic activation in humans. .* Hypertension, 1997. **29**: p. 137-43.

39. Michel, M.C., et al., *XVI. International Union of Pharmacology recommendations for the nomenclature of neuropeptide Y, peptide YY, and pancreatic polypeptide receptors.* Pharmacol Rev, 1998. **50**(1): p. 143-50.

40. Han, S., et al., *Direct evidence for the role of neuropeptide Y in sympathetic nerve stimulation-induced vasoconstriction.* Am J Physiol. , 1998. **274**: p. H290-4.

41. Franco-Cereceda, A. and J. Liska, *Neuropeptide Y Y1 receptors in vascular pharmacology.* Eur J Pharmacol. , 1998. **349**: p. 1-14.

42. Gradin, K., et al., *Neuropeptide Y2 receptors are involved in enhanced neurogenic vasoconstriction in spontaneously hypertensive rats.* Br J Pharmacol., 2006. **148**(5): p. 703-13.

43. Moreau, P., d.C. J, and N. Yamaguchi, *Alterations in circulating levels and cardiovascular tissue content of neuropeptide Y-like immunoreactivity during the development of deoxycorticosterone acetate-salt hypertension in the rat.* J Hypertens., 1992. **10**(8): p. 773-80.

44. Smyth, L.M., et al., *Release of beta-nicotinamide adenine dinucleotide upon stimulation of postganglionic nerve terminals in blood vessels and urinary bladder.* J Biol Chem, 2004. **279**(47): p. 48893-903.

45. Mutafova-Yambolieva, V.N., et al., *Beta-nicotinamide adenine dinucleotide is an inhibitory neurotransmitter in visceral smooth muscle.* Proc Natl Acad Sci U S A, 2007. **104**(41): p. 16359-64.

46. de Champlain, J., R.A. Mueller, and J. Axelrod, *Turnover and Synthesis of Norepinephrine in Experimental Hypertension in Rats.* Circ. Res., 1969. **25**: p. 285-291.

47. Smyth, L., et al., *Cotransmission from sympathetic vasoconstrictor neurons: differences in guinea-pig mesenteric artery and vein.* Auton. Neurosci., 2000. **86**: p. 18-29.

48. Stjärne, L., *Basic mechanisms and local modulation of nerve impulse-*

induced secretion of neurotransmitters from individual sympathetic nerve varicosities. Rev Physiol Biochem Pharmacol. , 1989. **112**: p. 1-137.

49. Striggow, F. and B. Ehrlich, *Ligand-gated calcium channels inside and out.* Curr Opin Cell Biol. , 1996. **8**(4): p. 490-5.

50. Yamakage, M. and A. Namiki, *Calcium channels--basic aspects of their structure, function and gene encoding; anesthetic action on the channels--a review.* Can J Anaesth. , 2002. **49**(2): p. 151-64.

51. Katz, B. and R. Miledi, *The role of calcium in neuromuscular facilitation.* J Physiol., 1968. **195**(2): p. 481-92.

52. Matthews, G., *Neurotransmitter release.* Annu Rev Neurosci. , 1996. **19**: p. 219-33.

53. Augustine, G., et al., *Molecular pathways for presynaptic calcium signaling.* Adv Second Messenger Phosphoprotein Res. , 1994. **29**: p. 139-54.

54. Littleton, J. and H. Bellen, *Synaptotagmin controls and modulates synaptic-vesicle fusion in a Ca(2+)-dependent manner.* Trends Neurosci. , 1995. **18**(4): p. 177-83.

55. Dunlap, K., J. Luebke, and T. Turner, *Exocytotic Ca2+ channels in mammalian central neurons.* Trends Neurosci. , 1995. **18**(2): p. 89-98.

56. Greengard, P., et al., *Synaptic vesicle phosphoproteins and regulation of synaptic function.* Science, 1993. **259**: p. 780-5.

57. Jackson, V. and T. Cunnane, *Neurotransmitter release mechanisms in sympathetic neurons: past, present, and future perspectives.* Neurochem Res. , 2001. **26**: p. 875-89.

58. Aldea, M., et al., *A perforated patch-clamp study of calcium currents and exocytosis in chromaffin cells of wild-type and alpha(1A) knockout mice.* J Neurochem. , 2002. **81**(5): p. 911-21.

59. Tsuda, K., et al., *Inhibition of norepinephrine release by presynaptic alpha 2-adrenoceptors in mesenteric vasculature preparations from chronic DOCA-salt hypertensive rats.* Jpn Heart J. , 1989. **30**(2): p. 231-9.

60. Todorov, L., et al., *Differential cotransmission in sympathetic nerves: role of frequency of stimulation and prejunctional autoreceptors.* J Pharmacol Exp Ther. , 1999. **290**(1): p. 241-6.

61. Miller, R.J., *Presynaptic Receptors.* Annu.Rev.Pharmacol.Toxicol., 1998.

38: p. 201-27.

62. Perälä, M., et al., *Differential expression of two alpha 2-adrenergic receptor subtype mRNAs in human tissues.* Brain Res Mol Brain Res. , 1992. **16**: p. 57-63.

63. Demel, S.L. and J.J. Galligan, *Impaired Purinergic Neurotransmission to Mesenteric Arteries in Deoxycorticosterone Acetate-Salt Hypertensive Rats.* Hypertension, 2008. **52**: p. 322-329.

64. Moreau, P., et al., *Alteration of prejunctional alpha 2-adrenergic autoinhibition in DOCA-salt hypertension.* Am J Hypertens. , 1995. **8**(3): p. 287-93.

65. Damase-Michel, C., et al., *The effect of yohimbine on sympathetic responsiveness in essential hypertension.* Eur J Clin Pharmacol. , 1993. **44**(2): p. 199-201.

66. Rana, B., et al., *Population-based sample reveals gene-gender interactions in blood pressure in White Americans.* Hypertension, 2007. **49**(1): p. 96-106.

67. Ekas, R.J. and M. Lokhandwala, *Sympathetic nerve function and vascular reactivity in Doca-salt hypertensive rats.* Am J Physiol. , 1980. **239**(3): p. R303-8.

68. Townsend-Nicholson, A., et al., *Localization of the adenosine A1 receptor subtype gene (ADORA1) to chromosome 1q32.1.* Genomics 1995. **26**(2): p. 423-5.

69. Silinsky, E.M., *Adenosine devreases both prysynaptic calcium currents and neurotransmitter release at the mouse neuromuscular junction.* J Physiol., 2004. **558**: p. 389–401.

70. Searl, T.J. and E.M. Silinsky, *Modulation of Calcium-Dependent and -Independent Acetylcholine Release From Motor Nerve Endings.* J. Mol. Neurosci. , 2006. **30**: p. 1559-1166.

71. Fredholm, B., et al., *International Union of Pharmacology. XXV. Nomenclature and classification of adenosine receptors.* Pharmacol Rev. , 2001. **53**(4): p. 527-52.

72. Karoon, P., A. Rubino, and G. Burnstock, *Enhanced sympathetic neurotransmission in the tail artery of 1,3-dipropyl-8-sulphophenylxanthine (DPSPX)-treated rats.* Br J Pharmacol. , 1995. **116**(2): p. 1918-22.

73. Jackson, E., *Role of adenosine in noradrenergic neurotransmission in spontaneously hypertensive rats.* Am J Physiol. , 1987. **253**: p. H909-18.

74. Eisenhofer, G., *The role of neuronal and extraneuronal plasma membrane transporters in the inactivation of peripheral catecholamines.* Pharmacol. Ther., 2001. **91**: p. 35–62.

75. Esler, M., et al., *Norepinephrine kinetics in essential hypertension. Defective neuronal uptake of norepinephrine in some patients.* Hypertension, 1981. **3**: p. 149–156.

76. Mandela, P. and G. Ordway, *The Norepinephrine transporter and its regulation.* . J. Neurochem., 2006: p. 310-333.

77. Rascher, W., et al., *Plasma catecholamines, noradrenaline metabolism and vascular response in desoxycorticosterone acetate hypertension of rats.* Eur J Pharmacol. , 1981. **75**(4): p. 255-63.

78. Esler, M., et al., *Assessment of neuronal uptake of noradrenaline in humans: defective uptake in some patients with essential hypertension.* Clin. Exp. Pharmacol. Physiol., 1980: p. 535–539.

79. Drolet, G., M. Bouvier, and J. de Champlain, *Enhanced sympathoadrenal reactivity to haemorrhagic stress in DOCA-salt hypertensive rats.* J. Hypertens. , 1989. **7**: p. 237-42.

80. Longhurst, P., et al., *Sensitivity of caudal arteries and the mesenteric vascular bed to norepinephrine in DOCA-salt hypertension.* Hypertension, 1988. **12**(2): p. 133-42.

81. Whall, C.W.J., M.M. Myers, and W. Halpern, *Norepinephrine sensitivity, tension development and neuronal uptake in resistance arteries from spontaneously hypertensive and normotensive rats.* Blood Vessels. , 1980. **17**: p. 1-15.

82. Zsotér, T. and C. Wolchinsky, *Norepinephrine uptake in arteries of spontaneously hypertensive rats.* Clin Invest Med. , 1983. **6**(3): p. 191-5.

83. Greenway, C. and G. Lister, *Capacitance effects and blood reservoir function in the splanchnic vascular bed during non-hypotensive haemorrhage and blood volume expansion in anaesthetized cats.* J Physiol. , 1974. **237**(2): p. 279-94.

84. Rothe, C., *Reflex control of veins and vascular capacitance.* Physiol Rev. , 1983. **63**(4): p. 1281-342.

85. Halliwill, J., C. Minson, and M. Joyner, *Measurement of limb venous compliance in humans: technical considerations and physiological findings.* J Appl Physiol. , 1999. **87**(4): p. 1555-63.

86. Greenway, C., *Role of splanchnic venous system in overall cardiovascular homeostasis.* Fed Proc., 1983. **42**(6): p. 1678-84.

87. Browning, K.N., et al., *Two populations of sympathetic neurons project selectively to mesenteric artery or vein.* Am. J. Physiol., 1999. **276**: p. H1263-72.

88. Hottenstein, O.D. and D.L. Kreulen, *Comparison of the frequency dependence of venous and arterial responses to sympathetic nerve stimulation in guineapigs.* J. Physiol., 1987. **384**: p. 153±167.

89. Kreulen, D.L., *Activation of mesenteric arteries and veins by preganglionic and postganglionic nerves.* Am. J. Physiol., 1986. **251**: p. H1267-H1275.

90. Gitterman, D. and R. Evans, *Nerve evoked P2X receptor contractions of rat mesenteric arteries; dependence on vessel size and lack of role of L-type calcium channels and calcium induced calcium release.* Br J Pharmacol. , 2001. **132**(6): p. 1201-8.

91. Park, J., et al., *Differences in sympathetic neuroeffector transmission to rat mesenteric arteries and veins as probed by in vitro continuous amperometry and video imaging.* J. Physiol., 2007. **584.3**: p. 819–834.

92. Harder, D., et al., *Norepinephrine effect on in situ venous membrane potential in spontaneously hypertensive rats.* Am J Physiol. , 1981. **240**(6): p. H837-42.

93. Ozono, K., Z.J. Bosnjak, and J.P. Kampine, *Effect of sympathetic tone on pressure-diameter relation of rabbit mesenteric veins in situ.* Circ Res, 1991. **68**(3): p. 888-96.

94. Safar, M.E. and G.M. London, *Arterial and venous compliance in sustained essential hypertension.* Hypertension, 1987. **10**(2): p. 133-9.

95. Nyhof, R., et al., *Splanchnic circulation in hypertension.* Fed Proc., 1983. **42**(6): p. 1690-3.

96. Martin, D., M. Rodrigo, and C. Appelt, *Venous tone in the developmental stages of spontaneous hypertension. .* Hypertension, 1998. **31**(1): p. 139-44.

97. Mark, A., *Structural changes in resistance and capacitance vessels in*

borderline hypertension. Hypertension, 1984. **6**: p. III69-73.

98. Willems, W., et al., *Sympathetic supraspinal control of venous membrane potential in spontaneous hypertension in vivo. .* Am J Physiol. , 1982. **243**(3): p. C101-6.

99. Julius, S., *Interaction between renin and the autonomic nervous system in hypertension.* Am Heart J, 1988. **116**(2 Pt 2): p. 611-6.

100. Sies, H., *Role of reactive oxygen species in biological processes.* Klin Wochenschr., 1991. **69**: p. 965-8.

101. de Champlain, J., et al., *Oxidative stress in hypertension.* Clin Exp Hypertens., 2004. **26**(7-8): p. 593-601.

102. Burdon, R. and C. Rice-Evans, *Free radicals and the regulation of mammalian cell proliferation.* Free Radic Res Commun. , 1989. **6**(6): p. 345-58.

103. Rao, G. and B. Berk, *Active oxygen species stimulate vascular smooth muscle cell growth and proto-oncogene expression.* Circ Res., 1992. **70**(3): p. 593-9.

104. Somers, M., et al., *Vascular superoxide production and vasomotor function in hypertension induced by deoxycorticosterone acetate-salt.* Circulation, 2000. **101**(14): p. 1722-8.

105. Campese, V.M., et al., *Reactive oxygen species stimulate central and peripheral sympathetic nervous system activity* Am J Physiol Heart Circ Physiol, 2004. **287**(2): p. H695-703.

106. Wu, R., et al., *Enhanced superoxide anion formation in vascular tissues from spontaneously hypertensive and desoxycorticosterone acetate-salt hypertensive rats.* J Hypertens. , 2001. **19**: p. 741-8.

107. Swei, A., et al., *Oxidative Stress in the Dahl Hypertensive Rat* Hypertension, 1997. **30**(6): p. 1628-33.

108. Rajagopalan, S., et al., *Angiotensin II-mediated hypertension in the rat increases vascular superoxide production via membrane NADH/NADPH oxidase activation. Contribution to alterations of vasomotor tone.* J Clin Invest. , 1996. **97**(8): p. 1916-23.

109. Touyz, R. and E. Schiffrin, *Reactive oxygen species in vascular biology: implications in hypertension.* Histochem Cell Biol. , 2004. **122**(4): p. 339-52.

110. Rodriguez-Iturbe, B., et al., *Antioxidant-rich diet relieves hypertension and reduces renal immune infiltration in spontaneously hypertensive rats.* Hypertension, 2003. **41**(2): p. 341-6.

111. Virdis, A., et al., *Role of NAD(P)H oxidase on vascular alterations in angiotensin II-infused mice.* J Hypertens, 2004. **22**(3): p. 535-542.

112. Park, J., et al., *Chronic treatment with a superoxide dismutase mimetic prevents vascular remodeling and progression of hypertension in salt-loaded stroke-prone spontaneously hypertensive rats.* Am J Hypertens. , 2002. **15**: p. 78-84.

113. Xu, H., G. Fink, and J. Galligan, *Nitric oxide-independent effects of tempol on sympathetic nerve activity and blood pressure in DOCA-salt rats.* Am J Physiol Heart Circ Physiol, 2002. **283**(3): p. H885-92.

114. Xu, H., G. Fink, and J. Galligan, *Tempol Lowers Blood Pressure and Sympathetic Nerve Activity But Not Vascular O^{2-} in DOCA-Salt Rats* Hypertension, 2004. **43**(2): p. 329-34.

115. Nishida, M., et al., *G alpha(i) and G alpha(o) are target proteins of reactive oxygen species.* Nature, 2000. **408**(6811): p. 492-5.

116. Dhalla, N.S., R.M. Temsah, and T. Netticadan, *Role of oxidative stress in cardiovascular diseases.* J Hypertens. , 2000. **18**(655-73).

117. Griendling, K., et al., *Angiotensin II stimulates NADH and NADPH oxidase activity in cultured vascular smooth muscle cells.* Circ Res. , 1994. **74**: p. 1141-8.

118. Dai, X., et al., *Increased $O_2^{\cdot-}$ production and upregulation of ETB receptors by sympathetic neurons in DOCA-salt hypertensive rats.* Hypertension, 2004. **43**(5): p. 1048-54.

119. Hassan, H. and I. Fridovich, *Intracellular production of superoxide radical and of hydrogen peroxide by redox active compounds.* Arch Biochem Biophys. , 1979. **196**: p. 385-95.

120. Girouard, H., et al., *Chronic antioxidant treatment improves sympathetic functions and [beta]-adrenergic pathway in the spontaneously hypertensive rats.* J Hypertens., 2003. **21**: p. 179-88.

121. Pinto, Y., M. Paul, and D. Ganten, *Lessons from rat models of hypertension: from Goldblatt to genetic engineering.* Cardiovasc Res., 1998. **39**: p. 77-88.

122. Gómez-Sánchez, E., M. Zhou, and C. Gomez-Sanchez, *Mineralocorticoids, salt and high blood pressure.* Steroids 1996. **61**(4): p. 184-8.

123. Schenk, J. and J. McNeill, *The pathogenesis of DOCA-salt hypertension* J Pharmacol Toxicol Methods. , 1992. **27**(3): p. 161-70.

124. Stjärne, L. and E. Stjärne, *Geometry, kinetics and plasticity of release and clearance of ATP and noradrenaline as sympathetic cotransmitters: roles for the neurogenic contraction.* Prog. Neurobiol., 1995. **47**: p. 45-94.

125. Tsukada, M. and S. Chiba, *Effect of Temperature on Responses of Dog Isolated Lingualand Mesenteric Arteries to Vasoactive Substances.* Clin. Exp. Pharmacol. Physiol., 2000. **27**: p. 876–880.

126. Webb-Peploe, M.M. and J.T. Shepherd, *Responses on the superficial limb veins of the dog to changes in temperature.* Circ. Res. , 1968. **22**: p. 737-746.

127. Park, J., et al., *In Vitro Continuous Amperometry with a Diamond Microelectrode Coupled with Video Microscopy for Simultaneously Monitoring Endogenous Norepinephrine and Its Effect on the Contractile Response of a Rat Mesenteric Artery.* Anal. Chem., 2006. **78**: p. 6756-6764.

128. Gonon, F., et al., *Fast and Local Electrochemical Monitoring of Noradrenaline Relesae from Sympathetic Terminals in Isolated Rat Tail Artery.* J. Neurochem., 1993. **60**: p. 1251-1257.

129. Gonon, F., F. navarre, and M. Buda, *In vivo monitoring of dopamine release in the rat brain with differential normal pulse voltammetry.* Anal. Chem., 1984. **56**: p. 573-575.

130. Gonon, F., M. Msghina, and L.Stjarne, *Kinetics of noradrenaline released by sympathetic nerves* Neuroscience 1993(56): p. 535-538

131. Brock, J.A. and J.H.C. Tan, *Selective modulation of noradrenaline release by a2-adrenoceptor blockade in the rat-tail artery in vitro.* Br. J. Pharmacol., 2004. **142**: p. 267–274.

132. Dunn, W.R., T.A. Hardy, and J.A. Brock, *Electrophysiological effects of activating the peptidergic primary afferent innervation of rat mesenteric arteries.* Br. J. Pharmacol., 2003. **140**: p. 231–238.

133. Stamford, J.A., et al., *Simultaneous "real-time" electrochemical and electrophysiological recording in brain slices with a single carbon-fibre*

microelectrode J. Neurosci. Methods., 1993. **50**: p. 279-290

134. Wightman, R.M., *Voltammetry with Microscopic Electrodes in New Domains* Science, 1988. **24**: p. 415 - 420.

135. Leszczyszyn, D., et al., *Secretion of catecholamines from individual adrenal medullary chromaffin cells.* J Neurochem. , 1991. **56**(6): p. 1855-63.

136. Bruns, D. and R. Jahn, *Real-time measurement of transmitter release from single synaptic vesicles.* Nature, 1995. **377**(6544): p. 62-5.

137. Mermet, C., F. Gonon, and L. Stjärne, *On-line electrochemical monitoring of the local noradrenaline release evoked by electrical stimulation of the sympathetic nerves in isolated rat tail artery.* Acta Physiol Scand. , 1990. **140**(3): p. 323-9.

138. Lane, R., et al., *Brain catecholamines: detection in vivo by means of differential pulse voltammetry at surface-modified platinum electrodes.* Brain Res. , 1976. **114**(2): p. 346-52.

139. McCreery, R.L., *Carbon electrodes: structural effects on electron transfer kinetics* Electroanalytical Chemistry 1990. **17**: p. 221-374.

140. McCreery, R.L., *Carbon Electrode Surface Chemistry: Optimization of Bioanalytical Performance, in Voltammetric Methods in Brain Systems.* Humana Press: New Jersey, 1995: p. 1-26.

141. Kawagoe, K.T., J.B. Zimmerman, and R.M. Wightman, *Principles of voltammetry and microelectrode surface states.* J. Neurosci. Methods., 1993. **48**: p. 225-240.

142. Bruno, F., M. Pham, and J. Dubois, *Polaromicrotribometric study of polyphenylene oxide film formation on metal electrodes by electrolysis of disubstituted phenols.* Electrochim. Acta., 1977. **22**: p. 451-7.

143. Runnels, P.L., et al., *Effect of pH and surface functionalities on the cyclic voltammetric responses of carbon-fiber microelectrodes.* . Anal. Chem., 1999. **71**(14): p. 2782–9.

144. Suaud-Chagny, M., et al., *High sensitivity measurement of brain catechols and indoles in vivo using electrochemically treated carbon-fiber electrodes.* J Neurosci Methods. , 1993. **48**: p. 241-50.

145. Asmussen, J. and D.K. Reinhard, *Diamond Films Handbook.* New York: Marcel Dekker., 2002.

146. Iwaki, M., et al., *Electrical conductivity of nitrogen and argon implanted diamond* Nucl. Instrum. Methods 1983. **209–210** p. 1129.

147. Swain, G.M., A.B. Anderson, and J.C. Angus, *Applications of diamond thin films in electrochemistry.* MRS Bull., 1998. **23**: p. 56-60.

148. Xu, J. and G. Swain, *Anthraquinonedisulfonate Electrochemistry: A Comparison of Glassy Carbon, Hydrogenated Glassy Carbon, Highly Oriented Pyrolytic Graphite, and Diamond Electrodes. .* Anal. Chem., 1998. **70**: p. 3146-54.

149. DeClements, R., et al., *Electrochemical and Surface Structural Characterization of Hydrogen Plasma Treated Glassy Carbon Electrodes.* Langmuir 1996. **12**: p. 6578–6586.

150. Park, J., et al., *Fabrication, characterization, and application of a diamond microelectrode for electrochemical measurement of norepinephrine release from the sympathetic nervous system.* Diam. Relat. Mater., 2006. **15**(4-8): p. 761-772

151. Cvacka, J., et al., *Boron-Doped Diamond Microelectrodes for Use in Capillary Electrophoresis with Electrochemical Detection.* Anal. Chem., 2003. **75**: p. 2678-2687.

152. Katz, B. and R. Miledi, *The effect of temperature on the synaptic delay at the neuromuscular junction. .* J. Physiol., 1965. **181**: p. 656-670.

153. Yang, X., et al., *Cooling blocks rat hippocampal neurotransmission by a presynaptic mechanism: observations using 2-photon microscopy.* J. Physiol. , 2005. **567**: p. 215-24.

154. Klyachko, V. and C. Stevens, *Temperature-dependent shift of balance among the components of short-term plasticity in hippocampal synapses.* J Neurosci., 2006. **26**: p. 6945-57.

155. Pyott, S. and C. Rosenmund, *The effects of temperature on vesicular supply and release in autaptic cultures of rat and mouse hippocampal neurons. .* J. Physiol. , 2002. **539**: p. 523–535.

156. Yamamoto, R., W.J. Cline, and K. Takasaki, *Effect of moderate cooling on endogenous noradrenaline release from the mesenteric vasculature of rats.* J. Auton. Pharmacol. , 1989. **9**: p. 347-55.

157. Webb-Peploe, M.M. and J.T. Shepherd, *Peripheral mechanism involved in response of dog's cutaneous veins to local temperature change.* Circ Res, 1968. **23**(6): p. 701-8.

158. Janssens, W. and P. Vanhoutte, *Instantaneous changes of alpha-adrenoceptor affinity caused by moderate cooling in canine cutaneous veins.* Am J Physiol. , 1978. **234**(4): p. H330-7.

159. Allen, S., et al., *Influence of cooling on mesenteric vascular reactivity.* Eur J Cardiothorac Surg., 1996. **10**(11): p. 1015-20.

160. Angus, J.C. and C.C. Hayman, *Low-pressure, metastable growth of diamond and "diamondlike" phases.* Science, 1988. **241**: p. 913-21.

161. Spiberg, P., et al., *In-situ Fourier transform IR emission spectroscopy of diamond chemical vapor deposition* Diam. Relat. Mater. , 1993. **2**: p. 708-712

162. Yater, J.E., et al., *Electron transport mechanisms in thin boron-doped diamond films.* J. Appl. Phys., 2004. **96**: p. 446-453.

163. Bennett, J.A., et al., *Pulsed Galvanostatic Deposition of Pt Particles on Microcrystalline and Nanocrystalline Diamond Thin-Film Electrodes I.Characterization of As-Deposited Metal/Diamond Surfaces.* J. Electrochem. Soc., 2005. **152**: p. E184-E192.

164. Fischer, A.E., Y. Show, and G.M. Swain, *Electrochemical Performance of Diamond Thin-Film Electrodes from Different Commercial Sources.* Anal. Chem., 2004. **76**: p. 2553-2560.

165. Wang, S. and G.M. Swain, *Spatially Heterogeneous Electrical and Electrochemical Properties of Hydrogen-Terminated Boron-Doped Nanocrystalline Diamond Thin Film Deposited from an Argon-Rich CH4/H2/Ar/B2H6 Source Gas Mixture.* J. Phys. Chem. C., 2007. **111**: p. 3986-3995.

166. Park, J., et al., *Diamond microelectrodes for use in biological environments.* J. Electroanal. Chem., 2005. **583**: p. 56–68.

167. Swain, G.M. and R. Ramesham, *The Electrochemical Activity of Boron-Doped Polycrystalline Diamond Thin Film Electrodes.* Anal. Chem., 1993. **65**: p. 345-351.

168. King, A.J., J.W. Osborn, and G.D. Fink, *Splanchnic Circulation Is a Critical Neural Target in Angiotensin II Salt Hypertension in Rats.* Hypertension, 2007. **50**: p. 547-556.

169. Ranganathan, S., T.-C. Kuo, and R.L. McCreery, *Facile Preparation of Active Glassy Carbon Electrodes with Activated Carbon and Organic Solvents.* Anal. Chem., 1999. **71**(16): p. 3574–3580.

170. Adams, R.N., *Probing brain chemistry with electroanalytical techniques.* . Anal. Chem., 1976. **48**(14): p. 1126A-1138A.

171. Stamford, J., *In vivo voltammetry: some methodological considerations.* J. Neurosci. Methods., 1986. **17**: p. 1-29.

172. Baur, J.E., et al., *Fast-scan voltammetry of biogenic amines.* Anal. Chem., 1988. **60**: p. 1268-72.

173. Rivot, J.P., L. Ory-Lavolleea, and C.Y. Chiang, *Differential pulse voltammetry in the dorsal horn of the spinal cord of the anesthetized rat: Are the voltammograms related to 5-HT and/or to 5-HIAA?* . Brain Res., 1983. **275**(2): p. 311-319.

174. Brock, J.A. and T.C. Cunnane, *Effects of Ca^{2+} concentration and Ca^{2+} channel blockers on noradrenaline release and purinergic neuroeffector transmission in rat tail artery.* Br. J. Pharmacol., 1999. **126**: p. 11 - 18.

175. Brock, J.A., et al., *Spontaneous release of large packets of noradrenaline from sympathetic nerve terminals in rat mesenteric arteries in vitro.* Br. J. Pharmacol., 2000. **131**: p. 1507 - 1511.

176. McElvain, J.S. and J.O. Schenk, *Studies of the mechanism of inhibition of the dopamine uptake carrier by cocaine in vitro using rotating disk electrode voltammetry.* . Ann. N. Y. Acad. Sci., 1992. **654**: p. 480-2.

177. Davidson, C., et al., *Effect of cocaine, nomifensine, GBR 12909 and WIN 35428 on carbon fiber microelectrode sensitivity for voltammetric recording of dopamineJoumal of Neuroscience Methods.* J. Neurosci. Methods., 2000. **101**: p. 75-83.

178. Zhang, L.L., et al., *Activation of transient receptor potential vanilloid type-1 channel prevents adipogenesis and obesity.* Circ. Res. , 2007. **13**: p. 1063-70.

179. AgerIII, J.W., et al., *Laser heating effects in the characterization of carbon fibers by Raman spectroscopy.* J. Appl. Phys., 1990. **68**(7): p. 3598-3608

180. Fauteux, C. and J. Pegna, *Radial characterization of 3D-LCVD carbon fibers by Raman spectroscopy.* Appl. Phys. A., 2004. **78**: p. 883–888.

181. Leveque, D. and M.-H. Auvray, *Study of Carbon-fiber Strain in Model Composites by Ramsn Spectroscopy.* Compos. Sci. Tech., 1996. **56**: p. 749-154.

182. Suzuki, H., *Effects of endogenous and exogenous noradrenaline on the*

smooth muscle of guineapig mesenteric vein. J. Physiol., 1981. **321**: p. 495–512.

183. Langer, S.Z., *25 years since the discovery of presynaptic receptors: present knowledge and future perspectives.* Trends Pharmacol. Sci., 1997. **18**: p. 95-99.

184. Ruff, R.L., *Effects of temperature on slow and fast inactivation of rat skeletal muscle Na+ channels.* Am. J. Physiol., 1999. **46**: p. C937-947.

185. Gonon, F.G., et al., *Electrochemical Treatment of Pyrolytic Carbon Fiber Electrodes.* Anal. Chem., 1981. **53**: p. 1386-1389.

186. Dong, H., et al., *Drug effects on the electrochemical detection of norepinephrine with carbon fiber and diamond microelectrodes.* J Electroanal Chem., 2009. **632**: p. 20-29.

187. Dunn, W.R., J.A. Brock, and T.A. Hardy, *Electrochemical and electrophysiological characterization of neurotransmitter release from sympathetic nerves supplying rat mesenteric arteries.* Br. J. Pharmacol., 1999. **128**: p. 174 - 180.

188. Herradón, E., M. Martín, and V. López-Miranda, *Characterization of the vasorelaxant mechanisms of the endocannabinoid anandamide in rat aorta.* Br J Pharmacol., 2007. **152**(5): p. 699-708.

189. Maxwell, R., *Guanethidine after twenty years: a pharmacologist's perspective.* Br J Pharmacol 1982. **13**: p. 35–44.

190. Smyth, L.M., I.A. Yamboliev, and V.N. Mutafova-Yambolieva, *N-type and P/Q-type calcium channels regulate differentially the release of noradrenaline, ATP and beta-NAD in blood vessels.* Neuropharmacology, 2009. **56**(2): p. 368-78.

191. Bard, A.J. and L.R. Faulkner, *Electrochemical Methods. Fundamentals and Applications 2nd Ed.* Wiley, New York., 2001.

192. Quintero, J.E., et al., *Amperometric measures of age-related changes in glutamate regulation in the cortex of rhesus monkeys* Exp Neurol. , 2007. **208**(2): p. 238-246

193. Dinkelacker, V., et al., *The readily releasable pool of vesicles in chromaffin cells is replenished in a temperature-dependent manner and transiently overfills at 37 degrees C.* J Neurosci. , 2000. **20**(22): p. 8377-83.

194. Nozaki, M. and N. Sperelakis, *Pertussis toxin effects on transmitter*

release from perivascular nerve terminals. Am J Physiol., 1989. **256**(2): p. H455-9.

195. Vanhoutte, P.M. and N.A. Flavahan, *Effects of temperature on alpha adrenoceptors in limb veins: role of receptor reserve.* Fed. Proc., 1986. **45**: p. 2347-54.

196. Harker, C., et al., *Cooling augments alpha 2-adrenoceptor-mediated contractions in rat tail artery.* Am J Physiol. , 1991. **260**: p. H1166-71.

197. Mason, J.N., et al., *Novel fluorescence-based approaches for the study of biogenic amine transporter localization, activity, and regulation.* J Neurosci Methods, 2005. **143**(1): p. 3-25.

198. Venton, B.J., et al., *Cocaine increases dopamine release by mobilization of a synapsin-dependent reserve pool.* J Neurosci. , 2006. **26**(12): p. 3206-9.

199. Suyama, S., et al., *Synaptic vesicle dynamics in the mossy fiber-CA3 presynaptic terminals of mouse hippocampus.* Neurosci Res. , 2007. **59**(4): p. 481-90.

200. Haynes, C.L., L.N. Siff, and R.M. Wightman, *Temperature-dependent differences between readily releasable and reserve pool vesicles in chromaffin cells.* Biochim Biophys Acta., 2007. **1773**(6): p. 728–735.

201. Kushmerick, C., R. Renden, and H. von Gersdorff, *Physiological temperatures reduce the rate of vesicle pool depletion and short-term depression via an acceleration of vesicle recruitment.* J Neurosci. , 2006. **26**(5): p. 1366-77.

202. Huidobro-Toro, J.P. and M.V.n. Donoso, *Sympathetic co-transmission: the coordinated action of ATP and noradrenaline and their modulation by neuropeptide Y in human vascular neuroeffector junctions.* Eur J Pharmacol., 2004. **500**: p. 27– 35.

203. Stjarne, L., et al., *Nerve activity-dependent variations in clearance of released noradrenaline: regulatory roles for sympathetic neuromuscular transmission in rat tail artery.* Neuroscience, 1994. **60**: p. 1021-1038.

204. Safar, M. and G. London, *Arterial and venous compliance in sustained essential hypertension.* Hypertension, 1987. **10**(2): p. 133-9.

205. Schobel, H., et al., *A centripetal shift in intravascular volume triggers the onset of early cardiac adaptation in hypertension.* J Hypertens Suppl, 1993. **11**(5): p. S94-5.

206. de Champlain, J., et al., *Circulating catecholamine levels in human and experimental hypertension.* Circ Res., 1976. **38**(2): p. 109-14.

207. Baba, A., et al., *Intracellular free calcium concentration, Ca++ channel and calmodulin level in experimental hypertension in rats.* Jpn Circ J. , 1987. **51**(10): p. 1216-22.

208. Westfall, T., et al., *Comparison of norepinephrine release in hypertensive rats: II. Caudal artery and portal vein.* Clin Exp Hypertens A., 1986. **8**(2): p. 221-37.

209. Monos, E., V. Bérczi, and G. Nádasy, *Local control of veins: biomechanical, metabolic, and humoral aspects.* Physiol Rev. , 1995. **75**(3): p. 611-66.

210. de Champlain, J., et al., *Peripheral neurogenic mechanisms in deoxycorticosterone acetate--salt hypertension in the rat.* Can J Physiol Pharmacol. , 1989. **67**: p. 1140-5.

211. Micheva, K. and S. Smith, *Strong effects of subphysiological temperature on the function and plasticity of mammalian presynaptic terminals.* J Neurosci. , 2005. **25**(33): p. 7481-8.

212. Dunn, T. and A. Mercier, *Synaptic modulation by a neuropeptide depends on temperature and extracellular calcium.* J Neurophysiol. , 2003. **89**(4): p. 1807-14.

213. Klöckner, U., A. Schiefer, and G. Isenberg, *L-type Ca-channels: similar Q10 of Ca-, Ba- and Na-conductance points to the importance of ion-channel interaction.* Pflugers Arch., 1990. **415**(5): p. 638-41.

214. Morris, G.J. and A. Clarke, *Effects of low temperatures on biological membranes.* London ; New York : Academic Press, 1981.

215. Fink, G.D., *Arthur C. Corcoran Memorial Lecture. Sympathetic activity, vascular capacitance, and long-term regulation of arterial pressure.* Hypertension, 2009. **53**(2): p. 307-12.

216. Ogilvie, R. and D. Zborowska-Sluis, *Compartmental vascular changes in dogs after nephrectomy, DOCA, and saline: effect of nifedipine.* Can J Physiol Pharmacol. , 1987. **65**(9): p. 1891-7.

217. Ricksten, S., T. Yao, and P. Thorén, *Peripheral and central vascular compliances in conscious normotensive and spontaneously hypertensive rats. .* Acta Physiol Scand. , 1981. **112**(2): p. 169-77.

218. Xu, H., et al., *Nitric oxide-independent effects of tempol on sympathetic*

nerve activity and blood pressure in normotensive rats. . Am J Physiol Heart Circ Physiol. , 2001. **281**(2): p. H975-80.

219. Touyz, R., *Reactive oxygen species, vascular oxidative stress, and redox signaling in hypertension: what is the clinical significance?* Hypertension, 2004. **44**(3): p. 248-52.

220. Cabassi, A., et al., *Norepinephrine reuptake is impaired in skeletal muscle of hypertensive rats in vivo.* Hypertension, 2001. **37**: p. 698-702.

221. El Midaoui, A. and J. de Champlain, *Prevention of hypertension, insulin resistance, and oxidative stress by alpha-lipoic acid.* Hypertension, 2002. **39**(2): p. 303-7.

222. Griendling, K.K., D. Sorescu, and M. Ushio-Fukai, *NAD(P)H oxidase: role in cardiovascular biology and disease.* Circ Res. , 2000. **86**(5): p. 494-501.

223. Dai, X., X. Cao, and D. Kreulen, *Superoxide anion is elevated in sympathetic neurons in DOCA-salt hypertension via activation of NADPH oxidase.* Am J Physiol Heart Circ Physiol, 2006. **290**(3): p. H1019-26.

224. Dröge, W., *Free Radicals in the Physiological Control of Cell Function* Physiol. Rev. , 2002. **82**(1): p. 47-95.

225. Macarthur, H., T.C. Westfall, and G.H. Wilken, *Oxidative stress attenuates NO-induced modulation of sympathetic neurotransmission in the mesenteric arterial bed of spontaneously hypertensive rats.* Am J Physiol Heart Circ Physiol, 2008. **294**(1): p. H183-9.

226. Giniatullin, A., et al., *SNAP25 is a pre-synaptic target for the depressant action of reactive oxygen species on transmitter release.* J Neurochem. , 2006. **98**(6): p. 1789-97.

227. Shokoji, T., et al., *Renal Sympathetic Nerve Responses to Tempol in Spontaneously Hypertensive Rats.* Hypertension, 2003. **41**(2): p. 266-73.

228. Beswick, R.A., et al., *NADH/NADPH oxidase and enhanced superoxide production in the mineralocorticoid hypertensive rat.* Hypertension, 2001. **38**(5): p. 1107-11.

229. Duffy, S., et al., *Effect of ascorbic acid treatment on conduit vessel endothelial dysfunction in patients with hypertension.* Am J Physiol Heart Circ Physiol. , 2001. **280**: p. H528-34.

230. Russo, C., et al., *Anti-oxidant status and lipid peroxidation in patients with essential hypertension.* J Hypertens., 1998. **16**(9): p. 1267-71.

231. Todorov, L., et al., *Evidence for the differential release of the cotransmitters ATP and noradrenaline from sympathetic nerves of the guinea-pig vas deferens.* J Physiol. , 1996. **496**: p. 731-48.

232. Fujii, S., et al., *L-arginine reverses p47phox and gp91phox expression induced by high salt in Dahl rats.* Hypertension, 2003. **42**(5): p. 1014-20.

233. Demel, S.L., et al., *Role of oxidative stress in the altered sympathetic neurotransmissoin in DOCA-salt hypertension. .* In preparation.

234. Davies, K.J., *Protein damage and degradation by oxygen radicals. I. general aspects.* J Biol Chem. , 1987. **262**(20): p. 9895-901.

235. Asaad, M. and M. Antonaccio, *Vascular wall renin in spontaneously hypertensive rats. Potential relevance to hypertension maintenance and antihypertensive effect of captopril.* Hypertension, 1982: p. 487-93.

236. Asano, N., et al., *Renal AT1 receptor: computerized quantification in spontaneously hypertensive rats and DOCA-salt rats.* Res Commun Mol Pathol Pharmacol, 1998: p. 171-80.

237. Heumüller, S., et al., *Apocynin is not an inhibitor of vascular NADPH oxidases but an antioxidant.* Hypertension, 2008. **51**(2): p. 211-7.

238. Zafari, A., et al., *Role of NADH/NADPH oxidase-derived H_2O_2 in angiotensin II-induced vascular hypertrophy.* Hypertension, 1998. **32**(3): p. 488-95.

239. Wu, L. and J. de Champlain, *Effects of superoxide on signaling pathways in smooth muscle cells from rats.* Hypertension, 1999. **34**(6): p. 1247-53.

240. Dean, R., C. Roberts, and W. Jessup, *Fragmentation of extracellular and intracellular polypeptides by free radicals.* Prog Clin Biol Res., 1985. **180**: p. 341-50.

241. McNamara, M. and R. Augusteyn, *The effects of hydrogen peroxide on lens proteins: a possible model for nuclear cataract.* Exp Eye Res., 1984. **38**(1): p. 45-56.

242. Kolo, L., T. Westfall, and H. Macarthur, *Nitric oxide decreases the biological activity of norepinephrine resulting in altered vascular tone in the rat mesenteric arterial bed.* Am J Physiol Heart Circ Physiol, 2004. **286**(1): p. H296-303.

243. Nishiyama, A., et al., *Systemic and Regional Hemodynamic Responses to Tempol in Angiotensin II-Infused Hypertensive Rats.* Hypertension, 2001.

37(1): p. 77-83.

244. Schnackenberg, C., W. Welch, and C. Wilcox, *Normalization of blood pressure and renal vascular resistance in SHR with a membrane-permeable superoxide dismutase mimetic: role of nitric oxide.* Hypertension, 1998. **32**(1): p. 59-64.

245. Bennett, M.R., *Autonomic neuromuscular transmission at a varicosity.* Prog Neurobiol, 1996. **50**(5-6): p. 505-32.

246. Brain, K.L. and M.R. Bennett, *Calcium in sympathetic varicosities of mouse vas deferens during facilitation, augmentation and autoinhibition.* J Physiol, 1997. **502 (Pt 3)**: p. 521-36.

247. Strosberg, A.D., *Structure, function, and regulation of adrenergic receptors.* Protein Sci, 1993. **2**(8): p. 1198-209.

248. Knapp, L.T. and E. Klann, *Superoxide-induced stimulation of protein kinase C via thiol modification and modulation of zinc content.* J Biol Chem, 2000. **275**(31): p. 24136-45.

249. Elroy-Stein, O. and Y. Groner, *Impaired neurotransmitter uptake in PC12 cells overexpressing human Cu/Zn-superoxide dismutase--implication for gene dosage effects in Down syndrome.* Cell, 1988. **52**(2): p. 259-67.

250. Mao, W., et al., *Norepinephrine induces endoplasmic reticulum stress and downregulation of norepinephrine transporter density in PC12 cells via oxidative stress.* Am J Physiol Heart Circ Physiol, 2005. **288**(5): p. H2381-9.

251. Pollock, D.M., *Endothelin, angiotensin, and oxidative stress in hypertension.* Hypertension, 2005. **45**(4): p. 477-80.